Dynamic Load Modelling in Real Time Digital Simulator (RTDS)

Abdulrasaq N. Gbadamosi

Technische Universiteit Delft

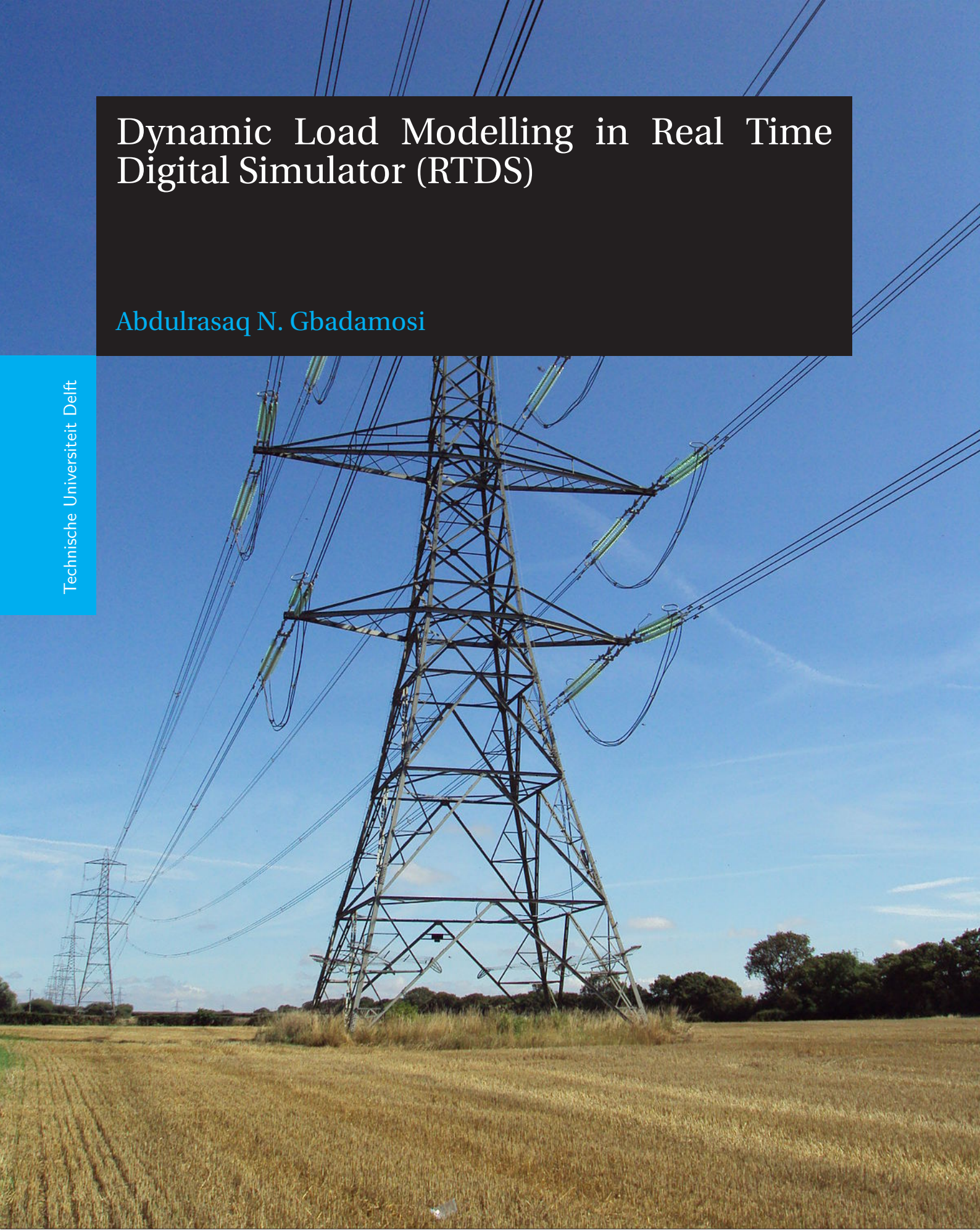

TU Delft Delft University of Technology

Challenge the future

DYNAMIC LOAD MODELLING IN REAL TIME DIGITAL SIMULATOR (RTDS)

by

Abdulrasaq N. Gbadamosi

A thesis submitted in partial fulfilment of the requirements for the degree of

Master of Science
in Electrical Engineering

at the Delft University of Technology,
to be defended publicly on Thursday 24th August, 2017 at 12:30 PM.

Supervisor:	Dr. ir. J. L. Rueda Torres	
Thesis committee:	Prof. dr. Peter Palensky	IEPG, TU Delft
	Dr. ir. J. L. Rueda Torres	IEPG , TU Delft
	Dr. ir. A. Rodrigo Mor	DCE&S, TU Delft

TU Delft Delft University of Technology

ACKNOWLEDGEMENTS

"Whoever is able to think deeply, would most definitely always be thankful" - *Yoruba adage*.

All praise is to Allah, the most Merciful, the most Compassionate, the Creator of all that exist.

I hereby express my sincerely gratitude to all those who supported me during the period of my research. Most notably, my deepest appreciation goes to my supervisor, Dr. Jose Rueda for his continuous support. I would not have been able to start nor finish this work without his constant support. He was very approachable, trustworthy and encouraging. His explanation during times of confusion generated new ideas to solve the problems. Furthermore, I would like to appreciate the excellent support of Da Wang. He took his time to review my work and gave very helpful feedbacks that helped me maintain focus.

Next I would like to thank Prof. Peter Palensky for chairing my thesis committee. Also to Dr. ir. Armando Rodrigo for agreeing to be part of my thesis committee, devoting considerable time to the evaluation of this work in a timely manner. My sincere appreciation also goes to the RTDS support staffs, especially, Onyi Ozimako for her guidance and explanation of the models used in this work. Her advice and comments gave me adequate understanding of the operation of the RTDS.

Most especially, my profound gratitude goes to my family, for their support throughout my academic journey so far. My sisters, Tobi and Kemi, were always there for me when I felt lonely away from home. I love you more than you can imagine. In particular, I am grateful to my Dad for his continuous support. Your advice, encouragement, principles, and extraordinary motivations helped me aspire to be the best I can possibly be in life. I would not be where I am without you!

Finally, I would like to appreciate my colleagues and friends that were in one way or the other involved in my successful stay in the Netherlands, Yinka, Dotun, Abdullah, Amira, Musab, Digvijay, Dedi, Zamroni, Jorge, Fabricio, Saliha, Halima, Harish, and others too numerous to mention. The moments we shared and the support received was immense. I wish you all success in your future endeavours.

Abdulrasaq N. Gbadamosi,
Delft,
August 2017.

CONTENTS

LIST OF FIGURES

LIST OF TABLES

ABSTRACT

The accuracy of modelling distribution networks plays a very important role in analysing the stability of transmission systems. In recent years, due to the surge in the integration of renewable energy resources via power electronic interfaces, distribution networks are evolving from passive networks to modern active networks. This means that their characteristics are time varying following the operating condition of renewable energy sources.

Real Time Digital Simulator (RTDS) is a specially designed hardware and software integrated computer system used to study Electromagnetic Transient (EMT) Phenomena in power systems. As the name implies, it can perform power system simulations at computational speeds equal to real-time operation. However, modelling of detailed distribution networks in RTDS would require many hardware resources. The goal of this thesis is to develop an equivalent dynamic load model for the stability analysis of transmission networks in RTDS, which should not only enhance RTDS's capability of simulating large power systems, but more importantly, improve the accuracy of model distribution networks. Most studies about transmission systems do not require a full representation of distribution networks. However, the dynamic behaviour of distribution networks still needs to be preserved. Therefore, the dynamic equivalent parameters of distribution networks must be sufficient to ensure an accurate representation for the analysis of transmission networks. In this thesis, the identification and optimization of parameters are done using Mean Variance Mapping Optimisation (MVMO), a unique heuristic optimisation technique.

The IEEE 34-Bus distribution system is used as a reference model for data collection and is developed in RSCAD, the RTDS software. An external grid is used to represent the transmission system wherein, several disturbances are simulated in order to compare the responses of the reference detailed model and the dynamic equivalent model. Furthermore, the validity of the developed DE load model is confirmed by comparing its behaviour to disturbances that were not implemented during the parameter optimization process.

1

INTRODUCTION

Over the last couple of years, the contribution of renewable energy resources (RES) to the energy mix has significantly escalated. Most recently, countries such as Germany and Portugal have reportedly supplied large portions of their energy demands using only renewable energy sources. Consequently, several technical challenges are being faced by utilities with respect to planning and operations of the modern power system. These challenges are mainly attributed to high penetration of RES in grid sections that have low demands. However, Such situations have led to numerous effort on research that investigates the influence of high influx of power electronics components in power systems [5] [6]. A major challenge of large scale integration of RES, especially at the distribution system level, is their behaviour and response to faults and other disturbances that might occur in the transmission system.

1.1. MOTIVATION

The power system is often regarded as the most enormous and complex system ever developed by man [7, 8]. It consists of numerous equipment like power transformers, synchronous generators, cables, capacitor banks, transmission lines, power electronic devices, thousands of buses etc. which enable safe and efficient generation, transmission and delivery of power to local and remote areas. This intricacy is why it is essential to ensure that the system is reliable and maintains a state of stability by carrying out different studies of possible disturbances. However, due to the continuous operation of the power system and the high cost of equipment, most researches are done on computer programs designed for simulations of the real system such that safety of the equipment and persons is not compromised.

Accordingly, the reliability of the power system must be maintained despite the continuous integration of different energy resources. Digital representations and simulations of dynamic components of power systems fosters better understanding and helps in real-life decision making on the operation of the complex systems [9]. New, efficient and accurate models of future active distribution network are therefore necessary in order to adequately design, plan and analyse possible contingencies in the network. These models are continuously becoming more complex to derive due to the connection of most recent RES to the grid through power electronic interfaces. Such models need to ensure that dynamic performance i.e. fast and slow transient phenomena of the network e.g. frequency and voltage fluctuations are well represented. This would ensure that proper planning and appropriate decisions can be made to ensure maintenance of power system stability and reliability.

The outcome of several studies [10, 11] show that load modelling is one of the most critical aspect of digital simulations of the power system. This was initially because of the fast rate at which

several devices and equipment such as induction motors, lighting, HVAC, personal computers, inverter-based electric heating, TVs etc. with different dynamics were added to the mix of system loads. Now, the importance is more driven by the increasing penetration of energy sources with power electronic interfaces leading to a more active distribution grid. This creates unpredictability in the system and makes it more complex to develop models that can accurately mimic the behaviour of the real system during contingencies and disturbances. Therefore, it is very significant to build load models that can aid system planning decisions and provide adequate insight into the effects of load on the network. Hence, this thesis project seeks to develop a dynamic equivalent load model of active distribution systems in Real Time Digital Simulator (RTDS).

1.2. PROBLEM DEFINITION

Very fast transients occur in power systems that are usually not captured by conventional power system digital simulators. The complexity of the power system implies that it may be costly and even dangerous to base decision making only on field information without adequate predictions. Simulation of power systems (or Power system analysis software) helps network operators and planners to forecast possible disturbances, provides adequate protection schemes and aids realistic future grid expansion. Most of the simulation software (packages) e.g. DigSilent Powerfactory, Powerworld Simulator, PSS/E etc. are based on RMS simulations. In these software, it is not feasible to represent all small components in the distribution network to perform some analysis. It would require a lot of computational resources and take too much time. Thus, aggregated or dynamic equivalent models are usually required to represent some part of the system while focus is given to the area of study which is modelled in detail.

Load modelling constitutes a major aspect of power system analysis and the continuous realization of active distribution networks as explained earlier makes it even more complex. Since most distributed energy sources are interfaced with power electronic devices, static or passive representation of load is no longer adequate [12]. The dynamics of load responses need to be accounted for to achieve better results close enough to expected values in actual situations. RTDS is an electromagnetic transient (EMT) simulation package that could provide more precise dynamic study results. Despite this, and just like RMS packages, it is computationally intensive to model each equipment in the distribution network. Especially when only a specific region (internal system) where contingencies are studied need full representation while the rest of the network (external system) can be reduced to equivalent models that provide similar responses.

Dynamic equivalent (DE) models are simple aggregated representation of a large network, able to provide similar responses and behaviours as the actual network for stability analysis. While numerous techniques have been proposed in literature to achieve adequate DE [5, 12, 13], most of them are based on RMS studies. There are not many dynamic equivalent models of loads in Electromagnetic Transient (EMT) applications. Therefore, the primary problem definition is to develop a DE model of an active distribution system in EMT that accurately represents current and future grids. This involves proper definition of the DE structure and development of adequate control systems for the model. Furthermore, it is imperative to ascertain the parameters of the DE that would provide accurate representation of the real system. Hence, the challenge is to implement a parameter identification technique in RTDS which would deliver sufficient parameters of the dynamic equivalent model. In this research, an automated technique was implemented to simplify the process of determining the parameters.

1.3. OBJECTIVE AND RESEARCH QUESTIONS

The objectives of this thesis project are defined as follows:

- Development of the dynamic equivalent model (layout, considered elements and controls,

etc.) of an active distribution network. This is done manually and with reference to methods available in literature.

- Identification of associated parameters of the DE model.

These are facilitated through the execution of a heuristic based optimisation algorithm, Mean Variance Mapping Optimisation (MVMO) for online DE parameter identification. A MATLAB script is used to link the models in RTDS with the MVMO algorithm through a TCP/IP connection as shown in Figure 1.1.

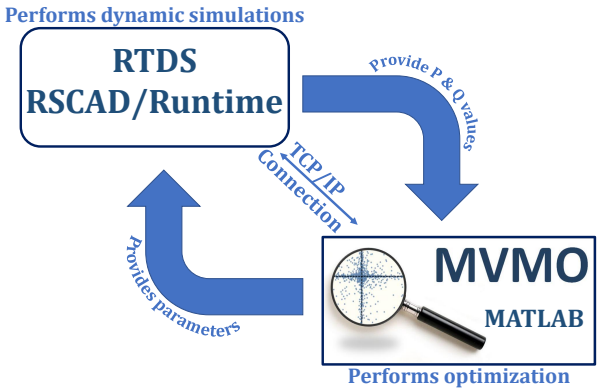

Figure 1.1: MATLAB and RSCAD/Runtime Interaction

Consequently, the following research questions will be answered upon the completion of this project:

1. How can a DE model for a future distribution system, dominated by solar PV generation, be defined for real-time digital simulation?
2. How accurate can the response of the DE model be when disturbance at transmission system side are simulated?
3. Is it feasible and computationally efficient to apply metaheuristic optimization to perform the parameter identification in an automated manner in RTDS?

1.4. RESEARCH APPROACH

To begin with, there is a need to have a detailed reference model that can provide relevant measurement data of the signals to be used for validating the developed DE model. This is due to the lack of field measurement data from Phasor Measurement Units (PMUs) or detailed load composition data. Due to computational constraints (number of racks) in RTDS, a relatively small size system, an existing IEEE benchmark distribution system model, the IEEE 34-Bus system is adopted as reference model. This helps to avoid the high computation time and complications involved in developing a new model. The model is modified in RTDS software (RSCAD) to represent an active distribution system with solar PV generation, connected to an external grid through a step-down transformer and a long transmission line.

The required signals are measured at the boundary bus between the active distribution system and the external grid by applying specific disturbances in the external grid. The equivalent model is developed by grouping the DS loads based on their characteristics (constant Z, I or P). A ZIP load model in RSCAD is then used to represent the loads on each phase. For more dynamics, induction machines are added to the DS and their level of contribution to the overall load determined the influence of the IM model in the DE. Besides that, the total PV generation added to the reference

model is used to determine the range of PV generation represented in the DE. Signals at the PCC of the external grid and the DE is also measured for subsequent identification of the DE parameters. The main aim is to limit the error between the signals derived from the reference grid and those from the DE model upon subjecting both to the same set of contingencies. Figure 1.2 illustrates the general approach used.

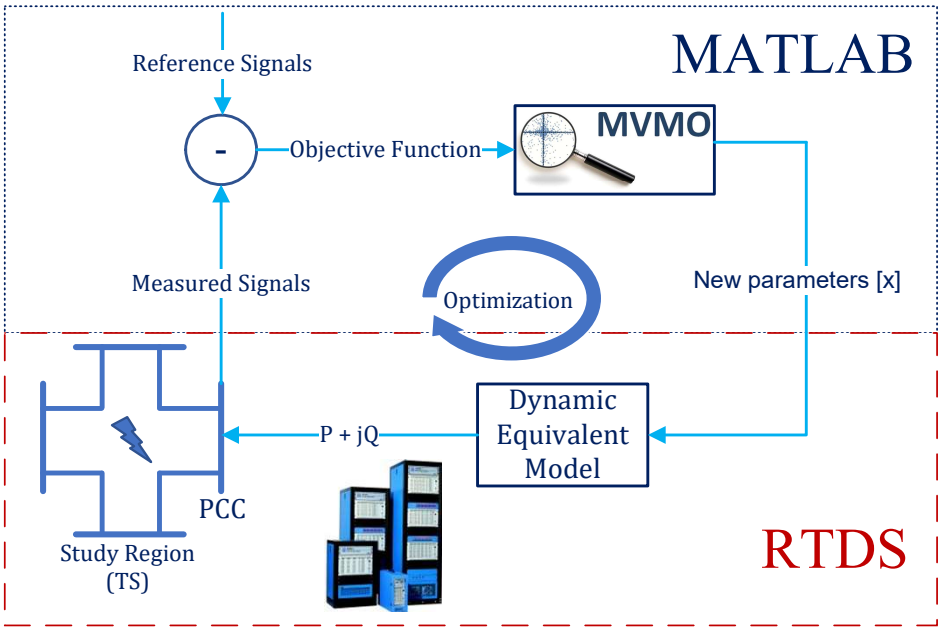

Figure 1.2: Flow chart of the research approach

From Figure 1.2, it can be deduced that the result of the comparison between the signals from the reference model and the measured signals obtained at the point of common coupling of the DE to the external grid are fed to MVMO algorithm as an objective function. Thereafter, the algorithm supplies new parameters, as a vector $\mathbf{x}$, to the DE model based on its internal evolutionary mechanism. The optimization process stops when the termination criteria is fulfilled. Then the best obtained parameters are updated to the model thus improving the ability of the DE to optimally mimic the behaviour of the reference system.

1.5. THESIS CONTRIBUTION

Though sufficient literature about dynamic load modelling already exist, most are based on RMS simulations while only a few are available with respect to EMT simulations. With the large-scale integration of DG in low and medium voltage networks, it is important to develop equivalent models that are suitable for representing the resulting ADN in dynamic studies involving EMT simulations of large power systems. Hence, this thesis seeks to contribute to the vast literature on load modelling by providing an adequate equivalent model developed in RTDS which can produce sufficient responses like those of a detailed active distribution system when subjected to various contingencies.

1.6. THESIS OUTLINE

This chapter gives a general synopsis of the purpose of this thesis. In Chapter 2, the description of existing load modelling methodologies as well as the techniques used to identify load model parameters is presented. The RTDS simulator hardware and software features are presented in

Chapter 3. The methodology to determine the reference data by modifying an existing IEEE test system and the process of developing the dynamic equivalent model of the load is explained in Chapter 4. Chapter 5 explains how the load model parameters are identified and optimized using the MVMO algorithm. Relevant results from this investigation are analysed and presented in Chapter 6. Lastly, Chapter 7 presents the conclusions derived from the performed analyses as well as suggestions for further research.

2

LOAD MODELLING

2.1. INTRODUCTION

Load modelling is generally known as the representation and implementation of electrical equipment, either individually or cumulatively, for power system studies. Such representations are usually mathematical, circuit based, physical component based, and so on, which describes the responses of load characteristics to expected or unexpected conditions and disturbances in the power system. This section highlights the need for accurate load models, describes the fundamental concept of load modelling, presents a synopsis of widely used load models, and explains the load modelling approach used in this thesis.

2.2. IMPORTANCE OF LOAD MODELLING

Power systems planners and operators require results derived from stability studies to make appropriate decisions on both short and long term basis. These studies are needed to assess the performance and limits of power system components upon subjection to several operating conditions which could compromise the stability of the system. Their results often determine the level of financial investments, capital expenditure and other economic choices executed to ensure continuous operation of the power system. Therefore, adequate modelling of all components is vital to obtain correct and realistic results. Among all power system components, the electrical characteristics of loads should be accurately modelled as a result of their substantial influence on the dynamic behaviour of the power system [14–16]. Evidence of the catastrophic consequences that inadequate load modelling can cause is available in history, for example, the Swedish blackout [17] and the collapse of Tokyo network [18] which occurred in 1983 and 1987 respectively.

Over the last few decades, the size of the distribution grid, especially with the inclusion of distributed generation, has grown due to increasing energy demands. The surge in the integration of RES in the distribution system is gradually changing the perspective of the transmission system operators (TSO) on the distribution network and their connected loads. The DS is experiencing a paradigm shift thereby evolving from a traditionally passive network to an active network with bi-directional power flow. Moreover, it would require a lot of computational resources, both hardware and software, to model the entire active distribution system. From the TSO's perspective, the transmission system can be completely modelled due to it's size relative to the distribution system. However, a suitable representation of the low voltage DS is required for stability analysis carried out in the HV transmission system [19]. This presents a need for aggregate models of the ADN that can accurately mimic its dynamic behaviour at the bus of coupling to the transmission system. Upon replacing large portions of the distribution system with their dynamic equivalent, computational efforts would be significantly reduced.

2.3. DYNAMIC EQUIVALENCE

The concept of dynamic equivalence (also referred to as network aggregation) is a vastly popular method that power system operators adopt to approximate the dynamics of large networks. The demand for accurate and detailed simulation is usually compromised by limited computation capability and time. Moreover, the scale of modern interconnected power systems can be so large that it is often impractical for any digital time domain simulation tool to run such models in which all the components are represented with the full modelling capability. Therefore, the goal of the concept is to replace a large part or the whole detailed model with a reduced model that exhibits similar dynamic characteristics as the real ADN.

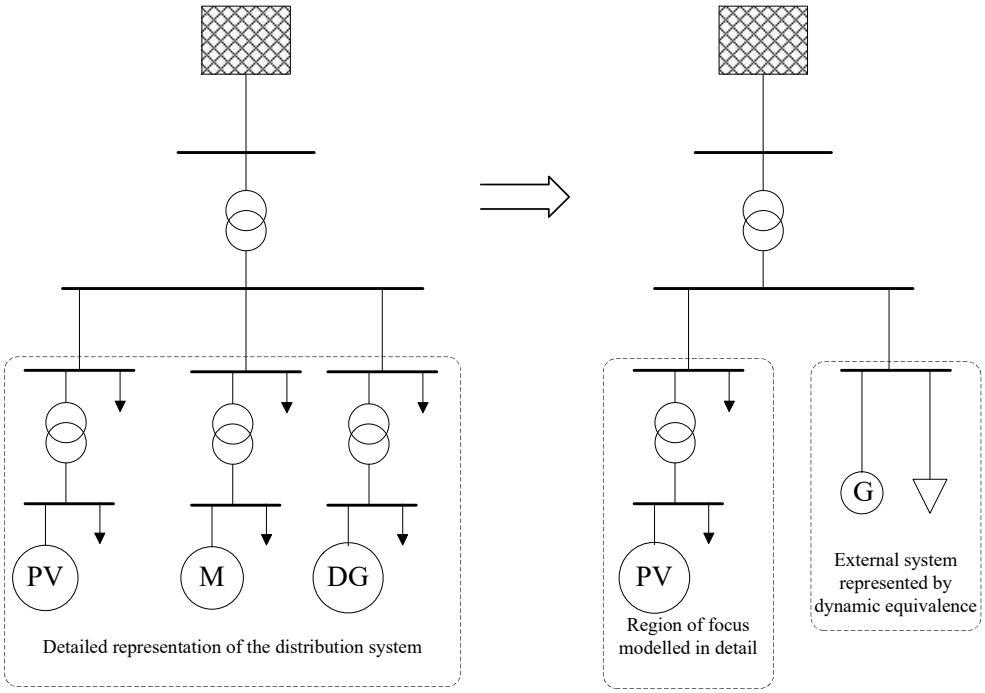

Figure 2.1: Concept of dynamic equivalence

Figure 2.1 shows an illustration of the concept. Much focus is placed on the region of the system where studies are to be done, so all the generators, loads, controls, etc. in this area must be modelled in detail. On the other hand, the behaviours of this region are also influenced by the interactions with the external system but a concise modelling of this part is not necessary. Therefore, a DE model is used to replace the sophisticated model of the external system. This simplified model should be able to reproduce to a reasonable extent, the responses of the main replaced system to disturbances that occur in the region of focus.

There has been many studies done on developing such aggregated models in several software like PSSE and DigSilent Powerfactory [20, 21]. However, few studies have been done on creating them in RTDS which is the focus of this thesis. Besides, there is still much research ongoing to determine the most suitable way to aggregate an active distribution network. The effectiveness of a dynamic equivalent model is related to the amount of computation time saved and the level of accuracy achieved for the phenomena under study. The next section gives an overview of the classification of load models (see Figure 2.2) and their methods of implementation.

2.4. IMPLEMENTATION OF LOAD MODELS

The choice of an appropriate load model is usually determined by the type of analysis to be done on power systems. There are many forms of load models in existence. However, results from surveys of utilities across the world show that some models are more widely used than others. The first of these surveys was done in the early 1990s by an IEEE task force established to focus on load modelling. They published three important papers, [22] in 1993, [15, 23] in 1995 on load modelling. These papers summarized the popular trends in static and dynamic load modelling, provided references to previous efforts on load models and gave recommendations on the appropriate load models to be used for power system dynamic studies.

However, since the mid-1990s, significant changes have developed in load composition and structure. More recently, the surge in DG technologies, both inverter interfaced and directly coupled, has re-established the need for appropriate load models. Consequently, a work group (WG) C4.605: "Modelling and aggregation of loads in flexible power networks" was established by CIGRE Study Committee in late 2009. They had five major objectives [3, 24, 25] as they strived to address trending issues related to load modelling. Their objectives were:

1. To provide a detailed and up to date synopsis of existing load models including their parameters for power system studies and also point out load classes and types for which appropriate models still do not exist;

2. To provide a thorough summary of current methodologies used to model loads, placing more focus on the component and measurement based approaches, thereby stating their advantages and disadvantages;

3. To recommend adequate and precise procedures for developing and validating load models, using either measurement or component based techniques, or a combination of both;

4. To develop load models for all devices that can be found in the power system as well as customer classes which currently have no existing models and suggest values and ranges for the parameter of such models;

5. To give recommendations on how to develop equivalent dynamic and static models of active distribution systems with large amount of DG, as well as microgrids.

To derive a general overview of the most recent load modelling practices for dynamic power system analysis, the work group carried out a survey of about 100 power system operators and energy utilities. The highlight of some of the main load models in use according to the findings of the survey is provided in the following subsections. The comprehensive report and detailed recommendations are available in [1].

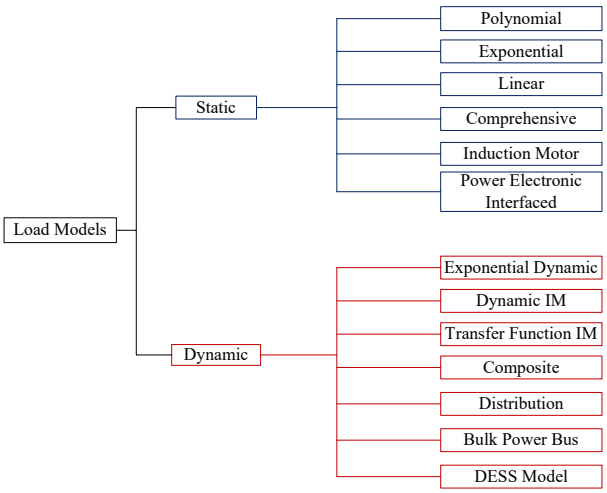

Figure 2.2: Load Model Classification (adapted from [1])

2.4.1. STATIC LOAD MODEL

Static load model (SLM) is one of the two main category of load models as shown in Figure 2.2. It is mostly used for representing general residential load that do not consist of large induction motors and drives. There are several groups of SLMs currently in use in the industry as described in Figure 2.2. Using an algebraic function of both frequency and voltage, the SLM describes the relationship between reactive and active power drawn by a load. However, there are no such things as "static loads". All loads respond to a large change in supply voltage or frequency in a finite way, taking some time for the transition from pre-disturbance to post-disturbance states. Nevertheless, static load models (SLMs) are used to represent loads which show simple time invariant changes in power demand due to slight deviation in supply voltage or frequency at the connecting bus. They can also be used to model loads that exhibit very fast dynamic response to voltage variations which are difficult to measure using measurement devices.

The general form of a static load model is given as:

$$P = f_P(U, f) \tag{2.1}$$

$$Q = f_Q(U, f) \tag{2.2}$$

where U is the voltage and f is the frequency.

POLYNOMIAL LOAD MODEL

The second order polynomial model is one of the most commonly used static load model. It can be implemented in different forms, either with frequency dependence considered or not. When frequency dependence is neglected, the load model is expressed as given in equations 2.3 and 2.4. The model is otherwise known as the "ZIP" model because it is characterised by constant impedance (Z), constant current (I) and constant power (P) load components [1].

$$P = P_n \left[p_1 \left(\frac{U}{U_n} \right)^2 + p_2 \left(\frac{U}{U_n} \right) + p_3 \right] \tag{2.3}$$

$$Q = Q_n \left[q_1 \left(\frac{U}{U_n} \right)^2 + q_2 \left(\frac{U}{U_n} \right) + q_3 \right] \tag{2.4}$$

where (p_1 and q_1), (p_2 and q_2), (p_3 and q_3) correspond to the relative involvement of Z, I, and P loads respectively. The overall sum of the proportion of each load component i.e. $(p_1 + p_2 + p_3)$ as

well as $(q_1 + q_2 + q_3)$ should be 1 p.u. This option is called the "constrained ZIP model" [12]. A more precise type is known as the "accurate ZIP model" [26]. Here, the individual p_i and q_i parameters can exceed 1 p.u. or have values below, but their sum must still equal 1 p.u.

An example of a commonly used polynomial load model with frequency dependence considered is expressed in equations 2.5 and 2.6 [27].

$$P = P_n \left[p_1 \left(\frac{U}{U_n} \right)^2 + p_2 \left(\frac{U}{U_n} \right) + p_3 \right] (1 + k_{pf} \Delta f), \sum_{i=1}^{3} p_i = 1 \tag{2.5}$$

$$Q = Q_n \left[q_1 \left(\frac{U}{U_n} \right)^2 + q_2 \left(\frac{U}{U_n} \right) + q_3 \right] (1 + k_{qf} \Delta f), \sum_{i=1}^{3} q_i = 1 \tag{2.6}$$

where Δf is the frequency deviation, k_{pf} and k_{qf} describe the change in load demand to variations in frequency. The typical values of k_{pf} are between 0 and 3.0 while k_{qf} are from -2.0 to 0 [16].

2.4.2. DYNAMIC LOAD MODELS

Dynamic loads are loads whose responses are dependent on the states in which the system and load previously were in time. Their models are usually expressed in differential equation forms relating the real and reactive power with voltage and frequency. They are often used to represent loads that have substantial amount of induction motors and electrical drives. The general mathematical formula of a dynamic load model (DLM) are similar to those of static load model. The difference is based on the addition of time dependency factor. If the dynamic model is known, then the static load model can be easily derived from it [1]. The existing DLMs can be categorized into 7 groups as shown in Figure 2.2. However, this thesis will focus on the dynamic model of induction motor and composite load model, so they are further discussed.

DYNAMIC MODEL OF INDUCTION MOTOR

The induction motor (IM) is the most widely used and customary type of electric machine in home, business and industry [28]. In most home applications, the single-phase induction machine is used while higher power industrial applications such as compressors, pumps, electric ships etc. require three phase induction machines [29]. For dynamic studies, the type of induction motor model used depends on the participation of induction machines in the load mix. When there is significant contribution of large induction machines with respect to other load types, the fifth order IM model should be used. Otherwise, it is sufficient to represent the dynamic load characteristics using the third order IM model. A fifth order, three phase IM model which is expressed using both differential and algebraic equations is given in equations 2.7 to 2.15 [30].

$$u_{ds} = R_s i_{ds} + \frac{\mathrm{d}\psi_{ds}}{\mathrm{d}\tau} - \omega_s \psi_{qs} \tag{2.7}$$

$$u_{qs} = R_s i_{qs} + \frac{\mathrm{d}\psi_{qs}}{\mathrm{d}\tau} - \omega_s \psi_{ds} \tag{2.8}$$

$$u_{dr} = R_r i_{dr} + \frac{\mathrm{d}\psi_{dr}}{\mathrm{d}\tau} - (\omega_s - \omega)\psi_{qr} \tag{2.9}$$

$$u_{qr} = R_r i_{qr} + \frac{\mathrm{d}\psi_{qr}}{\mathrm{d}\tau} + (\omega_s - \omega)\psi_{dr} \tag{2.10}$$

$$\frac{\mathrm{d}\omega}{\mathrm{d}\tau} = \frac{(M_e - M)}{\omega_b T_m} \tag{2.11}$$

with

$$M_e = X_m(i_{qs}i_{dr} + i_{ds}i_{qr})$$

$$\psi_{ds} = X_s i_{ds} + X_m i_{dr} \tag{2.12}$$

$$\psi_{qs} = X_s i_{qs} + X_m i_{qr} \tag{2.13}$$

$$\psi_{dr} = X_m i_{ds} + X_r i_{dr} \tag{2.14}$$

$$\psi_{qr} = X_m i_{qs} + X_r i_{qr} \tag{2.15}$$

where,
u_{ds}, u_{qs} - Stator voltage components
u_{dr}, u_{qr} - Rotor voltage components
i_{ds}, i_{qs} - Stator current components
i_{dr}, i_{qr} - Rotor current component
ψ_{ds}, ψ_{qs} - Stator flux linkages
ψ_{dr}, ψ_{qr} - Rotor flux linkages
R_s - Stator resistance
R_r - Rotor resistance
$X_s = X_m + X_{ys}$ - Shunt reactance
$X_r = X_m + X_{yr}$ - Rotor reactance
X_{ys} - Stator leakage reactance
X_{yr} - Rotor leakage reactance
X_m – Magnetizing reactance
ω_s - Synchronous angular speed
ω - Rotor angular speed
ω_b - Base angular frequency
M - Mechanical load torque
$\tau = \omega_b t$ - Normalized time
T_m - Mechanical time constant of the motor
M_e - Electromagnetic torque.

A third order model is derivable from the above fifth order model by neglecting the stator transients. This converts equations 2.7 and 2.8 to algebraic equations. In applications where the influence of induction motors are not emphasised, the corresponding third order model is usually adequate. Table 2.1 shows typical data of induction motor equivalents for different types of load.

Table 2.1: Parameters representing dynamic characteristics of IM

Load Type	**Rs**	**Xs**	**Rr**	**Xr**	**Xm**	**H**
Small Industrial motor	0.078	0.065	0.044	0.049	2.67	0.5
Large Industrial motor	0.007	0.0818	0.0062	0.0534	3.62	1.6
Commercial load	0.001	0.23	0.02	0.23	3.0	0.663

COMPOSITE LOAD MODEL

Most bulk supply buses serve loads that are a combination of several static and dynamic devices. This is particularly true for industrial load buses. Therefore, an appropriate load model should incorporate both static and induction motor components. The composite load model (CLM) consists of both dynamic and static load characteristics and has been subjected to many studies. There are several variants of composite load models due to the choice of their exact composition [31]. The static load section of the model can be represented by d and q current components of resistive and capacitive load [32], by conductance and susceptance in parallel [33] or by a ZIP model as implemented in [2, 34, 35]. To represent the dynamic attributes of load, most CLMs use the equations of a third order IM model due to their predominance. The equivalent circuit of the ZIP model with separated constant power, current and impedance components in parallel with a simple representation of an IM model is depicted in Figure 2.3.

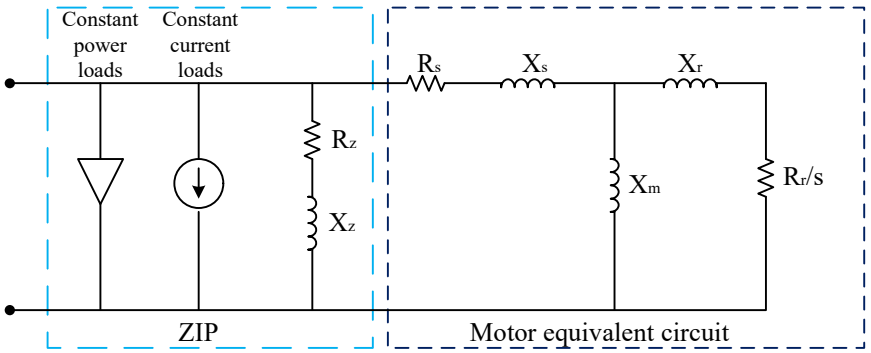

Figure 2.3: Composite Model (adapted from [2])

The ZIP part representing the static loads can be described similarly as equation 2.3 and 2.4. However, the constraints differ slightly as given below:

$$p_1 + p_2 + p_3 = 1 - K_{pm} \tag{2.16}$$

$$q_1 + q_2 + q_3 = 1 - \frac{Q_{motor}}{Q_o} \tag{2.17}$$

where K_{pm} represents the ratio of initial motor load to initial real load of the bus, Q_{motor} is the initial reactive power consumed by the motor and Q_0 is the initial reactive load of the bus [24]. The Induction motor part is described with the equations given in section 2.4.2.

2.5. DE MODEL STRUCTURE DEFINITION

From the implementation methods described in the previous section, a form of composite load model is adapted in this research. It comprises of the ZIP model in parallel with a third order IM model and a solar PV generator with its control system. This is depicted in Figure 2.4. Only the solar PV generator model was used because of its predominance in low voltage networks. Moreover, other RES were not included in the reference model due to the number of RTDS racks they would require. The ZIP model in the defined structure accounts for the static loads in the system while the IM model accounts for the dynamic loads. The third order IM model was adopted for its simplicity in representing the dynamic behaviour of induction machines. The overall structure preserves the characteristics of the reference system with respect to its load categories and distributed generation.

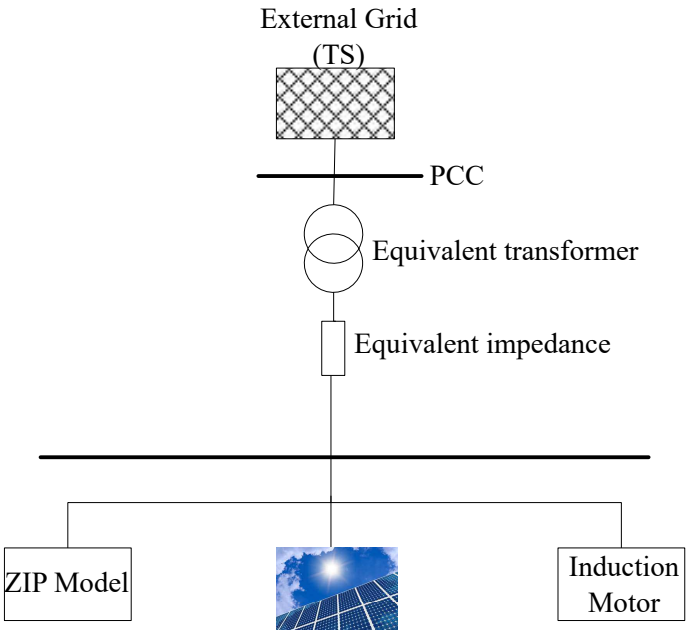

Figure 2.4: Load model used in this thesis

The description of each component of the above model and the actual implementation in RSCAD is thoroughly described in Chapter 4. Active Distribution Networks (ADN), whose DE structure is of major importance, are power system networks that contain significant amount of distributed generation (DG) and could either receive active power from the grid or supply it to the grid depending on the renewable source and load conditions. In some cases, they may also provide voltage and reactive power support to the grid. Generally, the composite model (i.e. ZIP and IM model) is a very common model used by utilities for dynamic stability studies. Nevertheless, the inclusion of a PV model with its control is to capture the effect of power electronic interfaced generation available in the detailed ADN network.

After the structure of the DE model is defined, the next step is to determine the parameters of its components that would ensure it produces similar responses as the reference system. In view of that, the dynamic behaviour of the reference distribution system and other data associated with it must first be collected. The approaches used for this are elaborated in the next section while the techniques used for parameter identification are discussed in section 2.7.

2.6. DETERMINATION OF LOAD MODEL DATA

The process of gathering the necessary system data for the development of correct aggregate load models has predominantly been approached by the power industry in two ways. i.e. component-based or measurement-based approach [36].

2.6.1. COMPONENT-BASED APPROACH

This approach which is also called the bottom-up approach relies on the knowledge of the individual load components to build an aggregate load model. The loads are divided into sectors such as residential, industrial, etc. Also, they are distinguished by categories such as resistive, inductive, power electronics etc. in a way that their mix within the total load demand are effectively represented. An illustration of this knowledge based approach is shown in Figure 2.5 [13]. The composition of individual load components in the aggregate model is usually expressed as a composite load model or represented using a second order polynomial model.

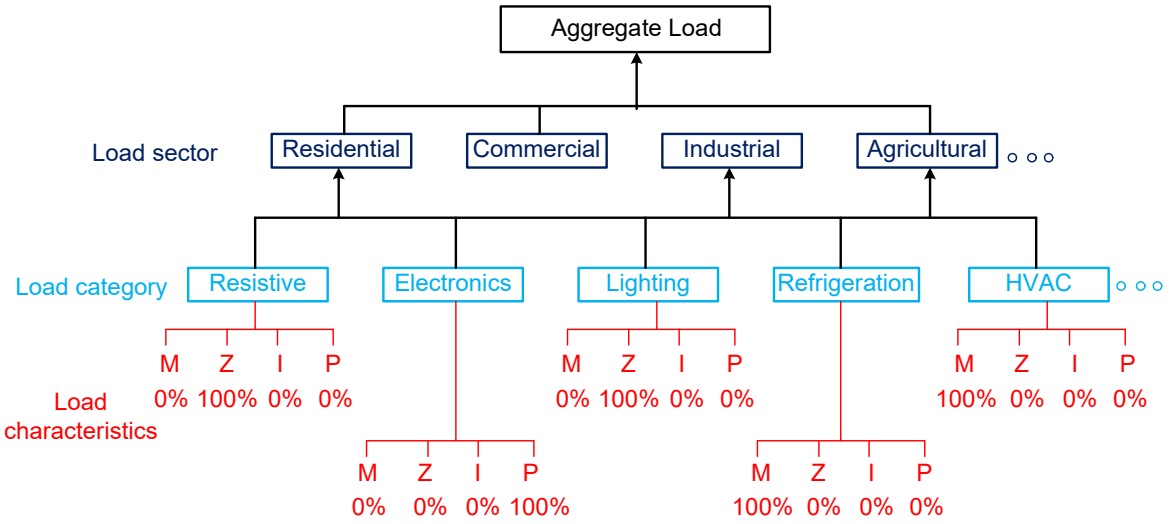

Figure 2.5: Component-based approach (adapted from [3])

The main advantage of the component based approach is its independence on field measurements of the power system. Therefore, aggregated load models can be developed from surveys or data found in literature. Nevertheless, its major drawback is that it does not account for changes in load structure or composition over time due to seasonal, behavioural or weather-related variations. Moreover, it is hard to accurately determine the composition of load nowadays.

2.6.2. MEASUREMENT-BASED APPROACH

This is a methodology in which system events at substations or feeders of interest are recorded to obtain data representing the characteristics of the connected load. These events could be small or large disturbances such as switching or lightning events that changes the system bus voltage and frequency. When a disturbance occurs, the load response i.e. active and reactive power variation is measured by measurement devices. Current and voltage transformers, phasor measurement units (PMU), power quality meters and fault recorders are some of the data acquisition devices installed in the actual power grid for this modelling approach [37, 38]. Figure 2.6 shows an illustration of this concept where CTs and VTs are monitored on representative feeders.

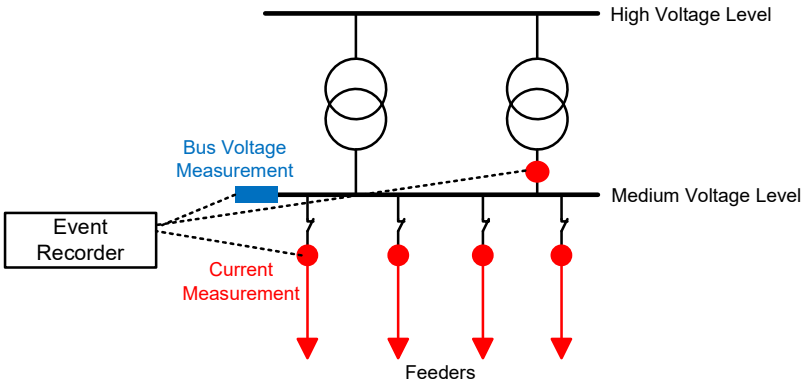

Figure 2.6: Measurement-based illustration (adapted from [3])

The measured data are fitted to estimate the parameters of the pre-defined load model such that the model can mimic the dynamic response of the load prior to, during and after a disturbance. The estimation is done using optimization and parameter identification techniques which are further explained in section 2.7.2. Examples of where this approach was used are detailed in [37, 39, 40]. The main advantages of this approach are the use of dynamic response data of the load from actual grid system and the simplicity of applying it to any kind of load. However, the main disadvantage is the lack of large disturbance measurement data needed for appropriate parameter estimation due to the robustness of the system. This limitation is resolved by using simulated data measured from a detailed reference system model as done in this research.

2.7. TECHNIQUES FOR DETERMINING DE LOAD MODEL PARAMETERS

Irrespective of the approach implemented to gather specified signals of the detailed system to be aggregated, two techniques are prominently used to define the parameters of their dynamic equivalent. They are system reduction and parameter identification techniques [41, 42].

2.7.1. SYSTEM REDUCTION TECHNIQUES

System Reduction techniques involves the combination or exclusion of some components available in the reference model. The two main methods commonly used to implement this aggregation technique are modal analysis [43, 44], and coherency based aggregation methods [45, 46]. In modal analysis, similar modes are combined while others that are not of interest are eliminated. However, this approach has two major downsides: it takes a lot of time, and it is purely mathematical in nature which means no structural identity. Thus, complex dynamics of the system cannot be properly captured following major disturbances.

Alternatively, coherency based method is classified as the more reliable process for system reduction. It identifies generators that exhibit coherent rotor angle swings and aggregates them as one generator. This is done through several methods such as the Zhukov's method and the Dimos method [47]. Other approaches such as pattern recognition and Lyapunov function etc. which are both linear models have also been applied to identify coherency. There are also well documented researches [48–51] of coherency identification which have been done without linearisation. Despite its preference, it is sometimes impossible to reduce some desired region of the system using coherency based method since it determines the regions that can be divided.

2.7.2. PARAMETER IDENTIFICATION TECHNIQUES

The system identification techniques involve using dataset derived at a boundary bus between the region of study in a system and the region to be reduced. This is the technique adopted for this research and the procedure to attain these data have been explained in Section 2.6.

Several methods have been deployed towards different identification problems. Trajectory sensitivity method and analysis was proposed in [52] to limit the amount of parameters considered in a composite model to the most significant ones. The study showed that some parameters have insignificant effect on the output and can be disregarded. It elaborated that including all parameters affects the variability of important ones which leads to inaccurate result. The analysis method was further extended to non-linear systems in [53] by applying a term selection approach. Furthermore, the Least absolute shrinkage and selection operator (Lasso) method was implemented to limit the count of parameters of a non-linear fifth-order IM model.

Other statistical methods that are well documented in literature include the least squares technique used to determine the IM model parameters in [54] and weighted least squares technique [55]. Weighted least square method was deployed to solve the high error variability effect by adding weights to each observation. However, it is difficult to assign proper weights and as a result, the algorithm becomes complex.

Meanwhile, the complexity of this load modelling technique is not limited to parameter identification but also the derivation of optimal values for the identified model parameters. In addition, optimization problem is usually formulated as a nonlinear, non-convex and multi-modal challenge. Consequently, further sophisticated optimization methods which are based on heuristics are proposed in many literature to resolve this issue. The well-established ones include Genetic Algorithms, (GA) [56, 57], Particle swarm optimization (PSO) [58, 59] and Levenberg–Marquardt algorithm [60].

Genetic Algorithm is a suitable method for dynamic load modelling as demonstrated in [61]. However, one of its major drawback is the high computational cost. Moreover, GA converges slowly because it explores wide search space rather than use neighbouring information to manoeuvre the best direction of search. Several versions of the algorithm which include population diversity-based GA (PDGA) [62] and adaptively adjusted GA [63] have been implemented in an attempt to improve its efficiency. The limitations of GA can be slightly improved by combining it with another technique that has better local search abilities. For instance, a form of hybrid algorithm was implemented in [64] where both Genetic Algorithm and Levenberg-Marquardt Algorithm were used for estimating the parameters of the composite load model which contained an IM component. Since the objective function used for load modelling optimization usually has multiple local minima [65], this combination was an attempt to upgrade the search capability of the algorithm. The Levenberg-Marquardt Algorithm has a good local search ability [60] while GA is reputable for its global search ability. Consequently, the convergence achieved was considerably more than the lone GA while the hybrid algorithm avoided being confined to a local optimum to which the distinct LMA would have been susceptible. However, the hybrid algorithm is still not fast enough due to the involvement of GA. Thus, a compromise between the cost of computation and its ability to search for global optimal solution is necessary. The complexity also increases due to the number of parameters to be heuristically determined.

In conclusion, Artificial Neural Networks (ANN) are the most predominant technique for optimization due to their intrinsic ability for modelling nonlinear systems [1]. Besides, they have been successfully implemented in many power system dynamics and stability applications [66–69]. The procedure is very suitable for dynamic load modelling because it does not require load composition information nor equivalent model structure. It adaptively adjusts and updates model parameters based on the measurement data gathered from the detailed model. Particularly, an ANN-based strategy was used to create a dynamic equivalence of an active distribution network

with many active DGs in [69]. Upon sufficiently training the ANN, it was able to replicate the behaviour of the main system and could interact with the retained part of the system. Accordingly, some impressive results have been reported on the application of Mean-Variance Mapping Optimization (MVMO) algorithm, a novel heuristic optimization algorithm, for identification of load modelling parameters [70, 71]. MVMO is a swarm intelligence based procedure with an enhanced search capability based on its incorporation of single parent-offspring technique which makes it suitable for real time applications. It exhibits exceptional convergence characteristics and an impressive performance with respect to the accuracy of the identified parameters [72]. Therefore, the MVMO algorithm is adopted in this thesis for parameter identification of the DE which is implemented in RTDS. A detailed description of the algorithm and its implementation in RSCAD-MATLAB is given in Chapter 5.

2.8. SUMMARY

This chapter presented the importance of load modelling in power system dynamics and stability studies. It highlighted the different types of load modelling methodologies and load models in existence based on the outcomes of an international survey on load modelling performed by CIGRE Work group C4.605. As previously stated, the survey results showed that static load models are still predominantly used, even for power system dynamic studies. Although, the results showed that about 30% of TSOs and utilities include some form of IM model to characterize dynamic loads. Nevertheless, the reports suggest that the count of dynamic load models currently implemented in actual studies is limited despite the variety of models in existence.

The concept of dynamic equivalence was explained and accompanied by the techniques used for aggregation of load models. According to the findings of the CIGRE work group, there are no aggregated load models for active distribution networks currently being used in practice by utilities. Admittedly, recommendations for dynamic equivalencing of ADN and micro-grids (MG) are in the most primitive stages and can mostly be referred from academic research. The report suggests the supplementary development of equivalent mathematical models for ADNs and MGs. These models should be able to adequately represent ADN for both steady-state and dynamic studies of medium and large power networks. Since some characteristics of ADN are difficult to represent using conventional dynamic equivalencing methods, the report suggests that system identification techniques should be exploited to tackle this challenge. Several parameter estimation techniques based on system identification have been proposed to derive appropriate aggregated models of complex power systems.

Furthermore, the structure of the dynamic equivalent that is adopted in this research was explained. This chapter also reviewed the two approaches used for determining load model data, i.e. the measurement and component-based approaches. This included their major advantages and disadvantages. Also, the two main techniques for determining DE parameters, system reduction and system identification techniques were discussed. The latter was adopted in this research by using the heuristic-based MVMO algorithm.

3

REAL TIME DIGITAL SIMULATOR

3.1. INTRODUCTION

Real Time Digital Simulator (RTDS) is a sophisticated hardware and software integrated computer system used to study Electromagnetic Transient (EMT) Phenomena in power system. As the name implies, it can perform power system simulations at computational speeds equal to those achieved during real-time operation. It is a commercially available system that is widely used by leading electrical power utilities, electrical equipment manufacturers and research institutions. The first application of the RTDS Simulator was to study the Nelson River Manitoba Hydro HVDC System. However, continuous improvement and development by RTDS Technologies has led to it being the world standard and benchmark tool for real-time digital power system simulation [73].

One of the main advantages of the RTDS is that it provides utilities with a safe and controlled platform to perform several tests and analyses. These analyses are usually for power system scenarios that seldom occur but are dangerous and very costly to incorporate in actual existing networks. Some areas of application of the RTDS by utilities and other electrical companies include pre-testing of new protection and control systems, Expansion Planning, Contingency and Reliability Analysis, HVDC and FACTS applications, Maintenance and Training [73]. The IEPG research group in the Electrical Engineering department at TU Delft is equipped with an RTDS Simulator similar to that shown in Figure 3.1. The module has 8-racks and a couple of them are simultaneously used for research within the MIGRATE project [74].

Figure 3.1: The RTDS Power System Simulator (www.rtds.com).

3.2. RTDS HARDWARE

RTDS employs high-speed Digital Signal Processor (DSP) chips and Reduced Instruction Set Computer (RISC) to achieve real-time computational speeds [75]. This is fostered by the utilization of cutting-edge parallel processing techniques. It is a modular system (cubicle) available in different sizes consisting of racks, DIN rails for input/output cards and power entry components. A rack is a 19-inch housing where RTDS processor cards and other cards are mounted as shown in Figure 3.2. Each rack is powered from a separate power supply installed at the bottom of the cubicle and delivers +5Vdc, +15Vdc and -15Vdc. However, their power switches are located on the front of the RTDS Cubicle's power panel. The cubicles have a reset button on the main power relay which must be pushed when AC supply voltage is restored. The Input/Output cards which are installed on the DIN rails enable the RTDS hardware to be interfaced with other equipment such as relays or controllers. They are powered by a 24Vdc, 100W power supply thus limiting their number.

3.2.1. GTWIF: GIGA TRANSCEIVER WORKSTATION INTERFACE CARD

This is the card responsible for communication between the parallel processing hardware and the host computer workstation. The connection is established via Ethernet LAN cable. The GTWIF card is usually installed on the far-right side of an RTDS rack. Its main functions are [75]:

1. Communication between the RTDS rack and the host PC running the RSCAD software. The link is established over an ethernet based LAN either connected directly to a computer workstation (for portable RTDS) or via an ethernet switch available in full size, mid-size and mini cubicles.

2. Facilitates data transfer with the computer workstation thereby enabling users to load, start and stop the simulation cases.

3. Communication with other racks participating in a simulation case. Each GTWIF card uses

its inter-rack communication channels to exchange data with up to six other racks while the simulation case is running.

4. Synchronization of racks for multi-rack simulation cases. This is done by the first rack in the simulation case which is designated as the master rack.
5. Communication of data between processors over the rack's backplane is coordinated by the GTWIF.
6. The GTWIF performs self-tests and runs diagnostics on other cards installed in its rack. The diagnostics are automatically run at power up and may be initiated by the user.

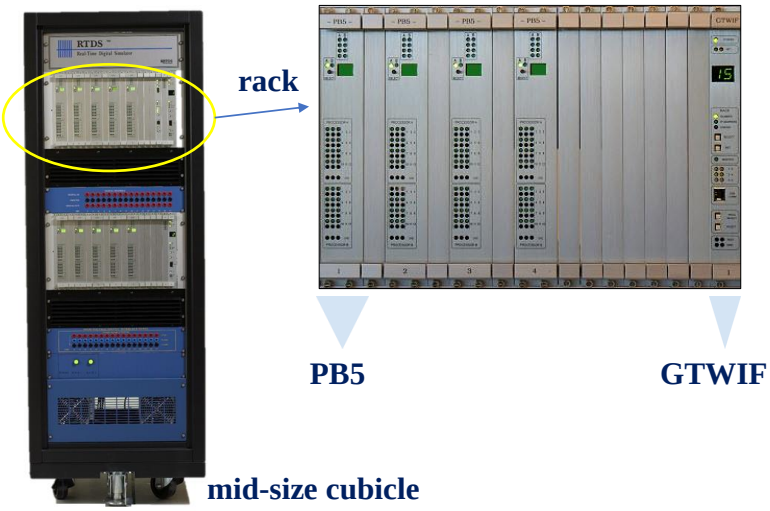

Figure 3.2: The RTDS Rack

3.2.2. PB5: PROCESSOR CARDS

The PB5 processor card shown in Figure 3.3 consists of 2 Power PC RISC processors, each running at 1.7 GHz. It utilizes communication ports for inter-processor data exchange. PB5 provides increased network solution and component modelling capabilities. A network solution processor is allowed only 72 nodes, thus a total of 144 nodes per PB5. However, a unique fiber enhanced backplane feature allows the number of nodes per processor to be increased to 90 implying a total of 180 nodes within a single rack [75].

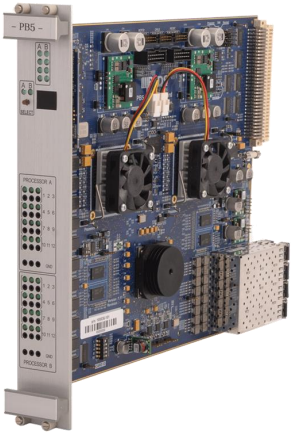

Figure 3.3: The RTDS PB5 processor card

3.2.3. GLOBAL BUS HUB

The Global Bus Hub (GBH) interface panel shown in Figure 3.4 is used to coordinate the operation of RTDS simulators consisting of 3 or more RTDS racks [75]. This is facilitated by connecting each rack to the GBH via a fibre optic cable available on their GTWIF card. If an RTDS simulator consists of only two racks, a direct connection is made between the optical ports on the GTWIF cards in the racks, therefore a GBH is not required. Usually, the GBH panel is placed in the rear of one of the RTDS cubicles. The configuration of the panel may include up to 3 hub cards. Each hub card can accommodate about 10 GTWIF cards. Therefore, a single GBH enables the interconnection of up to 30 racks. However, it is possible to ring 2 GBH panels, enabling a maximum of 60 interconnected racks.

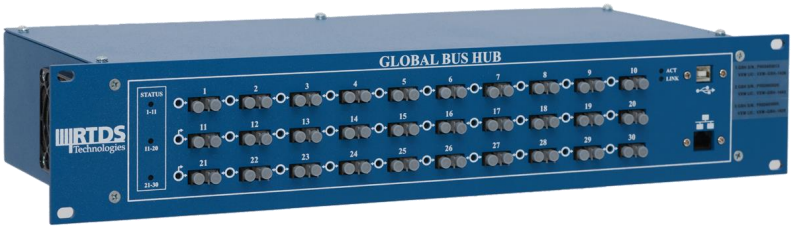

Figure 3.4: The RTDS Global Bus Hub

Furthermore, the GBH is configured to isolate consecutive racks which may be required for some simulation cases. This ensures that the remaining racks are available for other users to run simulations. For example, this thesis project initially required 3 racks out of the 8 racks available in the IEPG group. As such, the remaining 5 racks could be simultaneously used for other simulation cases. Multi-rack simulations of any combination are permitted by the GBH so long as the racks are consecutive [75]. Thus, an 8 rack RTDS is able to run 4 separate double rack cases and so on. Another important function of the GBH is the distribution of common timestep for all racks. The GTWIF in the first rack i.e. master rack assigned to a simulation case defines the timestep clock/signal and sends it via fibre optic connection to the GBH. This signal is then received by other racks i.e. slave racks involved in the simulation. Through the fibre optic link, racks also transfer other signals required for data synchronization and coordination of communication intervals to the GBH. The GBH can be accessed by RTDS software through its Ethernet LAN port located at the front of the panel. The Ethernet LAN parameters are initialized using a USB port also located at the front of the GBH. The GBH operation is configured by the software at the beginning of a simulation case, defining the master rack and number of slave racks required.

3.2.4. GIGA-TRANSCEIVER INPUT/OUTPUT (GTIO) CARDS

The GTIO cards are designed to interface analogue and digital signals between the RTDS Simulator and an external device. They are driven from the Giga-Transceiver (GT) optical ports available on the PB5 processor cards. Their connection is flexible and depending on the configuration, as many as 8 GTIO cards can be daisy-chained or connected to a GT port. A fibre optic cable with industry standard LC connectors is used as a link between the GTIO cards and the PB5. The link operates at 2Gbit/s bandwidth which allows the GTIO cards to be placed up to 35mm from the RTDS Simulator cubicles [75]. However, under normal configuration, they are mounted on DIN rails in the rear of the cubicle. There are four types of GTIO cards, two digital (GTDI and GTDO) and two analog (GTAI and GTAO) cards. These cards provide optically isolated input and output for connecting RTDS simulator to external devices.

3.3. RTDS SOFTWARE (RSCAD)

The RTDS Simulator has a state-of-the-art graphical user interface known as RSCAD. This interface includes several modules that are designed to enable the user to prepare, run and analyse simulation cases. The modules provide a communication platform between the user and the RTDS Simulator. These RSCAD modules are: FileManager, Draft, RunTime, TLine, Cable, MultiPlot, Convert and CBuilder [75].

3.3.1. FILE MANAGER

File Manager is the homepage of the RSCAD software from which all other modules can be launched. It facilitates the organisation of simulation projects and cases. Users can assess and share projects and cases within the Local Area Network depending on permission rights. Furthermore, it provides a link to a comprehensive manual set is provided as can be seen in Figure 3.5. The manuals include RTDS hardware manual, power and control system components manuals, tutorial manuals etc.

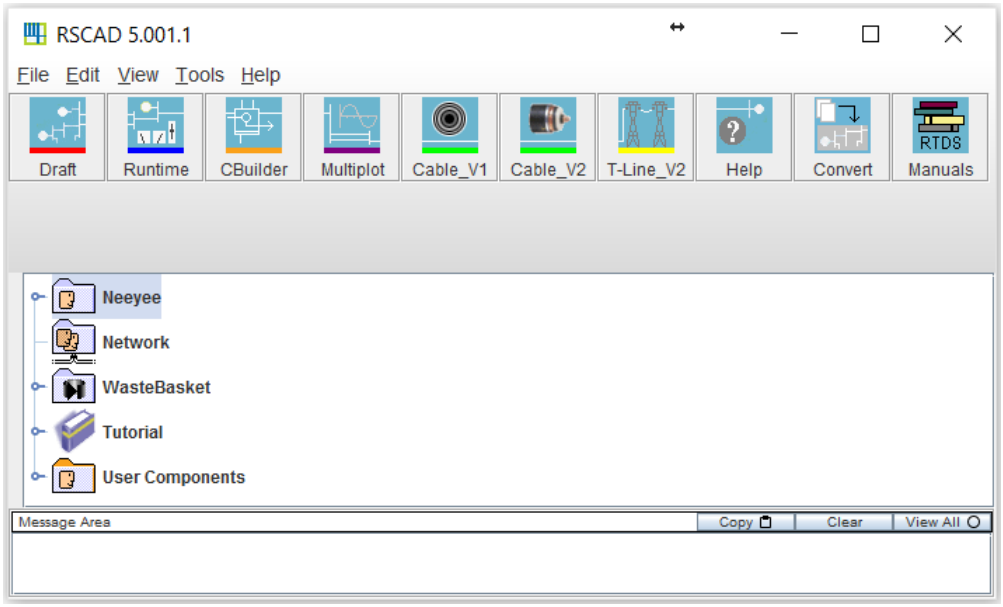

Figure 3.5: RSCAD File Manager module.

3.3.2. DRAFT

The RSCAD Draft module allows users to graphically assemble the circuit diagram of the system to be simulated. It contains on its right side, a comprehensive library of power system, control, protection and automation component models. Simulation circuits are created by simply copying the required component from the library and pasting it onto the window on the left side of the draft screen shown in Figure 3.6. A menu window is used to enter model parameters to customize their performance. After the circuit is completed, load flow calculations can be initialized, thus minimizing the start-up transient. Thereafter, the simulation case is compiled for the RTDS Simulator. The compilation process provides preliminary error checking of simulation components and parameters as well as creates the execution code for the simulator hardware. Furthermore, the draft module offers advanced features such as the single line diagram (SLD) format which allows users to toggle between single line and three-phase formats. The SLD view is easier to understand while the three-phase view allows for implementing more details such as unsymmetrical loading. For larger systems, it is also possible to collapse some parts into hierarchy boxes.

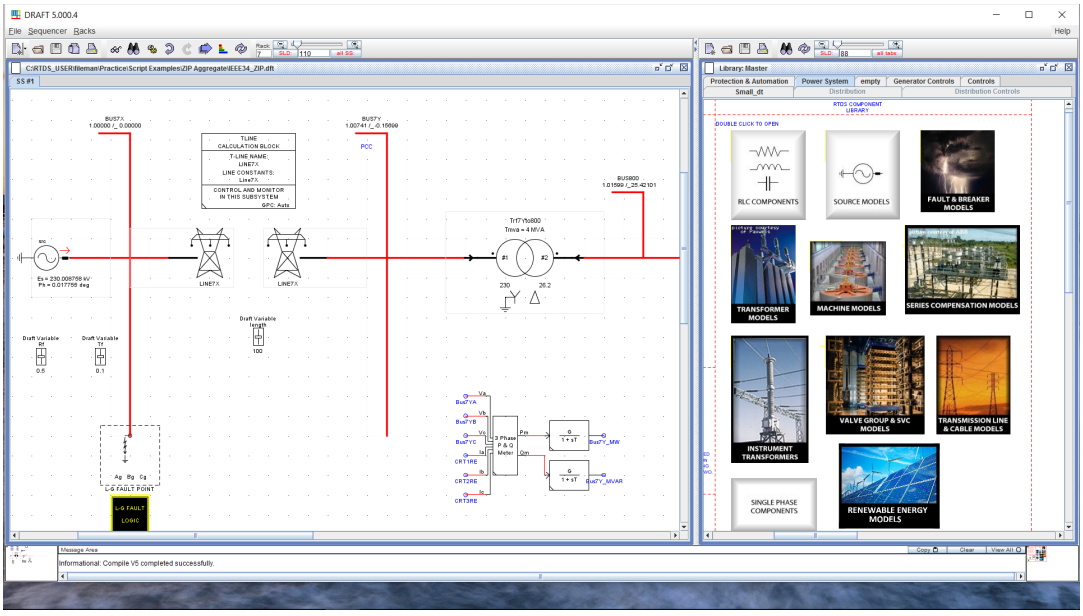

Figure 3.6: RSCAD Draft module.

RTDS LIBRARY

The right side of the draft module shown in Figure 3.6 contains the comprehensive RSCAD library. It includes power system, control system, protection and automation, and small time-step components libraries which can be used to build the desired simulation circuit. The Power System Component Library shown in Figure 3.7a contains models of most of the common equipment available nowadays in power systems. Examples of such models include: voltage and current sources, synchronous and induction machines, transmission lines, instrument transformers, HVDC, FACTS, filters, passive components (resistors, inductors, and capacitors), breakers, etc. The Control system component library shown in Figure 3.7b contains individual and composite control blocks used to interact with the power system model and other external programs. The control models are available as specialised group of components. These groups include maths functions, constants, data conversion, generator controls, logic functions, meters, signal processing, etc.

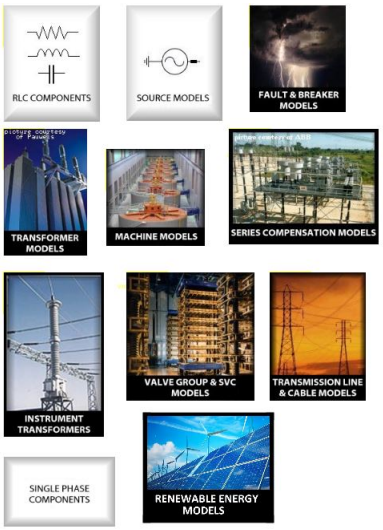

(a) Power system library

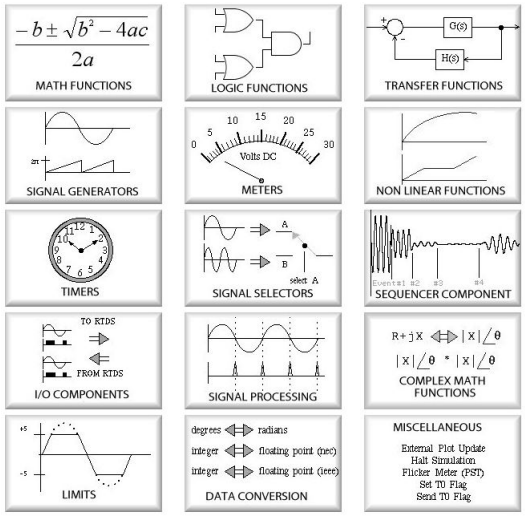

(b) Control system library

Figure 3.7: RSCAD Power system and Control system libraries.

3.3.3. RUNTIME

The Runtime module shown in Figure 3.8 ensures that the loading, controlling and running of the simulations is done entirely on the host computer. The Runtime software communicates with the GTWIF card's real-time operating system to exchange messages associated with plot updates and user initiated events. It serves as the Operator's Console because it is the platform through which the user interacts with the real-time simulation. The user can customize and adjust parameters through components like sliders, switches, buttons, dials, meters, plots, etc. while the simulation is in progress. These components can be placed in groups and minimized for better navigation of the platform. Timestamps, texts and annotations can also be included to aid the documentation of results. Plot data can be saved for further processing in Multiplot or in external software such as MS Excel or Matlab. Plots are automatically updated when the user interacts with the simulation. The plots can also be used directly in reports by saving them in different formats such as JPEG, PDF, COMTRADE and EMF format. Additionally, simulations can be run without user interference in a process called Automated batch operation. Users can create a script file to perform a sequence of events such as starting/stopping simulation cases, initiating events, changing set points including draft variables, saving results, etc. Script files can be created by using a record and replay feature or through an editor available in Runtime or on an external program like Matlab. Section 5.4 explains in more details how scripting was used in this research work.

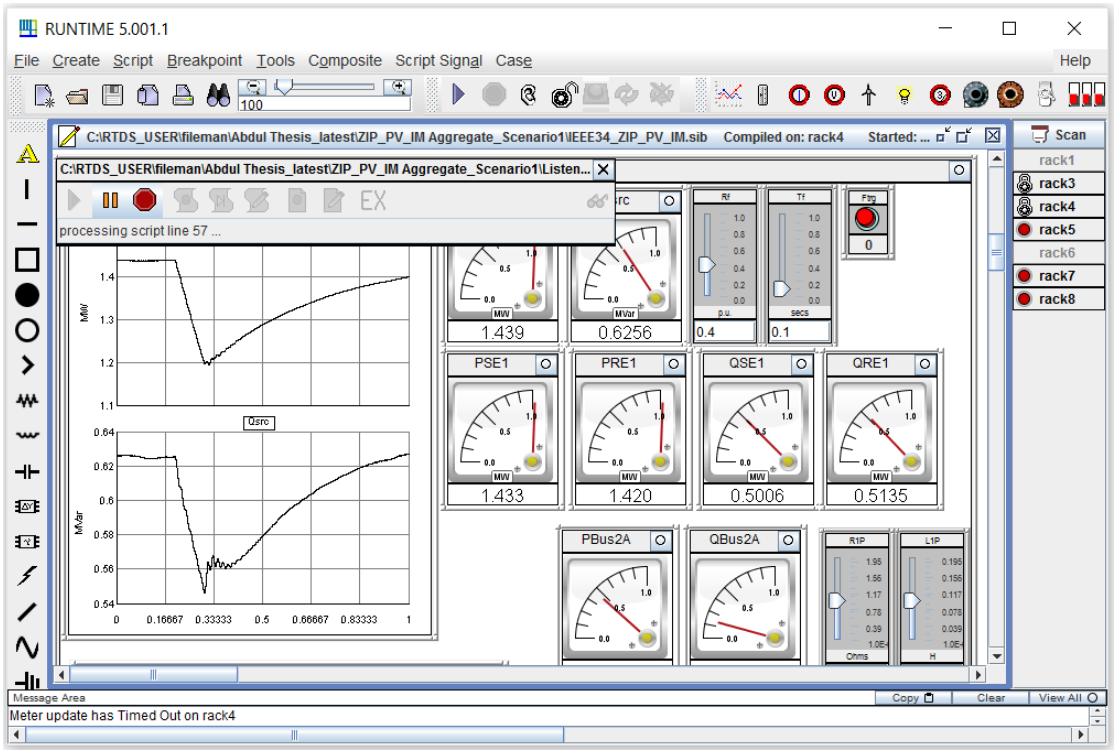

Figure 3.8: RSCAD Runtime module.

3.3.4. TLINE

The RSCAD TLine module is used to generate physical AC and DC transmission line data which is converted to a form usable in the Draft module. Generally, transmission lines are modelled using travelling wave algorithms within the RTDS [73]. The travelling wave models are distributed parameter representations of these lines. However, if the line is shorter than 15km which corresponds to a simulation time-step of 50 μsec, it is modelled using lumped R-L-C components assembled as a PI-circuit. The file containing the transmission line data must be specified in the

travelling wave transmission line component available in Draft.

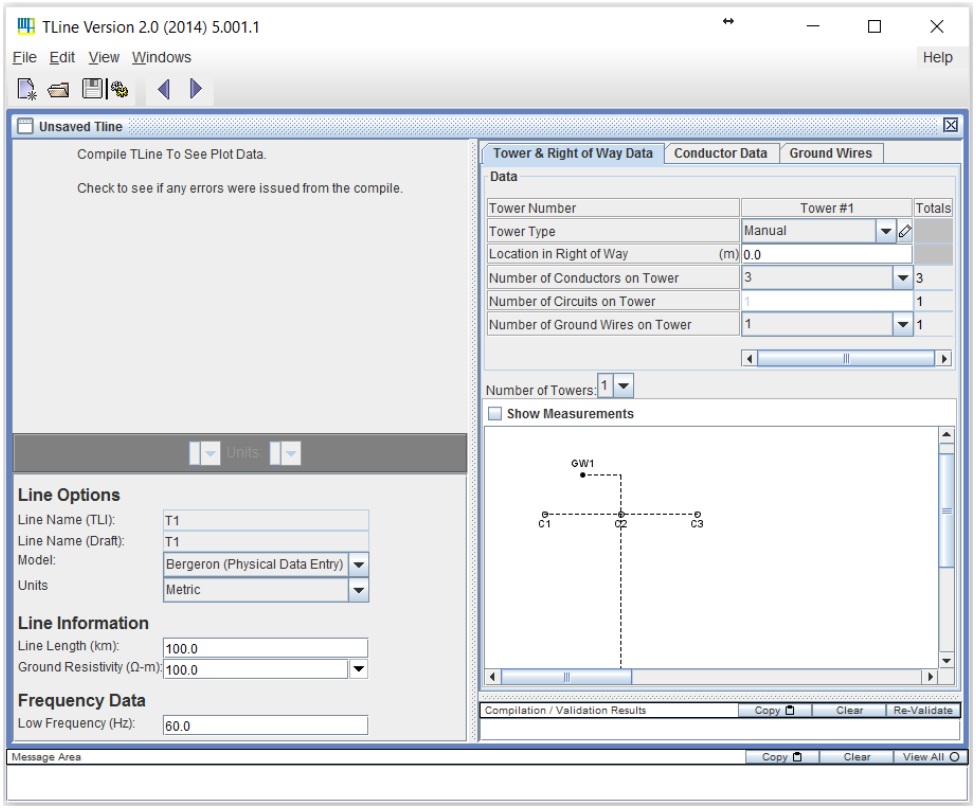

Figure 3.9: RSCAD TLine module.

The data for the commonly available Bergeron and frequency dependent travelling wave models can be calculated using the conductors' physical characteristics and their location relative to each other and earth as shown in Figure 3.9. Alternatively, the positive and zero sequence impedances can be used to generate these data.

3.3.5. CABLE

Like the TLine module, the RSCAD Cable module provides the conversion of physical cable data into a form usable in the Draft module. Cables can be modelled using travelling wave models or equivalent PI sections. Also, parameters for both Bergeron and frequency dependent models can be generated.

3.3.6. CONVERT

The Convert module is a special feature of RSCAD that allows the conversion of simulation files from PSS/E and MATLAB Simulink to RSCAD [75]. The conversion program takes load flow description (.raw), dynamic data (.dyr), and the sequence data file (.seq) which are input text files for the PSS/e program and produces graphical output files that are readable in the RSCAD Draft module. A screenshot of the module is shown in Figure 3.10. Simulink control models can be imported into RSCAD library through the Component Builder module discussed in the next section. This is facilitated by MATLAB's embedded coder which allows the model to be translated to C code for generating the CBuilder component.

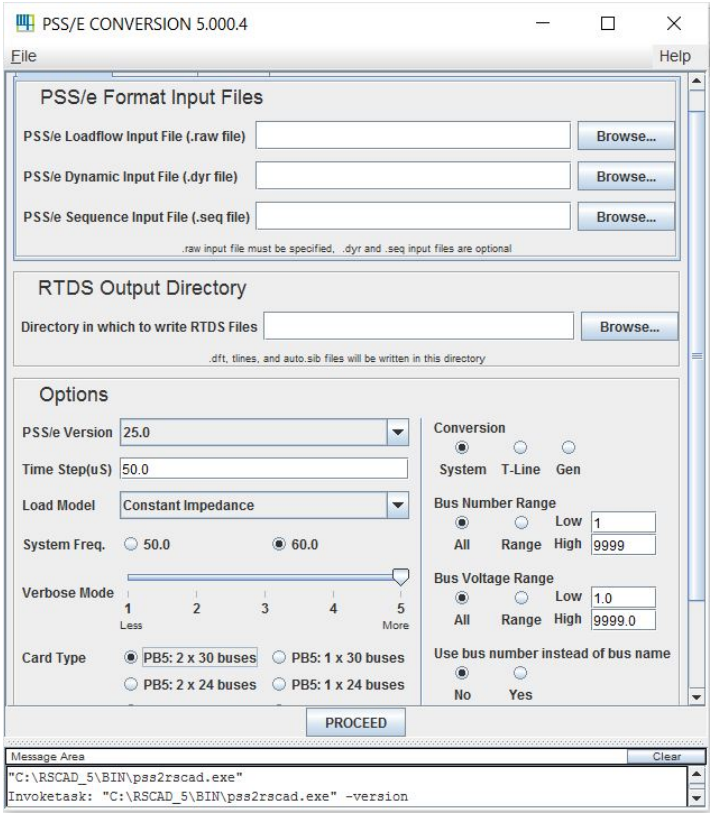

Figure 3.10: RSCAD Convert module.

3.3.7. CBUILDER

The RSCAD Component Builder (CBuilder) module facilitates the creation of customized components occasionally required by advanced users to be run on the RTDS Simulator. In this environment, users can draw the icon for new power system or control components as shown in Figure 3.11. Additionally, users can define the parameters, the input/output nodes and write the associating code. The code for CBuilder components is based on ANSI C. However, models built using the CBuilder can only run on PB5/GPC cards.

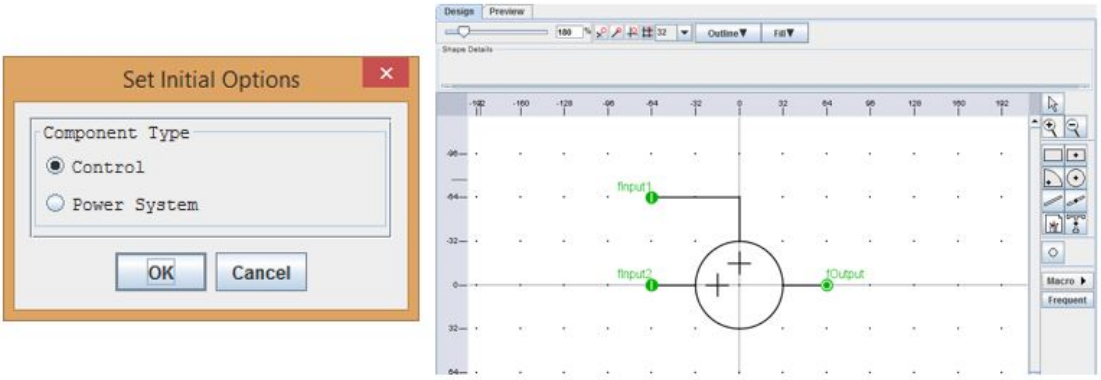

Figure 3.11: RSCAD CBuilder module.

3.3.8. MULTIPLOT

The Multiplot module shown in Figure 3.12 is used for post-processing, analysis and printing of results captured from the RTDS Simulator. It contains advanced data analysis, conditioning, and plotting functions. Data can also be exported for post processing in other application software (Matlab, Excel, etc.).

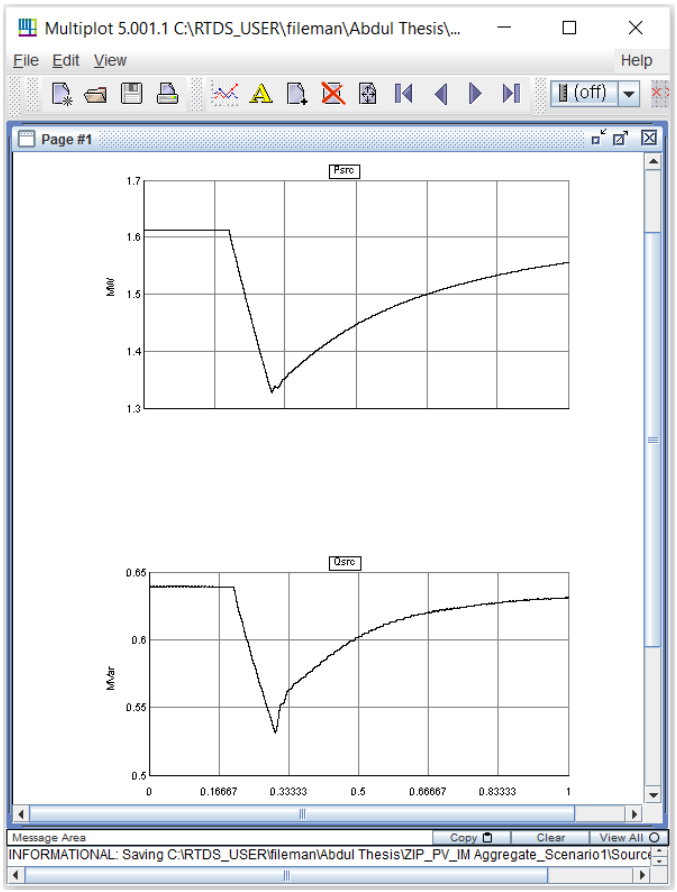

Figure 3.12: RSCAD Multiplot module.

3.4. RTDS OPERATION

For the RTDS to properly function, both the hardware and its software, RSCAD, must be properly set up and installed on a computer workstation respectively. A LAN communication is then established between the computer and the RTDS to allow the use to communicate with the simulator. As previously explained, RSCAD contains precise power system component models which are essential for representing various elements that are available in real power systems. Also, RTDS employs the nodal analysis technique to provide network solutions based on Dommel's solution algorithm introduced in [76]. This algorithm is used in almost all digital simulation software designed for the study of electromagnetic transients [75].

There are some simple steps required to prepare and run any new or existing simulation case, which may represent either a simple circuit or complex power system. These steps are as follows:

1. Start the RSCAD Software
2. Create new Project and Case directories in the File Manager module.
3. Start the RSCAD/Draft module

4. Create the new power system model and specify the starting rack number
5. Compile the new model from RSCAD/Draft
6. Run the simulation case using RSCAD/RunTime module
7. Plot and analyse simulation results using RSCAD/MultiPlot

The following sections seek to provide insight into some aspects of the simulation procedure in RTDS that a user should be cognisant with based on information in the RTDS Tutorial Manuals [75].

3.4.1. NODES

The point of connection between two power system component is known as a node. In RTDS, a node is a single-phase entity and is usually mathematically absorbed wherever possible due to its limited availability per processor. The maximum number of nodes per network solution on the PB5 processor card is 90 single-phase nodes (30 three-phase buses). However, a unique feature of the PB5 processor card is its ability to support dual network solutions (i.e. two subsystems) in a single rack. Therefore, the maximum number of nodes per rack is doubled to 180 (i.e. 2 x 90).

3.4.2. SIMULATION TIME STEP

The computation of the state of a power system network is done at integral instants of time. Node voltages and branch currents at any moment are dependent on their values from previous timesteps. Hence, it is important to select an appropriate simulation time step while preparing a new case to adequately represent real time quantities. The RTDS, through its parallel processing capability, must be able to solve all the equations representing the power system model within the user specified time step. The typical time steps for studies performed on RTDS or similar EMTP type simulations are in the range of 50 microseconds. However, such time steps are too high to accurately simulate high frequency switching circuits such as power electronic converters. To resolve this, RSCAD has a feature known as small time step simulation which employs several techniques to reduce the time step to a range of 1 to 2.5 microseconds. Overall, the complexity of the circuit to be simulated determines the actual time-step that would be used.

3.4.3. SUBSYSTEMS

The concept of subsystems is a very vital one in RTDS and other Electromagnetic Transients (EMT) Software. A subsystem is a decoupled portion of a power system model which is mathematically isolated from other portions of the system and can be solved independently. Subsystems are normally created using travelling wave transmission lines or cables whose length should be greater than 15km because of the typical RTDS timestep of 50μs. They can also be created using subsystem splitting transformer available in the RSCAD library. Due to the time required to solve a network with many nodes, splitting a system into two considerably reduces the computation time; moreover, subsystems can be solved in parallel. However, it is not necessary to split a model into subsystems if it fits onto a single rack of RTDS and has sufficient nodes. There can be more than one subsystem on a rack but a single subsystem cannot exceed one rack. Therefore, each rack usually corresponds to one RSCAD/Draft page.

3.5. POWER COMPONENT MODELS IN RTDS

There are several components in the RSCAD power system component library. This section covers a few of them which are directed related to this thesis.

3.5.1. SOURCE MODEL

RSCAD/Draft offers both single and three phase equivalent source models which can simulate infinite bus voltage signals behind a defined system impedance. The single-phase models can simulate purely sinusoidal ac, ac with superimposed harmonics, ac modulated and dc waveforms while the three phase models normally represent a balanced sinusoidal three-phase infinite bus voltage behind a specified impedance. For three phase models, the user can select individual positive and zero sequence impedance circuits. The positive sequence impedance circuit has four different configurations, R, L, R//L and R-R//L. One of them must be selected during the Draft session from the source configuration window shown in Figure 3.13. The voltage magnitude and other parameters such as frequency, phase angle, source impedance etc. of the source models can be dynamically varied using sliders created in the RSCAD/Runtime module while the simulations is running.

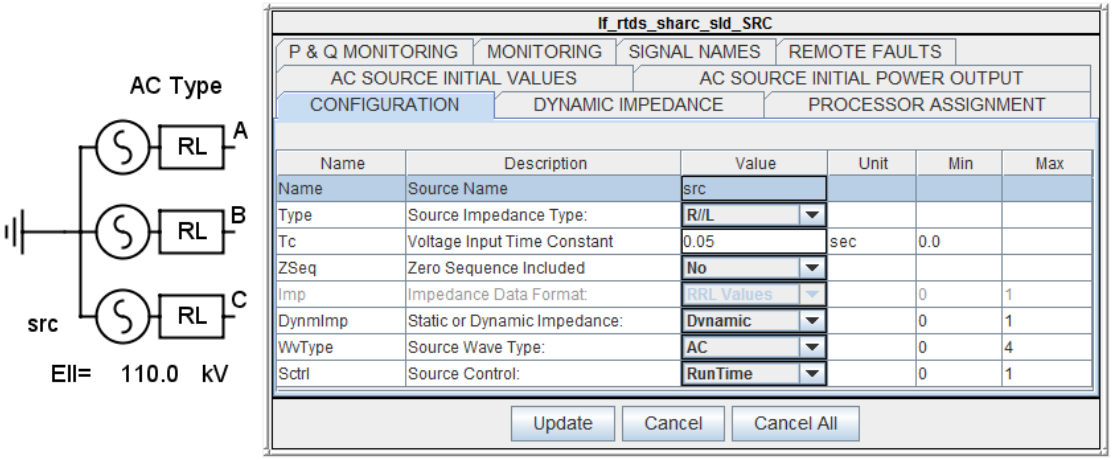

Figure 3.13: Three-phase source model

Furthermore, an internal fault can be simulated behind the source impedance by creating a sudden but timed reduction of the source voltage. The duration of the reduction and its magnitude can be defined through the remote fault tab on the configuration menu in Figure 3.13. The simulation of the internal fault can be repeated in RSCAD/Runtime using the push button component. A sequence of event which involves the push button can also be defined through a script as implemented in this thesis (see section 5.4.1).

3.5.2. TRANSFORMER MODEL

RTDS has different types of transformers which can be selected based on the intended application. However, only the power transformers and not measurement transformers are discussed further. The transformer models can represent either two or three winding configurations. Currently, the power system component library includes a single-phase two winding transformer model and three-phase two and three winding auto transformer models. The winding of the three phase transformers can be connected in either delta, wye-grounded or wye-ungrounded based on the user's selection in the transformer configuration menu shown in Figure 3.14. Furthermore, the three-phase two winding transformer can be modelled using any of three options: ideal, linear or saturating transformer.

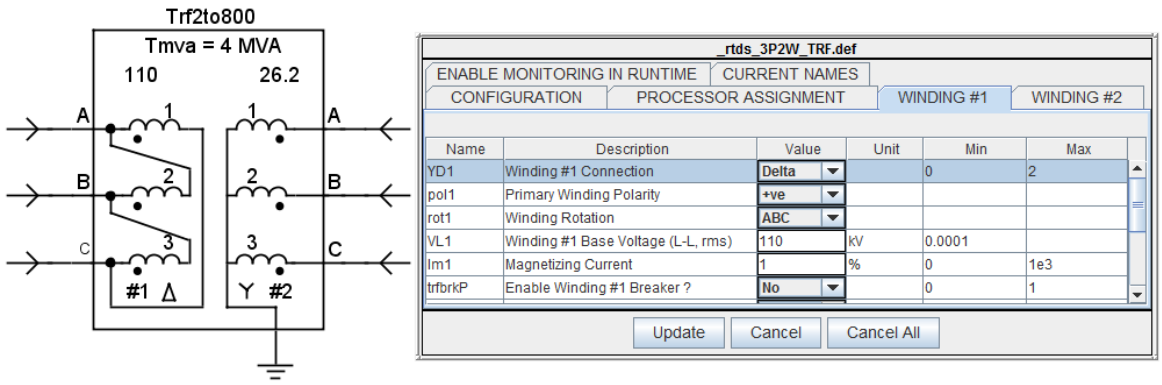

Figure 3.14: Transformer model configuration menu

Any of these options can be chosen in the transformer configuration menu. If the type option which determines whether the saturation and hysteresis feature is enabled is set to 'Yes', then the transformer is modelled as ideal. This means that no magnetizing inductance is included but only the stated leakage reactance. Otherwise, a magnetizing branch with the leakage reactance would be defined to represent a non-ideal transformer. Other items that can be configured in the usual manner through several menus are the ratings (in MVA), winding configuration (either wye or delta), number of coupled windings, leakage impedances, magnetizing currents, tap changers etc.

3.5.3. TRANSMISSION LINE MODEL

Transmission lines can be represented in RTDS either by travelling wave transmission line or PI section models as shown in 3.15. The former is preferred because they offer better accuracy due to their distributed parameter representation of long transmission lines and require lesser simulator hardware. In other words, travelling wave models need only one or two processors to represent an entire line with about 12 mutually coupled conductors unlike the PI section models which would require more due to their lumped parameter representation. Several PI sections have to be cascaded to represent a line while the nodes between each section also need to be modelled. However, for short transmission lines (less than 15km), the PI section model must be used. This is due to the calculation algorithm of the travelling wave model which limits the length of line to be represented. For the usual timestep of 50μs and assuming wave propagation velocity is at the speed of light, the waveform would travel approximately 15km. Therefore, lines that are less than 15km should be represented using a PI section. Moreover, as the length of lines reduces, so does the effect of approximations derived from using the PI section.

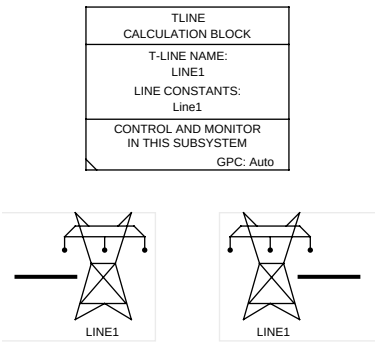

(a) Travelling wave model

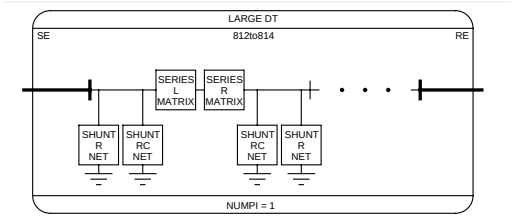

(b) PI section model

Figure 3.15: Transmission line models

In RSCAD, the TLINE module is used to define the line geometry, configuration and other relevant parameters. The output of the module (i.e. a .tlo file), which must be in the same simulation case folder, is used by the Draft module upon compilation of a case containing the line. As mentioned earlier, travelling wave line models are also used to split large power systems into mathematically isolated subsystems. In this thesis, both the PI section made up of R, L and C components and travelling wave transmission line models were used. The travelling wave model was used to connect the external grid to the distribution system and to split the overall system into two subsystems. Figure 3.15a shows the representation of the travelling wave model in Draft module. The distribution lines of the reference detailed model (see Chapter 4) were however represented using PI sections due to their length. Figure 3.15b shows the representation of the PI section model.

3.5.4. LOAD MODEL

Dynamic single phase and three phase load models exist in RSCAD power system component library to represent different loads in the power network. The dynamic models can be used to adjust the load to maintain real and reactive power set points using a variable conductance [75]. The load can be connected either in wye or delta configuration and modelled as series resistance and reactance (R-X) or parallel (R//X) connection. The power set points can be controlled using either sliders, control components or ZIP components through the '*cc*' option in the load model configuration menu shown in Figure 3.16. When Slider is selected, the P and Q set points are initialized with the corresponding sliders in RSCAD/Runtime module. However, if the '*cc*' parameter is set to ZIP component, the load computations are based on the percentages of the load which is constant power (PP, QP parameters), constant impedance (ZP, ZQ parameters) and constant current (IP, IQ parameters). When '*CC*' is chosen, the power set points can be adjusted through control input wires connected to other control components such as the exponential load computation blocks. Finally, the load can be modelled as a constant impedance by selecting 'ConstZ' option thus implying the load is not dynamic.

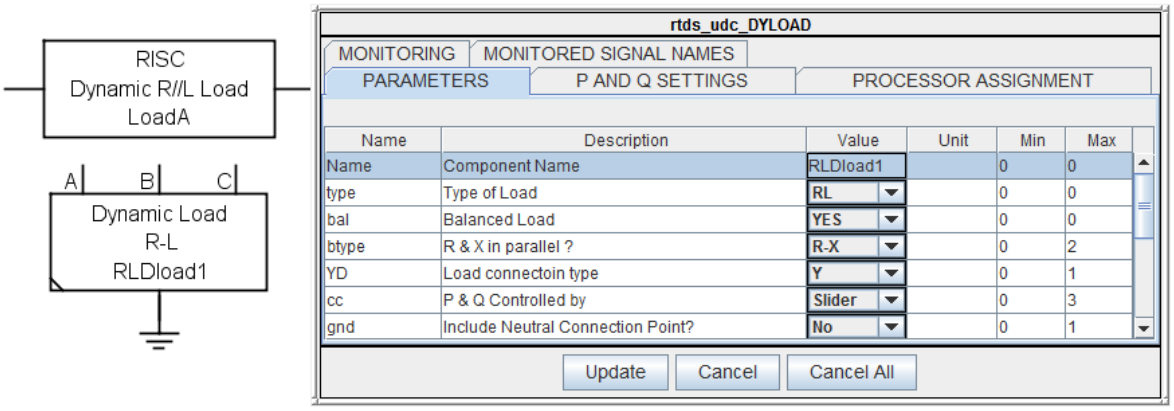

Figure 3.16: Load Model Configuration menu

4

MODELLING OF DETAILED AND DE SYSTEM IN RTDS

4.1. INTRODUCTION

This chapter presents the models of the detailed network and the dynamic equivalent from which the test cases for this research were implemented. For conducting load model analysis and implementing an aggregated model, a suitable distribution system that already exists was necessary on which comprehensive analysis can be performed. The system adapted is a well-known IEEE 34 Bus system, an actual distribution system in Arizona, and a test system provided by the IEEE Power Engineering Society [77]. The distribution feeder has a variety of components including distributed and spot loads which makes it an ideal system for this research. On the other hand, the transmission system was represented as an external grid due to the limited amount of racks available and the computation effort required to scale up the distribution system. Meanwhile, to accommodate the recent integration of distributed generation (DG) in the low and medium voltage grid levels, the IEEE 34 Bus test system was modified to include renewable energy sources. Hence, the distribution system was transformed from a passive network to an active network where the power flow is bi-directional.

4.2. IEEE 34-BUS SYSTEM

The IEEE 34-bus test system, shown in Figure A is one out of five benchmark distribution feeders published by the Distribution Subcommittee of the IEEE Power Engineering Society. It represents an actual feeder located in Arizona, USA. It is a lightly loaded and unbalanced system with uneven load distribution. The feeder operates at a voltage level of 24.9kV and the has nineteen distributed loads combined with six three-phase spot loads which sum up to 1.769MW/1.04MVar. These loads are specified as either delta or wye loads and are modelled as constant impedance (Z), constant current (I), and constant power (PQ) loads. The parameters and configurations of the feeder are available in Appendix A and published in [77] with the power flow results. Besides, the network elements available on the test feeder include a substation transformer, an in-line transformer, voltage regulators, shunt capacitors, overhead distribution lines of several configurations and loads. These network elements were modelled in RTDS using components from the power system, controls and generator controls libraries in RSCAD already explained in Chapter 3. However, due to the length of the distribution lines, they were modelled using approximate pi-model rather than the travelling wave which requires a minimum of 15km.

4.3. MODIFIED IEEE 34-BUS SYSTEM

To create an active distribution system for representing recent and future grids (and for reference data generation), a bi-directional power flow system must be achieved. Therefore, for the test cases used in this thesis, the IEEE 34-bus test feeder was modified to include distributed generators i.e. three PV modules at different nodes, thus representing an active distribution system. These PV generators supply about 0.4MW each. The modified network which is also the first test case is shown in Figure 4.1. Only PV modules were considered to represent power electronic interfaced based DG due to the number of racks available for this thesis. In addition, induction motors were also added at a few nodes to increase the contribution of dynamic loads in the detailed reference model. The results from disturbances applied to this modified IEEE 34 Bus system provide a benchmark for validating the proposed dynamic equivalent model. Furthermore, the generation of simulated data required for the estimating the parameters of the equivalent model using MVMO algorithm is discussed in detail.

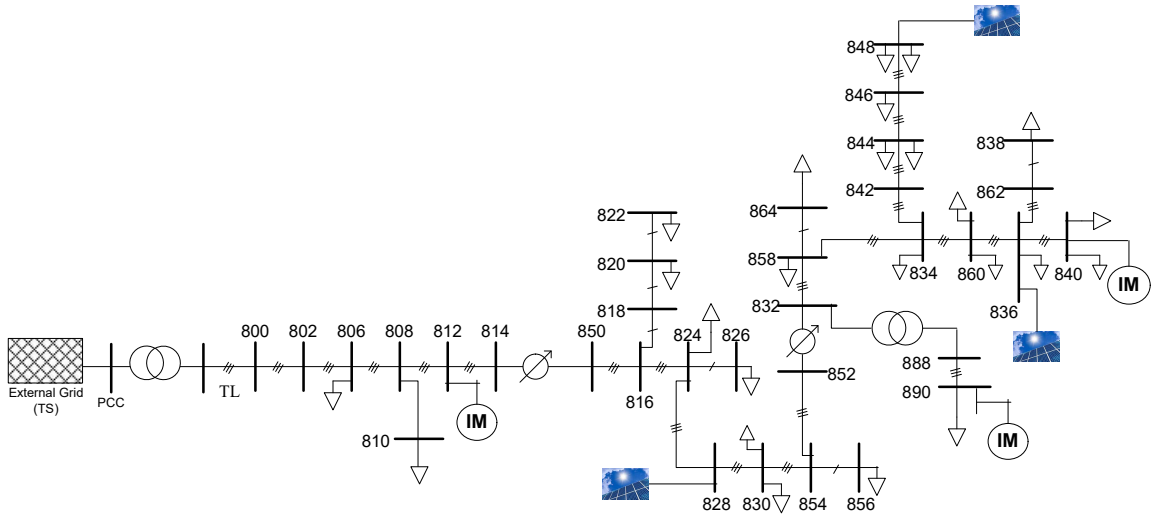

Figure 4.1: Modified IEEE 34 Bus system

4.3.1. EXTERNAL GRID MODEL

The external grid represents the transmission system and was modelled using a three-phase source model available in the RSCAD library. It operates at a voltage of 110kV and was connected to the IEEE 34-Bus distribution system using a delta-wye step down transformer and a 120km transmission line. The source impedance type used was a resistor in parallel with an inductor whose values are 1Ω and 0.1H respectively. Furthermore, the high voltage side of the connecting transformer was used as the point of common coupling between the transmission and distribution system. However, the source model has a feature which allows the user to monitor the active and reactive power at the source terminal. Hence it was used as the point of collecting the simulated data for validating the dynamic equivalent load model. The transmission line was modelled using the travelling wave transmission line model on the TLINE module which was previously explained in section 3.5.3.

4.3.2. PV MODEL

Solar energy development has recently surged due to advancement in electronic power conversion technologies and the world's push towards addressing climate change and other environmental issues. Grid-connected photovoltaic systems is gradually becoming a major contributor to the energy mix, so it is important to consider their characteristics while modelling a distribution grid.

A block diagram of the PV system model which was added to different buses on the IEEE 34-Bus distribution network and also used to represent the aggregate power electronic interfaced generation in the RSCAD/Draft environment is shown in Figure 4.2. The main components of the PV system are a solar array, electronic power converter with its controllers, and a grid interfacing transformer.

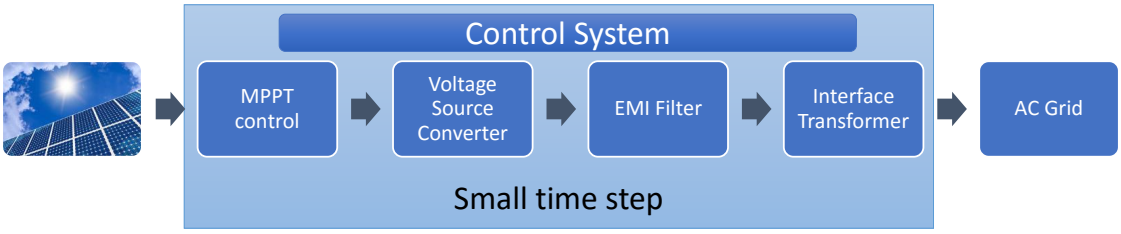

Figure 4.2: Block diagram of PV System Model

PV ARRAY

A solar cell is the fundamental component of a PV array which converts solar energy to electric energy due to photovoltaic effect. Solar cells are made from semiconductor materials of which silicon is the most commonly used. A simple silicon solar cell produces a relatively small voltage of about 0.7 V. To attain higher voltage and current levels, solar cells are connected in series and in parallel to form PV modules, which produce about 16V to 36V with a few watts of power. However, for practical applications, PV modules are connected in series and parallel to form PV arrays which produce large amounts of voltage (kV) and current (kA). Figure 4.3a shows the description of the PV array as formed from a solar cell.

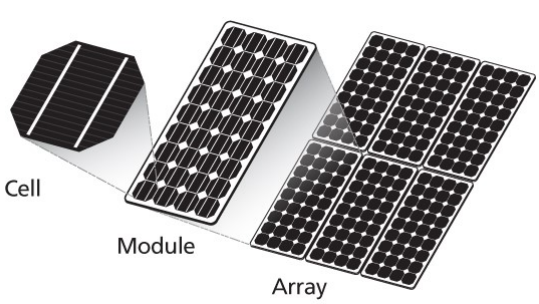

(a) PV array

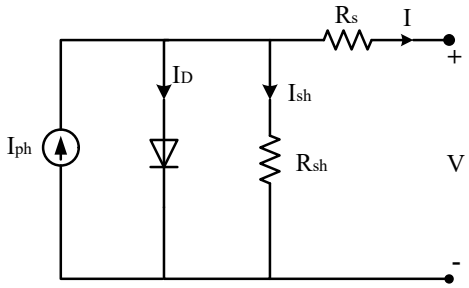

(b) Practical model of a solar cell

Figure 4.3: Description of a Solar cell

The typical behaviour of a solar cell can be represented by an equivalent circuit which includes a diode, a series and shunt resistance as shown in Figure 4.3b. The mathematical model of a PV cell which describes its current-voltage relationship is given by equations 4.1 and 4.2.

$$I = I_{ph} - I_D - I_{sh} \tag{4.1}$$

$$I = I_{ph} - I_o\left(exp\left(\frac{V + R_s I}{n_s a V_t}\right) - 1\right) - \left(\frac{V + R_s I}{R_{sh}}\right) \tag{4.2}$$

$$V_t = \frac{kT}{q} \tag{4.3}$$

Where,
I_{ph} is the photo-current induced by the incidence light on the PV cell and depends on the cell size, semiconductor material, insolation G (W/m2) and temperature T (K) while I_D is the total diffusion current through the diode. I_o is the diode reverse saturation current, a is the diode ideality factor which measures the closeness of the diode to being ideal. R_s is the series resistance which is the sum of structural resistances in the PV cell while R_{sh} is the leakage current of the p-n junction of the semiconductor material [78]. ns is the number of PV cells connected in series. V_t is the diode thermal potential difference which is dependent on temperature T (in K) as described in equation 4.3. Where k is the Boltzmann constant ($1.38x10^{-23}J/K$) and q is the magnitude of an electron charge ($1.602x10^{-19}C$). Furthermore, the standard test condition (stc) for solar irradiance is usually $G_{stc} = 1000W/m^2$ at a temperature, $T_{stc} = 25°C$. Further details about the PV cell model and how its complexity can be reduced are well documented in [78].

RSCAD/Draft contains a PV array model shown in Figure 4.4 which can be configured by the user to the desired number of modules in series and parallel to produce an appropriate power output. The parameters of the PV array modelled in this thesis are given in Table 4.1. The model takes the insolation (Watts/m^2) and temperature (°C) as inputs and provides the positive and negative DC node voltages VDC_p and VDC_n as outputs. Under simulation circumstances, the PV array characteristics is simply approximated as the superposition of the characteristics of the PV modules. Therefore, the array output voltage is the number of parallel modules multiplied by the module output voltage while its output current is the number of modules connected in series multiplied by the module output current [79].

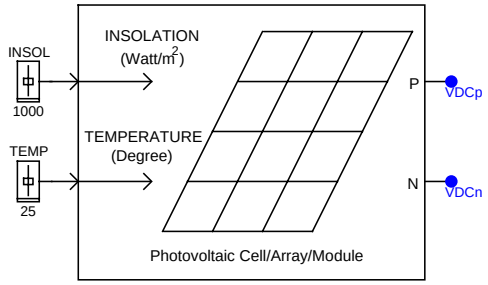

Figure 4.4: PV array model in RSCAD component library

Table 4.1: PV Array Parameters

Voc_stc	21.7 V
Isc_stc	3.35 A
Vm_stc	17.4 V
Im_stc	3.05 A
Ki	0.065 %/°C
Eg	1.11eV
Prated	1.74 MW
Ncs	36
Ncp	1
Ns	115
Np	285

PV System Power Converters

To connect PV arrays to the grid, power converters whose function is to convert the PV output DC power to meet the requirements of the AC grid are required. There are two main topologies, single-stage or dual-stage converter topology, through which PV arrays can be interfaced with the grid. These are shown in Figure 4.5.

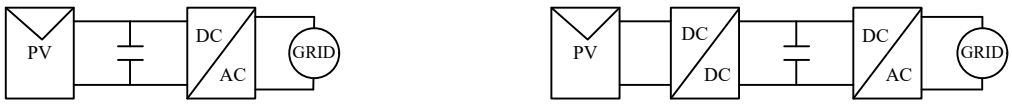

(a) Single stage (b) Dual stage

Figure 4.5: PV converter topology

The structure of the single stage topology is simpler and provides a higher power efficiency than the dual stage. Its control system is however more complex than the dual stage as the DC/AC inverter solely ensures maximum power transfer from the PV array to the grid [80]. Due to the inverter's efficiency, the DC-side voltage is about 1.63 times more than the AC-side under normal operation. In this thesis, the single stage grid connected system shown in Figure 4.6 was adopted as implemented in [81]. The system uses a DC capacitor to limit the oscillations on the DC voltage. The Voltage Source Converter (VSC) controls the DC link voltage and active power supply to the grid and also ensures grid synchronization. A delta-wye transformer steps up the VSC AC-side voltage to grid level voltage and reduces harmonic current injection to the grid. Capacitor filters and interface reactors are placed at the point of common coupling (PCC) between the VSC and the grid to further minimize the converter harmonics injected to the grid [82].

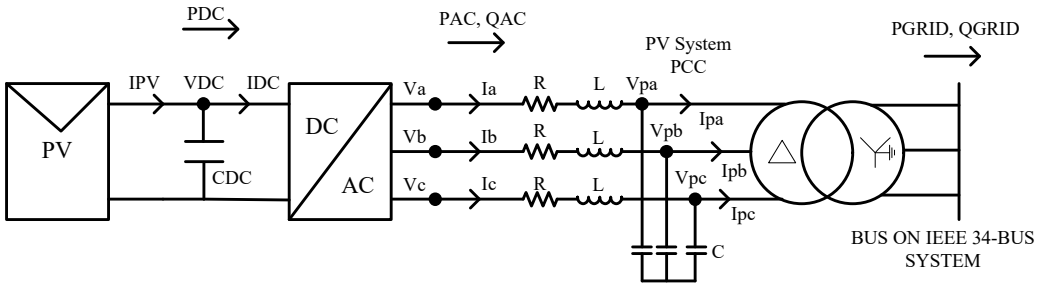

Figure 4.6: Single-Stage, Grid-connected PV system

Many DC/AC converter topologies can be used to interface PV arrays to the grid. Frequently used among them is the two-level voltage source converter (VSC) shown in Figure 4.7. The three phase VSC has three legs, each containing two valves made of insulated-gate bipolar transistor (IGBT) semiconductor switching device in parallel with a diode. Each of the VSC legs is connected to one phase of the grid which can adopt either of two voltage levels, $+V_{DC}$ or $-V_{DC}$ [82]. The AC side phase voltage is positive when the top switches are ON and negative when the bottom ones are ON relative to the DC side mid-point [82].

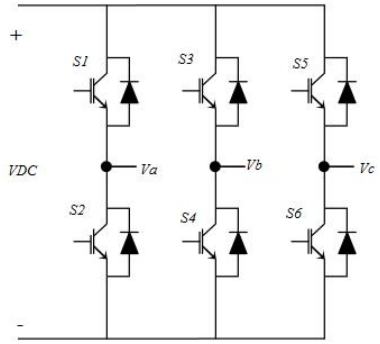

Figure 4.7: 3-phase, 2-level Voltage Source Converter

Sinusoidal pulse width modulation (SPWM) is used for switching the six valves of the VSC due to its minimized lower order harmonics and simplicity [83]. SPWM involves the comparison of a high frequency triangular carrier wave with a low frequency sinusoidal modulation signal to generate firing pulses for controlling the switching procedure of each valve. This leads to the generation of the output voltage waveforms. The magnitude of the output voltage and its harmonic content depend on the frequency modulation index, m_f, and the amplitude modulation index, m [83]. m_f is the ratio of frequency of the carrier signal to the frequency of the modulation signal as given in equation 4.4 while m is the ratio of the amplitude of the modulating signal, A_m, to the amplitude of the carrier signal, A_c given in equation 4.5. The VSC functions in a linear modulation range between the carrier and the output voltage signals when $-1 \leq m \leq 1$. However, over modulation occurs when $m > 1$ leading to a lower quality of the output voltage waveforms [83]. Furthermore, m_f must be an integer multiple of trice the modulation frequency, k, i.e. $m_f = 3k$, to ensure generation of a symmetric three-phase modulating waveform [83].

$$m_f = \frac{f_c}{f_m} \tag{4.4}$$

$$m = \frac{A_m}{A_c} \tag{4.5}$$

The VSC switching frequencies are usually in the range of 1 to 4kHz. Due to these, the two-level VSC is modelled in RSCAD within a small time step sub-network shown in Figure 4.8 . This sub-network is solved within a time step range of 1.4 to 3 μsecs, allowing the simulation of the high switching frequencies of the VSC in RSCAD [75]. Moreover, the PV array is simulated with a large time step of 50 μsecs and was interfaced with the 2-level, VSC simulated with a small time step of 2.5 μsecs using a large time step to small time step transmission line interface model in RSCAD as shown in Figure 4.9.

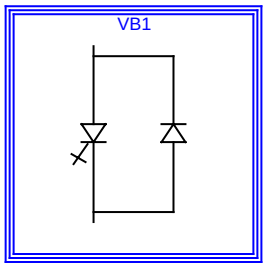

Figure 4.8: Small time-step subnetwork in RSCAD/Draft

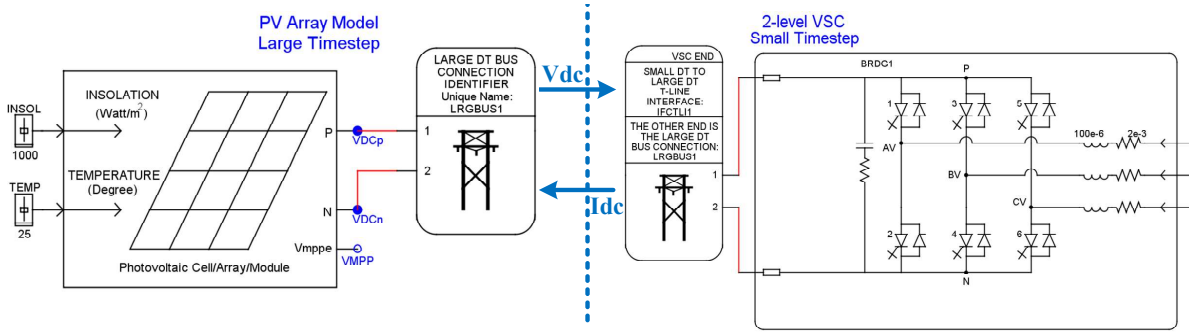

Figure 4.9: Large to small time-step connection in RSCAD/Draft

MODELLING OF THE PV CONTROL SYSTEM

The main objectives of the PV control system are to ensure maximum power transfer from the PV to the grid through maximum power point tracking (MPPT) and to enable adequate inverter-grid connection [84]. The components in the control systems library of RSCAD were used to implement these control objectives. PV generators always have a maximum power point for every operating condition and operating at this point of PV output is necessary. Maximum power point tracking aids the realization of this point despite changes in level of insolation and temperature and ensures the PV cells operate at their highest efficiency. Several algorithms are used for MPPT based on either direct method such as perturbation & observation (P&O) and incremental conductance (INC) methods or indirect methods such as Lambert approximation, fuzzy logic etc. The direct methods are commonly preferred due to their reduced computational requirement and non-complexity [85]. Hence, the incremental conductance algorithm whose flow chart is shown in Figure 4.10 was used to obtain the DC bus reference. The MPPT algorithm increases or decreases the DC bus reference for any given insolation and temperature, thereby tracking the new maximum power output.

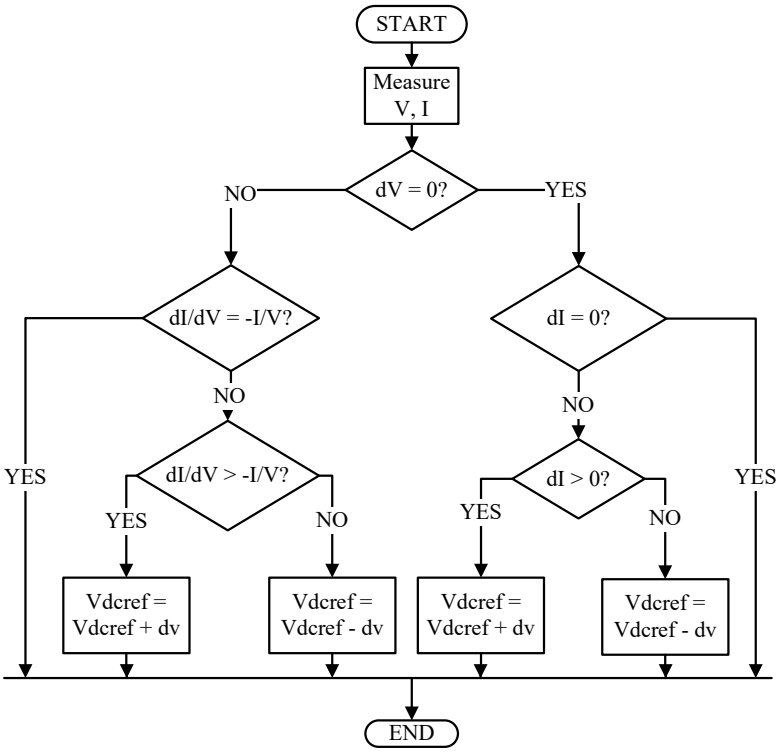

Figure 4.10: Flowchart of incremental conductance algorithm

The second objective which is to properly connect the inverter to the grid is discussed here. The exchange of real and reactive power between the PV system and the grid is implemented in the dq reference frame using the fundamental decoupled current control scheme [82]. This scheme ensures a robust dynamic response to disturbances in the PV system and also protects the VSC against high current conditions [84]. Figure 4.11 describes the full control scheme implemented in this thesis while the various control blocks are provided in Appendix B. The instantaneous AC voltages and currents are transformed by the dq reference frame control into DC signals thus simplifying the parameter tuning process and control design [82]. By tracking the frequency and angle of the grid side AC voltage (delta side of the transformer) using a phase locked loop (PLL) controller, a transform angle ρ is obtained and used to transform the AC voltages and currents to the dq reference frame. The PLL control was designed using a prebuilt PLL component accessible in the RSCAD library [75]. The decoupled current controllers provide modulation signals, md and mq, as outputs. These are transformed to three-phase sinusoidal signals, ma, ma, mc, using a dq-abc transformation block and serve as the modulation waveform in the SPWM control. Thereafter, the SPWM control block generates the firing pulses of the VSC valves.

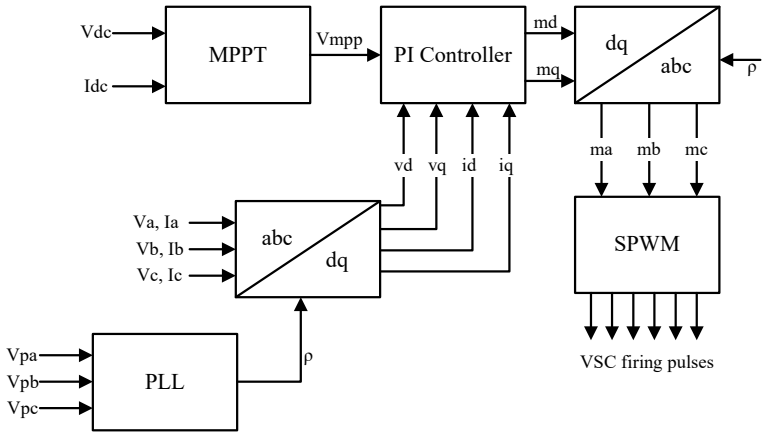

Figure 4.11: PV system Control

RUNTIME SIMULATION OF THE PV SYSTEM

The description of the simulation and control of the PV system in the RSCAD/Runtime module is given in Figure 4.12. At the standard test condition of insolation, $1000 W/m^2$ and temperature, 25(°C), the PV system is designed to deliver about 1.8MW at the DC bus voltage. The AC side of the inverter is interfaced to the selected bus on the distribution system using a 0.8MVA, 0.48/14.38kV, delta-wye VSC interface transformer. The filter capacitance is set to 2500μF.

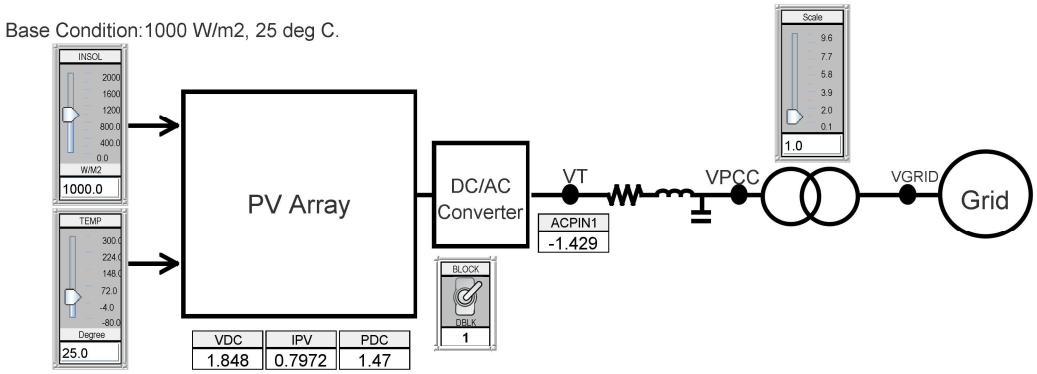

Figure 4.12: PV Simulation on RSCAD/Runtime

The variation of the DC bus voltage and the output power of the PV array to change in insolation from $500W/m^2$ to $1000W/m^2$ is shown in Figure 4.13. The voltage on the DC side of the VSC as the insolation increases, thereby increasing the power output to the grid. This reflects the intermittency of the power derivable from renewable energy resources. The 'Scale' slider shown in Figure 4.12 is a special feature which can be used to control the output of the PV beyond the VSC interface transformer and is further discussed in section 4.4.2.

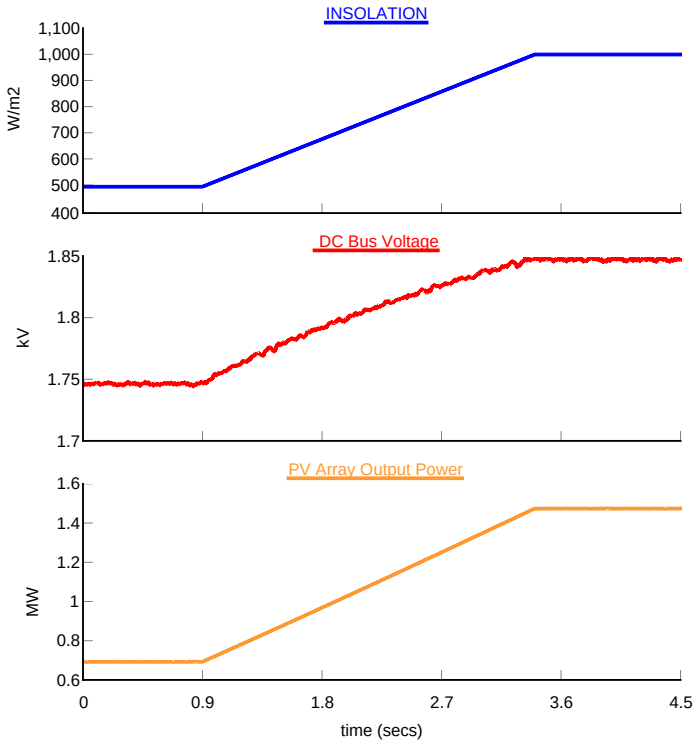

Figure 4.13: DC Bus voltage and PV power response to change in insolation

4.3.3. INDUCTION MOTOR MODEL

As indicated in Chapter 2, induction motors form a significant percentage of dynamic loads in most power systems; therefore, it is important to model them properly for system stability studies. RTDS has a three-phase induction motor model which can either be used as a generator or a motor. The IM operates as a motor when a negative value of the input mechanical torque is used or when the speed is less than the synchronous speed as described in Table 4.2. Control signals are used to select either the torque or speed mode as input to the IM model.

Table 4.2: Induction Machine operating mode

Mode	Generator	Motor
Torque	Positive Torque	Negative Torque
Speed	>synchronous speed	<synchronous speed

To account for industrial loads in the IEEE 34-Bus distribution system, IMs were connected to some of the buses to form test cases. An IM with a double cage construction and a rated output of approximately 0.137MVA was used. It was connected through a breaker to a 400V bus which is connected to the selected buses through a transformer. The parameters of the transformer are: Y-Δ, 0.18MVA, 24.9kV / 400V, leakage = 0.15pu. The mechanical and electrical parameters of the

IM were based on the data given in [86]. However, the saturation characteristics of the machine is not specified. Therefore, the default saturation curve data given in the RTDS induction machine component was maintained. Just like other components, the parameters were specified via the configuration menu of the component.

To form the test cases used in this thesis, the PV model and IM model were connected to different buses as described in Table 4.3. For the first test case, the PV generation accounts for approximately 40% of the load while the IM adds about 15% additional load. For the second test case, the PV generates about 1MW (≈65%) of the load with IMs constituting 10% of the load.

Table 4.3: Test cases implemented in the thesis

Parameters	**Test Case 1**	**Test Case 2**
Number of PVs	3	3
% of load supplied	40%	65%
Buses of PV connection	Bus 828, 848, 836	Bus 828, 848, 836
Number of IMs	4	3
% of load contribution	15%	10%
Buses of IM connection	Bus 834, 890, 840, 812	Bus 890, 840, 812

4.4. DYNAMIC EQUIVALENT MODEL

As previously explained, stability studies are usually confined to a certain region of the network (internal system). Thus, the bulk of the network (external system) which is outside this region can be represented by a dynamic equivalent model (also referred to as an aggregate model). This would reduce the computational resources required and save simulation time. Recall from Figure 2.4, the structure of the DE that is adopted in this thesis. The DE model includes a composite model (with ZIP and IM load models in parallel) and a solar PV generator model. These are connected through an equivalent impedance and transformer, to the point of common coupling of the external TS grid and the reference ADN. The modelling of each of these components of the DE in RTDS is hereby discussed.

4.4.1. ZIP MODEL

The ZIP load model represents the summation of all the loads in the network excluding the induction machine loads. Although the specific composition of the loads in the reference IEEE 34-Bus distribution system is unknown, their categories with respect to being either constant impedance (Z), constant current (I) or constant power (PQ) loads are given. Table 4.4 shows the details of these loads and how they are distributed on each of the phases.

Table 4.4: Load categories on IEEE 34-Bus reference system

Load Category	**Phase 1**		**Phase 2**		**Phase 3**	
	kW	kVar	kW	kVar	kW	kVar
Z	202	138	167	121	276	173
I	177	91	242	123	159	82
PQ	227	128	175	100	144	88
Total	**606**	**357**	**584**	**344**	**579**	**343**

As explained in section 3.5.4, the dynamic load model in RSCAD, through its configuration menu, provides the option to specify ZIP component as the means of controlling the active and reactive power of the load. Earlier versions of RSCAD had a separate ZIP control component

which is used as input to the dynamic load model. After choosing the ZIP component, a tab is included in the configuration menu for determining how the parameters of the ZIP are initialized or controlled. Since MVMO can access model parameters through sliders in RSCAD/Runtime, Runtime was chosen from the menu in RSCAD/Draft as shown in Figure 4.14, to control the P and Q ZIP fractions which are parameters to be optimized (see equations 2.3 and 2.4).

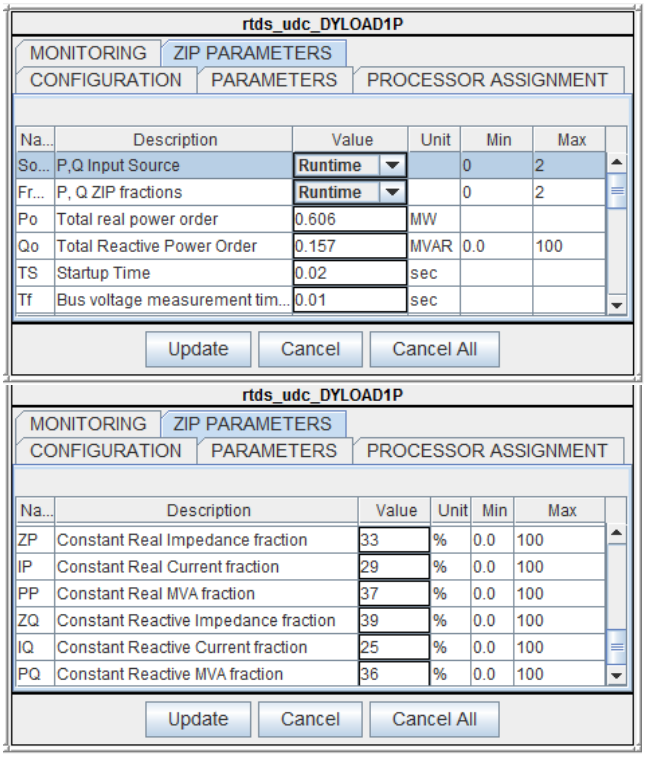

Figure 4.14: ZIP parameter configuration menu

The six parameters associated with the ZIP are then accessible in the Runtime environment as sliders as shown in Figure 4.15. The fractions of each parameter were initialized according to the data in table 4.4. A total of 18 parameters (6x3-phase) were then initialized in MATLAB by setting their minimum and maximum values. MVMO tunes the parameters within these boundaries and changes the value of the sliders with the generated de-normalized parameters before every evaluation.

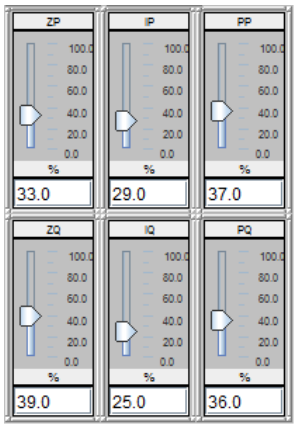

Figure 4.15: ZIP sliders in RSCAD/Runtime

4.4.2. AGGREGATED PV MODEL

Section 4.3.2 already explains in detail how the solar PV generator was modelled in RTDS. In addition to that, the PV system model has a feature which makes it easy to adapt as an aggregate model. The small time-step VSC interface transformer has a scale factor which can be used to increase the current injection from the small time-step to the large time-step grid side. Therefore, by selecting "Yes" for the option to 'include scaling influence on large DT' in the configuration menu shown in Figure 4.16, the scale factor was used to control the solar PV generator power output without changing the array and control parameters.

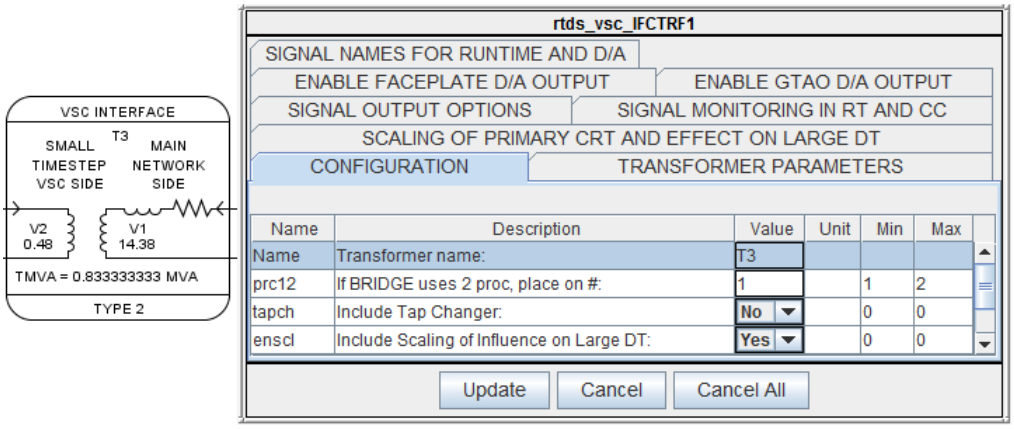

Figure 4.16: Configuration menu to enable scaling PV power output

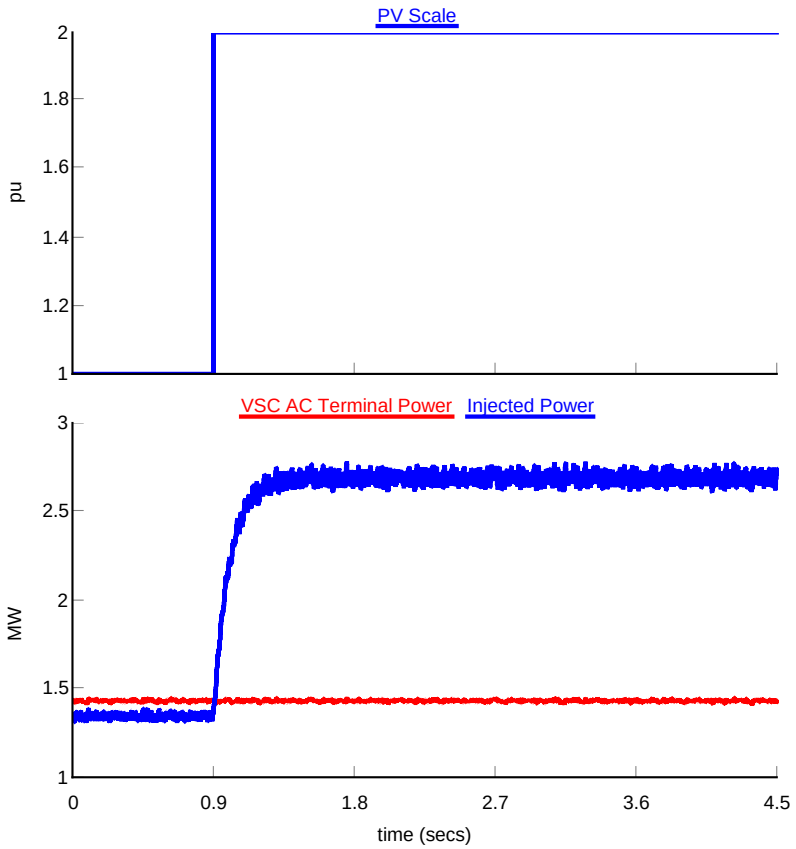

Figure 4.17: Scaling effect on PV power output

The scale factor is also chosen as one of the parameters to be optimized by MVMO. The influence of increasing the scale factor on the power injected into the grid by the PV can be seen in Figure T. As the scale was increased from 1 to 2pu, the output power doubled as well from about 1.4MW to 2.8MW. The control system of the PV is the same as that described in section 4.3.2.

4.4.3. AGGREGATED INDUCTION MOTOR MODEL

The mechanical and electrical parameters of the induction motor used as an aggregate were based on the data given in [16]. For the first test case, the induction motor load that were added to the reference system contributed 15% of the load i.e. about 0.3MW while they contributed approximately 0.2MW, 10% of the total load in the second test case. Accordingly, the addition of the demands of the induction motors in the reference model was used to determine the ratings of the aggregate IM models used in both test cases. However, the amount of induction machine loads inherent in the reference distribution system is not specified but was considered when designing the aggregate IM. Table G shows the ratings of the induction motors that were used in both test cases. The parameters that were selected for optimization are mentioned in section 5.3. Their search ranges were defined in the MVMO algorithm based on data available in [16].

Table 4.5: Ratings of the IM used in test cases

Test Cases	IM rated output (MVA)	Voltage level (kV)	Transformer
1	0.63	2.3	Y-Δ, 1MVA, 24.9kV / 400V, leakage = 0.15pu
2	0.34	400	Y-Δ, 0.5MVA, 24.9kV / 2.3kV, leakage = 0.15pu

4.5. NETWORK VALIDATION CRITERIA

As previously discussed, the response of the DE load model to specific faults in the external network is compared with those of the simulated detailed distribution network subject to the same faults. The voltage reduces at the HV side of the transformer due to remote faults in the external grid and this point of common coupling is the point where the validation signals are measured. For comparison of the two models, the variables that were used are:

- Active Power (P)
- Reactive Power (Q)

The fitness measurement was performed based on these signals and the comparison was focused on the period of fault occurrence.

4.6. REFERENCE SIGNALS AND SYSTEM DISTURBANCES

The reference data required for identification of the DE parameters and its validation are collected from the detailed simulated network. The terminal of the external grid, which is on the HV side of the step-down transformer is the point of common coupling where these data were collected. The signals were measured during system disturbances in the external grid and stored in the folder containing the DE model as a *.csv* file. They are transmitted to MATLAB when the script containing the objective function requests them for calculating the error.

The disturbances used were simulated by instantaneously varying the level of the source voltage behind the source impedance. The three-phase source model in RSCAD has a remote fault feature as shown in Figure 4.18 which allows faults to be initiated in the external grid. However, the faults are always three-phase faults thus limiting the number of scenarios that can be analysed.

Table 4.6: Fault scenarios

Fault Voltage (pu)	Source Impedance (ohms)	Fault Duration (ms)
0.2	1.0	100
0.4	1.0	100
0.5	1.0	100
0.6	1.0	100
0.8	1.0	100

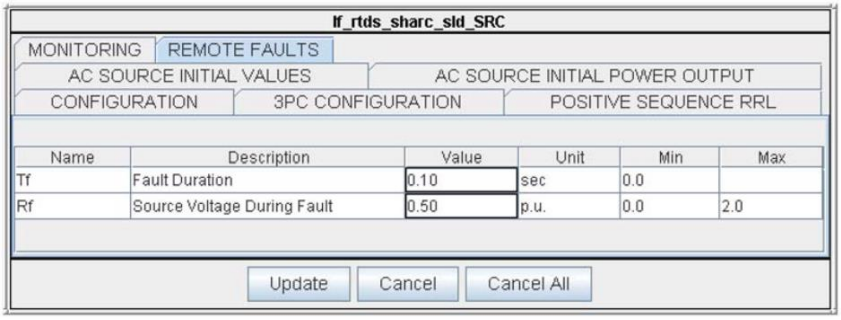

Figure 4.18: External Grid Remote Fault Menu

The percentage drop in the source voltage during faults (Rf) represents the occurrence of fault at various places within the external transmission system grid. Meanwhile, the duration of fault can also be specified through the 'Tf' parameter. The process of automating the fault application in RSCAD/Runtime module using a MATLAB script while parameter identification is in progress is explained in section 5.4.1. The faults implemented for both test cases are given in Table 4.6.

5

PARAMETER IDENTIFICATION

5.1. INTRODUCTION

The gradual transition of distribution networks from passive to active networks due to the integration of various DG technologies increases the complexity of the power system. Although there are various simulation platforms currently being used by utilities, it is still a herculean task to perform dynamic analysis of complex interconnected systems in real time. Therefore, representation of the less important areas (i.e. external systems) with dynamic equivalents while modelling the study area (i.e. internal system) in detail remains the most feasible way to reduce system complexity and save computation time and resources.

Based on the literature review on dynamic equivalence presented in Chapter 2, system identification techniques are the most preferred means for developing appropriate equivalent models. Dynamic stability studies of such systems using optimization algorithms are often formulated as non-linear, non-convex and multi-objective equations. These are difficult to solve using classical optimization techniques. Consequently, more sophisticated optimization techniques, most notably, heuristic based methods have recently been adopted to provide qualitative solutions. Though not entirely perfect, they provide practically accurate solutions within very reasonable computation time.

In this thesis, an innovative form of heuristic optimisation technique known as Mean Variance Mapping Optimization (MVMO) algorithm is used. This choice is motivated by MVMO's enhanced search capability and its ability to reach a global optimum while avoiding premature convergence. Other available techniques are more prone to hasty convergence and local stagnation when dealing with multi-objective problems. Moreover, results derived from the application of MVMO to several power system problems, especially on identification of dynamic equivalents, prove its potential as a sufficient optimization method for achieving satisfactory solutions. Therefore, this research was channelled towards implementing MVMO on RTDS, which is an advanced real-time EMT simulation package currently striving in the power systems industry.

5.2. MVMO ALGORITHM

The mean–variance mapping optimization (MVMO) is a recent variant of population-based, evolutionary optimization algorithm. Its main feature is its unique search mechanism for optimization variables within a normalized range of the search space. It also adopts a single parent-offspring approach. Moreover, the core of MVMO is based on a special mapping function used for its mutation operation where n-best solutions are stored in an archive which is recurrently updated. The mean and variance of the best optimization variables achieved so far and saved in the archive are used to guide the generation of further appropriate solutions. Besides, the algorithm

maintains a global search due to the shape of the mapping function and ensures a balance between diversification and intensity [87]. As a result, it exhibits fast convergence characteristics and efficiently avoids premature convergence. However, MVMO initially propagates randomly selected variables onto the corresponding mapping function, which thereafter leads to gradual generation of best solutions. Figure 5.1 illustrates the procedure of the algorithm implemented in this research. The following subsections further elaborate on each of the steps.

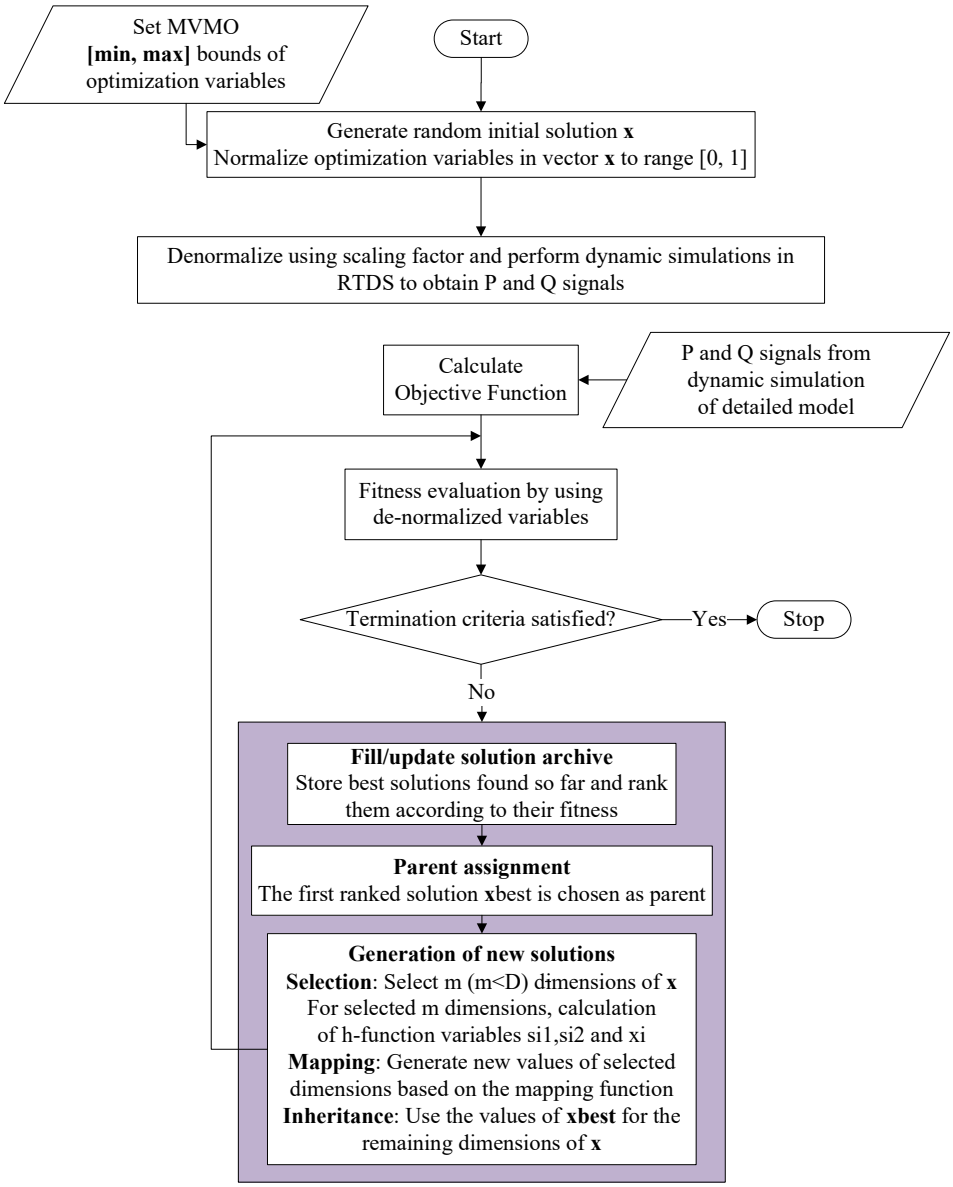

Figure 5.1: Flowchart of the approach used for identification of parameters of DE with MVMO (adapted from [4])

5.2.1. PROPOSED APPROACH

Figure 5.1 illustrates the overall procedure of MVMO algorithm as implemented in this research. Since this is a major aspect of this thesis, each of the stages are further explained in the following subsections.

After the determination of the structure of the dynamic equivalent model, a set of disturbances that will facilitate the identification of its parameters are defined. Prior to this, the same set of disturbances were used to collect simulated data at the boundary bus (i.e. bus between the

transmission and distribution system). A list of the disturbances applied in this research are summarized in table 4.6.

The general overview of the algorithm's procedure is as follows: Firstly, the parameters of the model are initialized with their upper and lower bounds. At the beginning of the optimization process, MVMO generates an initial solution vector by randomly sampling the optimization parameters within the defined [min, max] bounds as given below:

$$x_i^{ini} = x_i^{min} + rand(x_i^{max} - x_i^{min}), \qquad i = 1.....D \tag{5.1}$$

where D is the number of optimization parameters.

Secondly, these sampled parameters are normalized to values between [0,1] range. This feature is unique to MVMO and ensures that the generated offspring always remain within the search boundaries. Thereafter, the parameters are transformed from [0,1] to their original [min, max] dimension which are given to the model (in RSCAD/Runtime) for dynamic simulations. As the iteration progresses, the desired signals from the model are given to the fitness evaluation script for comparison with the simulated reference signals. A fitness value is derived from the objective function which determines whether the solution is included or not in the solution archive. Based on the best solution achieved so far, a parent is assigned from which new candidate solutions are generated through mutation operators and crossover. Lastly, the solutions are again de-normalized and supplied to the model for simulations. The iterative process continues until a predefined termination criterion is fulfilled. The criterion is usually defined as a specified number of function evaluations which was the case in this thesis.

As illustrated in Figures 1.2, the MVMO algorithm is coded in MATLAB. Hence, the calculation phases that enable MVMO's search procedure i.e. initialization and offspring creation, are structured in a script. This script does not require any modification by the user and runs in less than a second. However, the function evaluation used to determine the value of the objective function for the optimization problem is created in another script. It is within this script that the connection between MATLAB and RSCAD (explained in section 5.4) is established. Time delays were included in this script to allow RTDS compile and run the model which impacted the overall optimization time. Further, there is a main script which controls the entire iteration process of the function evaluation and provides the final solution at the end of the stipulated number of evaluations.

5.2.2. OBJECTIVE FUNCTION FORMULATION

The aim of MVMO algorithm is to find the values of parameters that effect the closest match between the behaviours (i.e. boundary bus signals) of the aggregated model and the detailed model. To do this, the active and reactive power at the boundary bus or point of common coupling were the chosen signals for comparison. Based on the difference between the simulated reference signals and the dynamic equivalent model signals, the objective function for this optimization problem was formulated as follows:

Minimize

$$OF = \sum_{n=1}^{p} \alpha_n \int_0^{\tau} \left(\sqrt{(P_n - P_{n_{ref}})^2 + (Q_n - Q_{n_{ref}})^2} \right) dt \tag{5.2}$$

Subject to

$$x_{min} \leq x \leq x_{max} \tag{5.3}$$

where P_n and Q_n are the active and reactive power signals of the DE, while $P_{n_{ref}}$, $Q_{n_{ref}}$ are the corresponding signals from the detailed model. p is the number of disturbances, α_n is the

probability of the nth disturbance and τ is the simulation period. Also, x is the solution vector that constitutes the set of DE parameters to be optimized while x_{min} and x_{max} are the minimum and maximum values defined for each parameter in x. Equation 5.2 is based on the Euclidean function which calculates the point to point error distance between two signals.

5.2.3. FITNESS EVALUATION

Following the de-normalization of the variables to their real values [min, max], the corresponding response signals are fed to the mathematical model for evaluation of the objective function given in equation 5.2. For a candidate solution being evaluated at any instance in the iteration, the fitness value basically corresponds with the objective function. Since no constraints were defined in this optimization process, the fitness value therefore corresponds to the objective function which is based on the Euclidean distance between the P and Q signals of the detailed and DE models for the applied disturbances.

5.2.4. SOLUTION ARCHIVE

The solution archive is one of the key features of MVMO algorithm. It serves as the knowledge database which guides the algorithm's search direction. Essentially, the n-best solutions that MVMO has derived at any point in iteration, with their corresponding fitness value, d factors and shape, are stored in the archive. The archive size for the entire process is fixed at the beginning in the main script. Insight from previous applications on power system optimization problems reveals that an archive size between 2 and 5 is adequate. In this research, it was maintained at a size of 4. Figure 5.2 shows a typical structure of the MVMO solution archive.

Ranking	**Fitness**	**x_1**	**x_2**	**…**	**x_D**
First best	F_1				
Second best					
⋮	F_2		Optimization Parameters		
Last best	F_A				
Mean	---	$\bar{x}_1$	$\bar{x}_2$	…	$\bar{x}_D$
Shape	---	s_1	s_2	…	s_D
d-factor	---	d_1	d_2	…	d_D

Figure 5.2: MVMO solution archive to store n-best solutions

Furthermore, the archive is gradually filled up in a descending order of fitness as the iteration progresses. When the archive is full, it is only updated if a newly generated solution has better fitness than those already stored in the archive. After each update, the mean and shape variables of every optimization parameter x_i are calculated using equations 5.4 and 5.5 respectively.

$$\bar{x}_i = \frac{1}{n}\sum_{j=1}^{n} x_i(j) \tag{5.4}$$

$$s_i = -\ln(v_i).f_s \tag{5.5}$$

where the variance v_i is computed as follows:

$$v_i = \frac{1}{n}\sum_{j=1}^{n}(x_i(j) - \bar{x}_i)^2 \tag{5.6}$$

Initially, $\bar{x}_i$ is the same as the randomly generated value of x_i, and v_i is set to 1. The geometric characteristics of the mapping function is highly influenced by the shape variable s_i, thus, the reason for s_i being dependent on the user defined scaling factor f_s. Moreover, s_i facilitates the control of the mapping function hence the search process.

5.2.5. PARENT SELECTION AND MUTATION

The process of generating offspring or child solution can be distinguished into 3 sections. First is the selection of parent, then crossover and finally, mutation. Each of these steps are explained in the following subsections.

PARENT SELECTION

As already mentioned, MVMO adopts a single parent-offspring approach. This implies that only one parent vector is used to create offspring vector. The solution available in the first-ranked position in the solution archive is chosen as the parent (x_{parent}) for subsequent creation of the child solution. Alternatively, the parent could also be selected through the combination of best solutions in the archive. In this thesis, the first solution updated to the solution archive is chosen as the parent.

CROSSOVER

For the next iteration in the process, the offspring vector (i.e. child solution) $x_{child} = [x_1, x_2, x_3 \ldots\ldots x_D]$ is generated by combining a subset of D-m variables derived from the parent vector and m selected variable that will undergo mutation. The value of m depends on the optimization problem however the choice of which m variables to be mutated is done by a random sequential selection scheme illustrated in Figure 5.3 below.

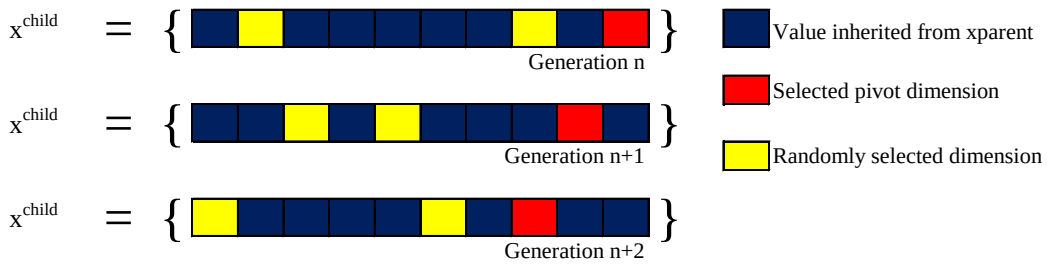

Figure 5.3: Random sequential selection strategy. The illustration considers a 10-dimensional solution vector with m = 3, done over three successive generations. One pivot of the m variables is sequentially selected from the last to the first dimension of the parent vector array while the remaining m - 1 variables are randomly selected.

MUTATION

After $m < D$ variables are randomly selected from the parent vector, they go through a mutation process implemented by a mapping function based on the real values of x_i and s_i. The new value of each selected dimension x_i is calculated using equation 5.7 below:

$$x_i = h_x + (1 + h_1 + h_0).x_i^{'} - h_0 \tag{5.7}$$

where x_i is a variable randomly changed with uniform distribution within [0, 1] while h denotes the mapping function which changes dynamically as the algorithm continues its search for optimal values and is defined by equation 5.8.

$$h(\bar{x}_i, s_1, s_2, x) = \bar{x}_i.(1 - e^{-x.s_{i1}}) + (1 - \bar{x}_i).e^{-(1-x).s_{i2}} \tag{5.8}$$

Here, subscript i denotes the ith dimension selected from the parent vector. xi is the mean of the best solution in the archive while s_1 and s_2, derived from the variance of the stored solution, are the shape factors. To recall equation 5.8, h_x, h_1, and h_0 are the outputs of the mapping function and are computed as expressed in equations 5.9 - 5.11 below:

$$h_x = (u_i = x_i^{'}) \tag{5.9}$$

$$h_0 = h(u_i = 0) \tag{5.10}$$

$$h_1 = h(u_i = 1) \tag{5.11}$$

The scope of both input and output of the mapping function is always between [0, 1]. The shape of the mapping function is determined by the mean x_i and the shape factors s_{i1} and s_{i2}. As the mean x_i value varies, the mapping curve shifts between the lower and upper limits of the normalized search range. However, the variation of the shape factors s_{i1} and s_{i2} influences the curve's degree of bent. Accordingly, emphasis is placed on either exploration (i.e., high bent shape) or exploitation (flattered shape) during stages of the search process. Since a balance between exploration and exploitation is desirable, as well as enhanced search performance, MVMO strategically varies the shape factors such that the asymmetric characteristic of the mapping function is well controlled. The strategy is illustrated as follows:

$s_1 = s_2 = s_i = -\ln(v_i) \cdot f_s$
if $s_i > 0$ then
  $\Delta d = (1 + \Delta d_0) + 2 \cdot (rand - 0.5)$
  if $s_i > d_i$
    $d_i = d_i \cdot \Delta d$
  else
    $d_i = d_i / \Delta d$
  end if
  if $rand \geqslant 0.5$ then
    $s_1 = s_i; s_2 = d_i$
  else
    $s_1 = d_i; s_2 = s_i$
  end if
end if

It is worth mentioning that the values of x_i, v_i, s_{i1}, and s_{i2} related to the candidate solution are not calculated until a certain amount of solutions have been updated to the solution archive. Their evaluation begins with at least two solutions in the archive. Otherwise, it is done after the archive has been completely filled. This implies that the search is performed with $s_{i1} = s_{i2} = 0$, corresponding to a linear shape of the mapping function between 0 and 1. In this situation, the mean value does not influence the mapping function. Finally, setting the shape factor (f_s) to a high value ($f_s > 1$) shifts the algorithm towards exploration while a low value ($f_s < 1$) tends it towards exploitation.

5.3. SENSITIVITY ANALYSIS

To determine the parameters of the dynamic equivalent model that significantly influence its behaviour, a sensitivity analysis was performed. The active and reactive power signals were used in this thesis as the basis for the analysis. Some of the parameters were chosen based on recommendations available in literature while others were based on the results of the analysis. The parameters chosen from each block of the DE, i.e. ZIP load model, induction model and the PV model are shown in Table 5.1.

Table 5.1: Parameters selected for optimization

Model	**Parameters**					
IM Model	Rr	Rs	Xr	Xs	Xm	H
ZIP Model	ZP	IP	PP	ZQ	IQ	PQ
	ZPcc2	IPcc2	PPcc2	ZQcc2	IQcc2	PQcc2
	ZPcc3	IPcc3	PPcc3	ZQcc3	IQcc3	PQcc3
PV Model	PVScale	Vsdref				
TX Line	length					

Percentages of the constant Z, I and P for both active and reactive power as illustrated in the polynomial ZIP load model equations (see equation 2.3 and 2.4) were selected. These components determine the power consumed by the load with respect to the voltage and are frequently used to represent static loads in most load model analysis. Their initial values were set based on the cumulative value of the loads in the detailed model. From the PV model, the scale factor (discussed in section 4.4.2) which determines the contribution of PV generation to the DE and reference voltage (Vsdref) were chosen. From the induction motor model, R_s, R_r, X_r, X_s, X_m and H (see section 2.4.2 for definitions) were selected for optimization. Also, the aggregated line length which corresponds to the equivalent resistance and reactance of the line is optimized. The line resistance and reactance could not be directly used because they are defined within a separate module Tline in RSCAD and only the length of the line can be varied in Runtime.

MVMO algorithm requires the definition of a search space within which it searches for optimal values of each parameter. This is done by specifying lower [min] and upper [max] bounds for every parameter within the parameter vectors. MVMO's search for the global optimum is highly dependent on these search ranges specified by the user. Table 5.2 shows the boundaries that were set for the optimization parameters during one of the identification process. These ranges were based on observations from the sensitivity analysis and attempts made towards getting a steady state dynamic equivalent before performing the optimization. Some of the ranges were changed (either expanded or reduced) during some simulation cases based on observation of their influence on the result. For example, the PV scale range was different for both test cases due to the penetration of solar PV generation in each of them.

Table 5.2: Search range of parameters to be optimized

Rr	[0.05, 0.3]	ZP	[30, 40]	ZPcc2	[27, 31]	ZPcc3	[30, 50]
Rs	[0.04, 0.055]	IP	[25, 35]	IPcc2	[36, 43]	IPcc3	[25, 40]
Xr	[0.04, 0.08]	PP	[35, 40]	PPcc2	[28, 32]	PPcc3	[23, 36]
Xs	[0.075, 0.095]	ZQ	[37, 45]	ZQcc2	[30, 37]	ZQcc3	[20, 60]
Xm	[2.5, 3.5]	IQ	[20, 30]	IQcc2	[32, 38]	IQcc3	[20, 50]
H	[0.55, 0.65]	PQ	[32, 40]	PQcc2	[27, 35]	PQcc3	[24, 50]
PVScale	[0.2, 0.6]	Vsdref	[0.39, 0.6]	length	[70, 80]		

5.4. IMPLEMENTATION OF MVMO IN MATLAB-RSCAD

This section addresses key steps involved in the implementation of MVMO algorithm on RTDS. The Runtime environment in RSCAD includes a scripting feature which allows the user to execute dynamic functions automatically. This implies that user interaction during simulations, especially on large systems are eliminated. A record and playback feature is available in RSCAD Runtime module to record actions initially performed by the user, store them as RTDS commands in a script file and re-execute them using a run function. Examples of common actions that would be recorded in a script file include starting and stopping a simulation, pushing a button, changing a slider set point, saving a plot etc. Furthermore, the script file can be modified to include or remove time delays and contain functions such as 'for loops', if-else or while statements etc. as used in 'C' programming language. This enhances the capability of the script to run many simulations lasting several hours or days. However, since the MVMO algorithm used in this thesis is written in MATLAB, it was essential to facilitate information exchange between it and RSCAD Runtime.

To establish a communication link between the two programs, the TCP/IP which is the most widely adopted network communication protocol was used. Consequently, one of the programs needs to be a server while the other is the client. A server is a network component that offers a service (e.g. a website) and the client requests access to such service. Therefore, RSCAD represented the server while MATLAB served as the client. Both programs are on the same computer and local network. Alternatively, the connection can be established via the internet such that the two programs are operated on different computers during the optimization process. However, this would create time delays in communication and render the optimization process inefficient.

A brief pseudocode of the connection process is given below:

1. OPEN the script feature in RTDS/Runtime.
2. Declare number of iterations.
3. Specify communication port for connection with MATLAB.
4. WAIT for MATLAB to connect.
5. Run MATLAB script which connects to Runtime through opened port.
6. CLOSE port after simulation in each iteration has ended.
7. RETURN to 4.
8. END connection when number of iterations is reached.

RSCAD/Runtime as a server, uses the 'ListenOnPort()' command which is one of the commands in the Runtime script feature to open a specific communication port for an external application to connect. Then it waits for an incoming connection request from the application, in this case MATLAB to enable assess to the Runtime environment. Once the connection is established, the port can be considered as a bi-directional or duplex communication channel. This means that both applications can send as well as receive data through the port. The code to establish this link is written in a .scr script created by using the Script tab in Runtime and selecting 'New'. The script must be saved in the same directory as the model. The script implemented in this thesis is described as follows:

```
float myArrayValues;
int myArraySize;
string mystring;
int j;
for (j=1; j<301; j++)
{
fprintf(stdmsg, "Runtime is now acting as TCP Server...\n");
fprintf(stdmsg,"Evaluation Number: %d\n",j);
ListenOnPort(4575, true);
}
fprintf(stdmsg, "Runtime is now finished acting as TCP Server\n");
```

The three variables *myArrayValues*, *myArraySize* and *mystring* are responsible for taking the data entering or leaving the port. The port number used for communication in this case was port 4575. *Fprintf* command displays messages in the Runtime message area, thus allowing the user to monitor the state of the simulation. The for loop was necessary in this case because of the number of evaluations specified for MVMO algorithm. After every evaluation, the connection to the server is terminated to allow the script return to the waiting state. This ensures that MVMO can start the simulation at the beginning of subsequent iterations. The value used in the for loop (301 in this case) must be greater than the number of evaluations specified in MVMO to ensure completion of the optimization.

Furthermore, the basic functions used in MATLAB to communicate with RSCAD are detailed below:

- *JTCPOBJ = jtcp (' REQUEST ' , Host, Port)* represents a request from MATLAB to RSCAD to establish a TCP/IP connection on the specified port opened by RSCAD. The host can be represented by an IP address string (e.g. '192.168.0.10') or by a hostname. Since both applications are on the same host, a loopback address ('127.0.0.1') was used. Port is an integer number between 1025 and 65535 which must be open by the server to enable connection.
- *jtcp ('writes', JTCPOBJ, msg)* sends the specified information contained in the 'msg' variable to RSCAD through the TCP/IP connection.
- *rmsg = jtcp ('read', JTCPOBJ)* reads the information that is sent from RSCAD through the communication port and stores it in a variable 'rmsg'.
- *jtcp ('close', JTCPOBJ)* closes the port thereby ending the TCP/IP connection between RSCAD and MATLAB.

The variable 'JTCPOBJ' stores all the necessary information flowing through the communication port which are needed by the remaining functions of the algorithm.

5.4.1. SENDING DATA FROM MATLAB TO RSCAD

This section describes in more detail, how the data (the de-normalized parameters in this case) are sent from MATLAB to the Runtime environment in RSCAD.

While the optimization is in progress, some of the network parameters i.e. those to be optimized should be updated in real-time at the beginning of each iteration without interruption by the user. The Runtime module contains components such as sliders, switches, buttons and dials whose value or status can be changed while the simulation is running. The parameters chosen for optimization in this simulation were represented with sliders, whose initial value, lower and upper bounds were specified in their configuration input window as shown in Figure 5.4.

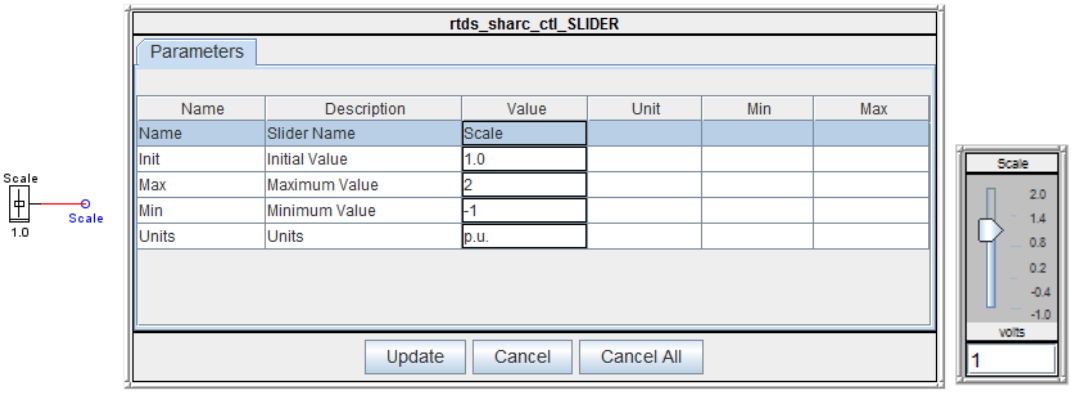

Figure 5.4: Slider component with its configuration window in Draft and its module in Runtime

During the simulation, changes to the sliders cannot be done manually, but through the interaction between MVMO algorithm and RSCAD. MATLAB instructs the sliders to get the new de-normalized values of the candidate solution generated by the algorithm. To illustrate this, the following function enables the MVMO algorithm on MATLAB to change the scale parameter of the PV model during its search for global optimum.

msg = sprintf('SetSlider "Subsystem#1 : CTLs : Inputs : Scale" = %f; ', xx_yy(2));
jtcp('writes' , JTCPOBJ, msg);

The critical point here is the construction of msg variable which contains the new values to be sent to RSCAD to change the appropriate sliders. The msg variable is a string and the syntax should be as stated in ref 1. The path to the location of the signal is represented by *"Subsystem#1 : CTLs : Inputs : Scale"* and can be different for other signals. Besides, there are some pre-processor variables embedded in the configuration of components in the Draft module which cannot be represented by normal sliders in Runtime. Such variables are known as draft variables and can still be varied in Runtime by introducing a '$' sign to their name and using a draft variable slider as shown in Figure H. Their interactive function in MATLAB is given as:

msg = sprintf('SetSlider "DraftVariables : Tf" = %f;' ,xx_yy(21));

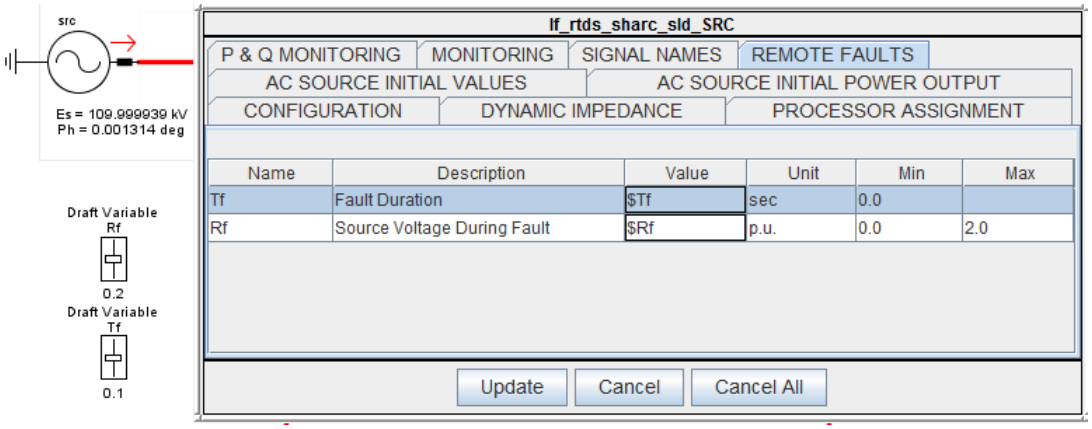

Figure 5.5: Draft Variable slider setup

The total number of parameters that accept their values from MATLAB during the simulation,

and therefore the number of necessary sliders, is 27. These have already been listed in Table 5.1.

Another example of a function used to control the simulation from MATLAB is the given below. Its purpose was to implement faults in the external grid using the push button component in Runtime. The "SUSPEND" function is used to stipulate the duration of the fault.

```
jtcp( 'writes' ,JTCPOBJ, 'PushButton "Subsystem#1 : Sources : src : Ftrg" ;' );
jtcp( 'writes' ,JTCPOBJ, 'SUSPEND 1.0;' );
jtcp( 'writes' ,JTCPOBJ, 'ReleaseButton "Subsystem#1 : Sources : src : Ftrg" ;' );
```

5.4.2. SENDING DATA FROM RSCAD TO MATLAB

To perform the opposite flow of data, i.e. to send some signals from the result of the simulation in RSCAD/Runtime to MATLAB for further processing, some prior steps need to be taken. At first, all the variables to be read by MATLAB must be represented by meters or plots in the Runtime environment. Meters always indicate the numerical value of the selected variable in the network while plots show the signal variation relative to time or other variables. Secondly, some necessary variables such as 'myArrayvalues' and 'mystring' mentioned earlier are declared in the Runtime script. The variable 'myArrayvalue' is a floating-point number value to be used as a container or temporary storage for meter values. The 'mystring' variable as the name implies is a string that will store the token string generated from RSCAD/Runtime. Finally, data is transmitted from Runtime to MATLAB using a script command named 'ListenOnPortHandshake()'. The data is parsed from Runtime through the token string using a regular expression given in 5.12 [88]. The regular expression describes how a text based string can be parsed with a pattern. Therefore, the token string from Runtime must follow the pattern defined in the expression.

$$expr = 'myArrayValues\s^* = \s^*(?<var\_arrayvalues>(-)?\d+(.\d+)?)\s^*END'; \quad (5.12)$$

The 'ListenOnPortHandshake()' command is also used to ensure synchronization of the two applications by making sure that all the previous commands sent are executed. Since the data transmission through the port is done in several packets, it is possible that some fragments of the string are not transmitted. Therefore, the regular expression strictly ensures that data transmission is complete and MATLAB can proceed with the parsing of the token string. More information about the Runtime commands and the regular expression can be found in RSCAD/Runtime manual [75] and [88] respectively. In this thesis, the regular expression was used to determine the array size of the power signal at the PCC and for synchronization of RSCAD/Runtime and MATLAB as previously explained. However, it takes a large amount of time to execute the data retrieval section of the code. Therefore, a more efficient MATLAB command i.e. 'importdata()' was used to parse the power signal data upon saving the plot using the following expression:

```
jtcp( 'writes' ,JTCPOBJ,'SavePlot "Source","folderpath\Source.mpb";');
```

The data is saved as a '*.mpb*' file which automatically creates a '*.out*' file from which the data can be imported to MATLAB. It is necessary to create a time delay to allow RSCAD/Runtime sufficient time to generate the '*.out*' file.

6

RESULTS AND DISCUSSION

The results of the two case studies implemented in this thesis are presented in this chapter. In the first test case, solar PV generation accounted for about 40% of the load while it supplies about 65% of the load demand in the second test case. Faults are applied within the equivalent external grid and the P and Q signals were measured at the PCC for optimization of the DE parameters. All the faults are three-phase faults with a duration of 100ms.

6.1. TEST CASE 1

The MVMO algorithm was configured to optimize 27 parameters (see table 5.1) of the dynamic equivalent model. It searches for the best values of these parameters within a specified range defined in table 5.2. The algorithm attempts to minimize the Euclidean distance between the P and Q signals at the PCC of the external TS grid to the detailed and DE models. The closer the final value is to zero after the defined number of evaluations, the more identical the signals would be. Therefore a good optimization process would result in a final value between 0 and 1. Figure 6.1 shows the convergence graph which indicates the gradual process of minimizing the error between the signals. It takes less than 50 evaluations for the distance value to reduce to a single digit number, which reflects the fast convergence characteristics of MVMO.

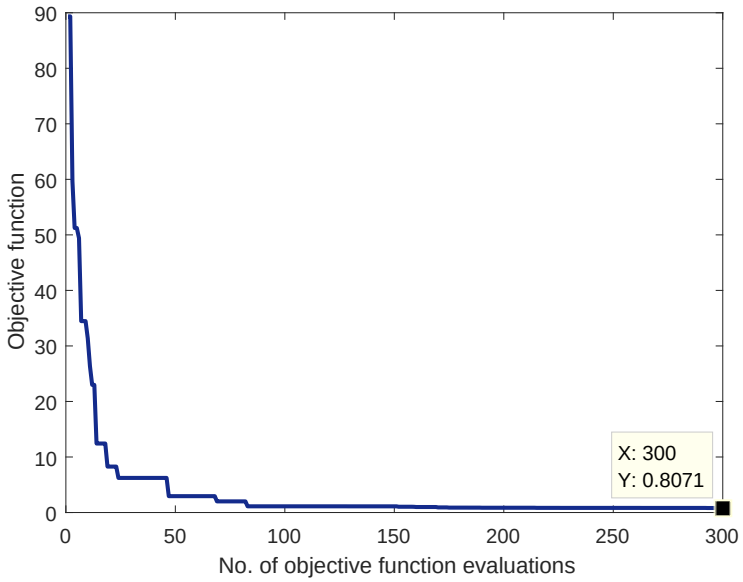

Figure 6.1: Convergence of MVMO algorithm in test case 1

This test case required 300 evaluations to achieve acceptable distance margin. Although more evaluations were used at times, the general observation is that about 200 to 400 evaluations are sufficient to reach a very low value. The graph indicates that the error was reduced over 90%. With deliberate time delays included, it took about 3.5 hours for MVMO to execute this identification problem.

Following a successful convergence of the algorithm, the associated response of the DE model is compared to those of the detailed network as shown in Figure 6.2 and 6.3. The graphs present the voltage, active power (P) and reactive power (Q) at the boundary bus of the external grid to the models i.e. the HV side of the transformer.

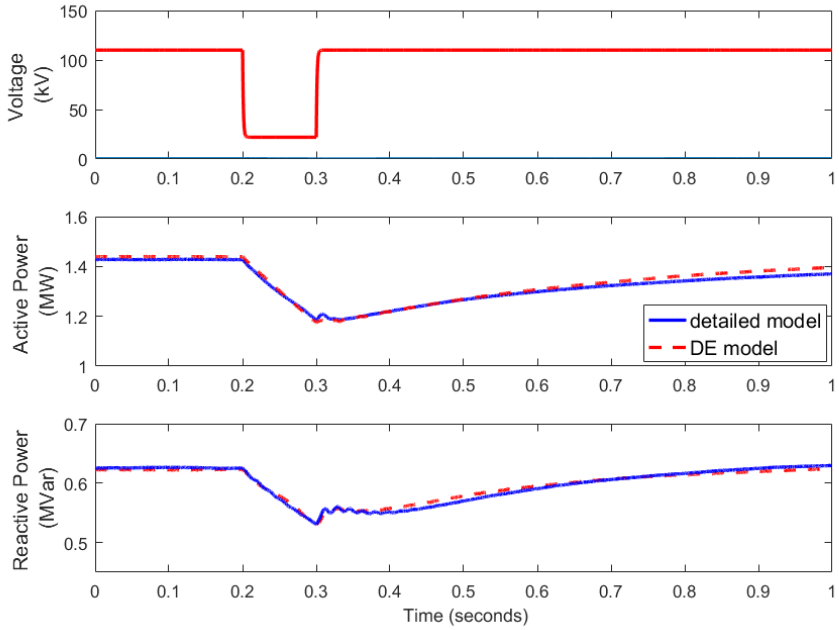

Figure 6.2: Fault scenario created by 0.2 pu voltage

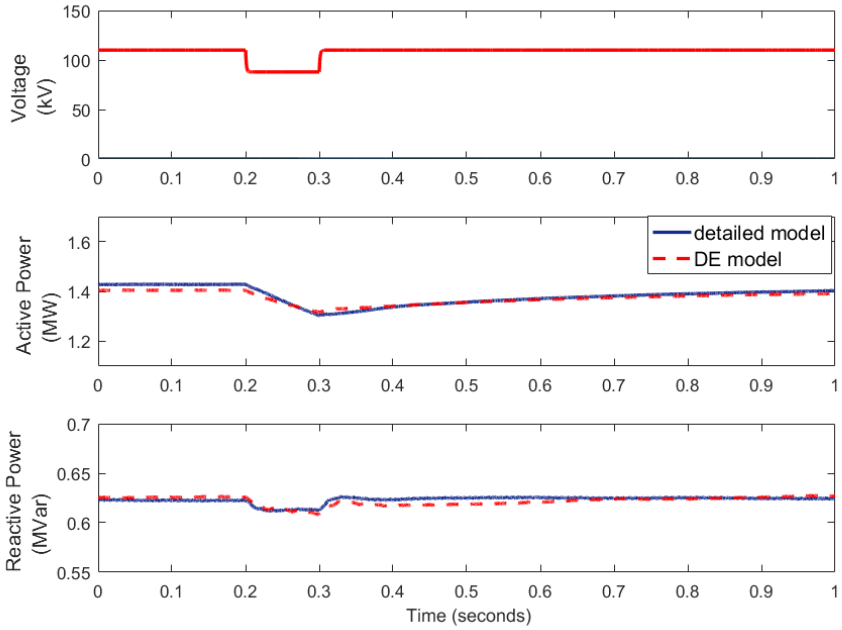

Figure 6.3: Fault scenario created by 0.8 pu voltage

For validation of the DE model, its response to a fault that was not used to define its parameters were measured. The fault scenario randomly applied to the DE model is 0.4 pu. The model parameters had been derived using a 0.2 pu fault. Figure 6.4 shows that the response of the DE is similar to that of the detailed network, thus showing the suitability of the model to respond to other external disturbances.

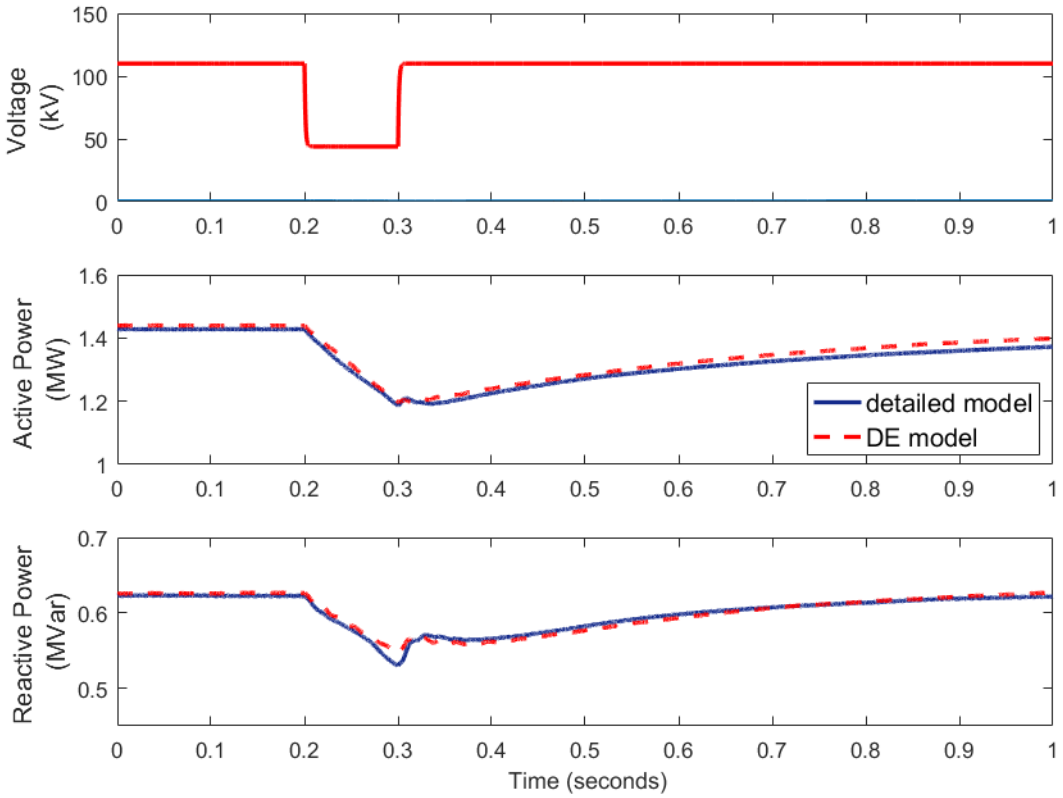

Figure 6.4: Random fault scenario created by 0.4 pu voltage

Furthermore, it is important to point out that the DE model reduces computational resources and also simulation time. Two RTDS racks were required to simulate the detailed network while the DE model only required one rack. This provides an extra rack for other research work to be done simultaneously. This advantage cannot be overstated as racks are very limited resource especially when large transmission systems need to be simulated. The same remark applies to the amount of time it takes to complete a simulation case. There was a 60% reduction in simulation time used on the detailed model. It took only about 3 seconds to run the DE model during the optimization process while it takes the detailed model over 10 seconds to run during normal start up.

The values of the optimized parameters delivered by MVMO at the end of the evaluation process which had the lowest objective function are given in table 6.1.

Table 6.1: Optimized parameters for test case 1

IM Model		ZIP Model						PV Model		Line (km)	
Rr	0.147	ZP	38.47	ZPcc2	28.92	ZPcc3	43.53	PVScale	0.69	length	58.89
Rs	0.0205	IP	17.64	IPcc2	41.34	IPcc3	29.05	Vsdref	0.586		
Xr	0.0605	PP	39.79	PPcc2	34.61	PPcc3	26.83				
Xs	0.0682	ZQ	23.49	ZQcc2	26.68	ZQcc3	34.3				
Xm	2.8153	IQ	32.29	IQcc2	32.43	IQcc3	32.14				
H	0.99	PQ	36.67	PQcc2	28.51	PQcc3	37.51				

6.2. TEST CASE 2

In this test case, the contribution of the solar PV generators was increased to about 65% of the overall demand while the induction motor contribution was reduced to 10%. This can be compared to a possible future distribution grid where the integration of PV is really high. Just like the first test case, 27 parameters were optimized and the objective function (see equation 5.2) is based on the Euclidean distance index which is the sum of the straight line, point to point distances between the power signals of the detailed and DE model. The termination criteria for the optimization process was 300 evaluations. After these evaluations, the objective function value was between 0 and 1 which means that there is high similarity between the signals compared. Figure 6.5 shows the plot of the objective function values against the evaluations. Once again, it can be seen that MVMO converges fast and reaches very low values after 100 evaluations. Therefore, it can be concluded that MVMO is a suitable heuristic optimization tool for RTDS-based simulations. Moreover, setting the number of evaluations to above 300 would result in lower values of the objective function but to save time, this was not implemented.

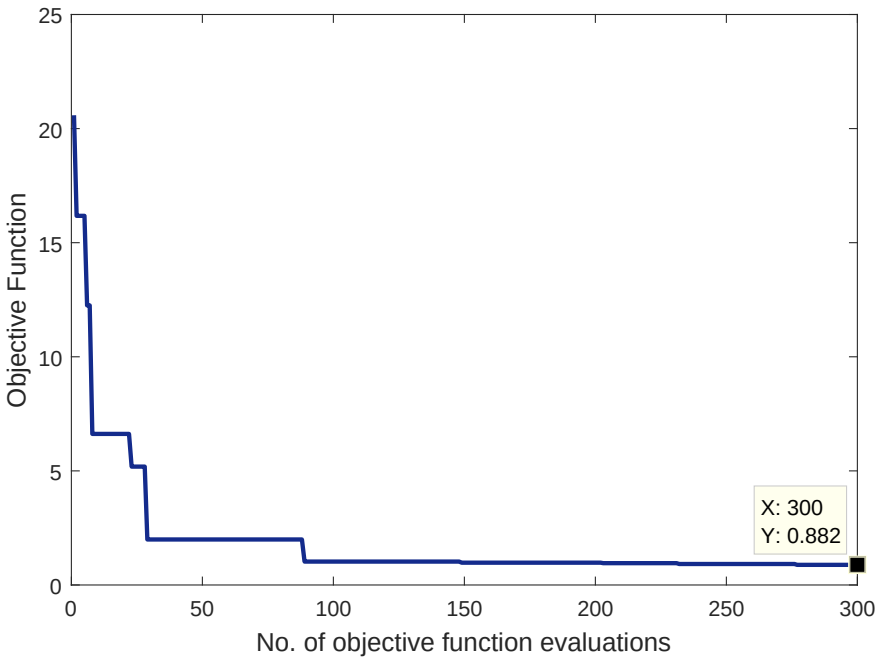

Figure 6.5: Convergence of MVMO algorithm in test case 2

MVMO achieved a 95% reduction of the distance between the signals and Figure 6.6 and 6.7 show their similarities after 0.5 pu and 0.2 pu three-phase faults were applied in the external grid respectively.

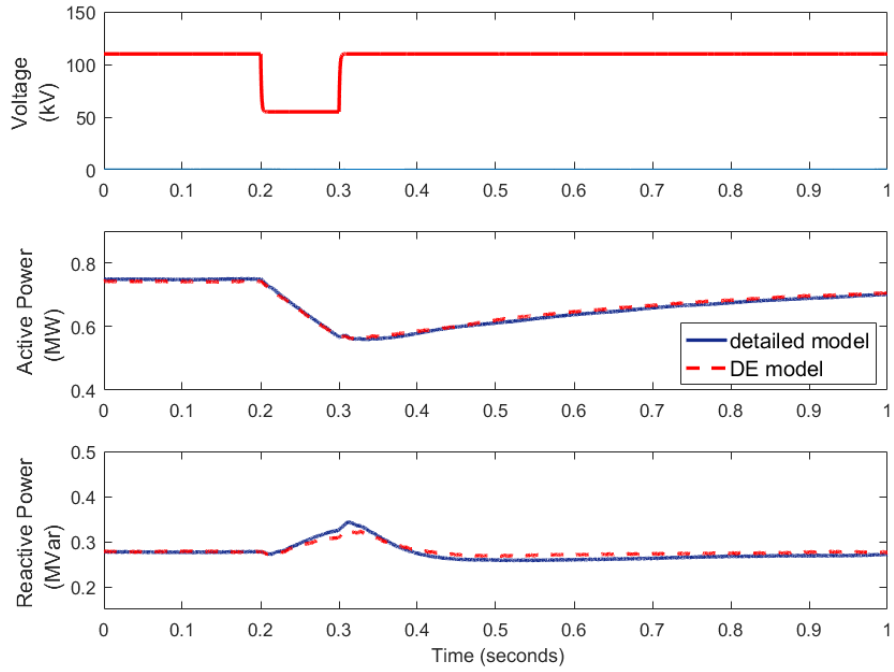

Figure 6.6: Fault scenario created by 0.5 pu voltage

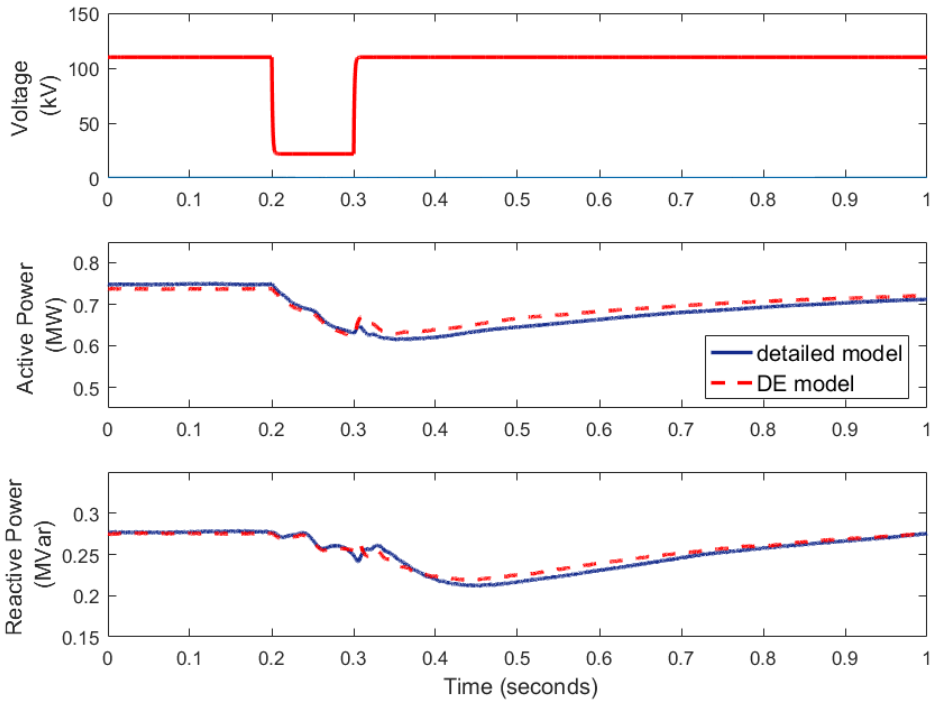

Figure 6.7: Fault scenario created by 0.2 pu voltage

The DE model parameters were once again validated by checking how the model responds to a fault that was not used during the optimization. Figure 6.8 shows the result of applying a 0.8 pu fault scenario to the DE model whose parameters were optimized using 0.5 pu fault. It shows that the DE is able to mimic the response of the detailed model even to such randomly selected fault. Therefore, the developed model is an acceptable, simplified representation of the detailed network.

The slight mismatch noticeable in the power signals can be attributed to the inability to directly use transmission line impedance and reactance as optimization variables in RTDS/Runtime but only the line length. Also, the control system of the solar PV generator model does not include reactive power injection capability which could support the grid voltage during faults.

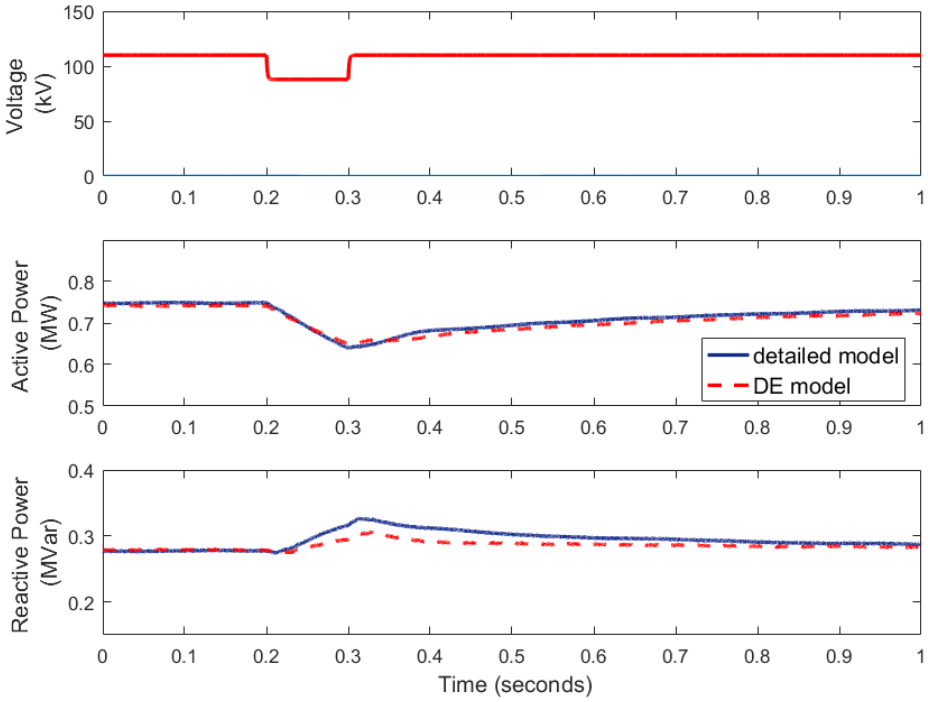

Figure 6.8: Fault scenario created by 0.8 pu voltage

The optimized parameters delivered by the algorithm after the specified number of evaluations are listed in table 6.2.

Table 6.2: Optimized parameters for Test case 2

IM Model		ZIP Model						PV Model		Line (km)	
Rr	0.2737	ZP	43.93	ZPcc2	41.63	ZPcc3	36.6	PVScale	0.9	length	71.82
Rs	0.0468	IP	26.75	IPcc2	35.42	IPcc3	34.47	Vsdref	0.4366		
Xr	0.0381	PP	25.17	PPcc2	40.91	PPcc3	31				
Xs	0.0621	ZQ	38.33	ZQcc2	30.55	ZQcc3	25.26				
Xm	2.6902	IQ	36.24	IQcc2	24.91	IQcc3	25.46				
H	1.1832	PQ	35.87	PQcc2	32.74	PQcc3	33.78				

7

CONCLUSIONS & RECOMMENDATIONS

This chapter includes the main conclusions that can be drawn from the research as well as the answers to the research questions presented at the beginning. Some recommendations are also given for possible future work that can done.

7.1. CONCLUSIONS

Here are some of the conclusions derived from the research work done:

1. Developing dynamic equivalent models for active distribution networks is paramount for simplified stability analysis of future grids. Having an adequate aggregated version of large power networks saves huge computational resources and simulation time. This advantage was evidence during this research as the DE only required one rack unlike the detailed system which needed two racks.

2. It is possible to represent solar PV generators with a simple aggregated model in RTDS without changing it's control parameters of PV array configuration. A scaling factor enables the output to be proportioned as required.

3. The dynamic response during disturbances was analysed using the Euclidean distance. The values derived at the end of the optimization are quite low, thus reflecting that the generated parameters are nearly accurate.

4. An optimization-enabled EMT simulation is successfully implemented on RTDS by communicating with MATLAB. The speed of process can be improved by ensuring that both software are on a very strong local area network.

5. Analyses of larger transmission systems on RTDS can be fostered by representing the distribution system with the developed DE. The racks of RTDS that would have been used by the detailed DS can accommodate additional parts of the transmission network.

6. The communication procedure between RTDS and MATLAB can be further explored for other power system analysis such as software and hardware in the loop applications.

7.2. RESEARCH ANSWERS

In the first chapter, some research questions were asked. Here are their respective answers based on insights drawn from the thesis.

1. **How can a DE model for a future distribution system, dominated by solar PV generation, be defined for real-time digital simulation?**
   The structure of the DE implemented in this thesis i.e. a composite load in parallel with an aggregated solar PV generator, achieved quite remarkable responses similar to the detailed ADN. The equivalent PV model can be easily adapted to represent any size of penetration without changing its configuration as used in this research through the scale factor. However, the control system of the PV model can be enhanced with low voltage ride through (LVRT) and reactive power dispatch capabilities. These features are set to be predominant in future distribution systems.

2. **How accurate can be the response of the DE model when disturbance at transmission system side are simulated?**
   The DE parameters were optimized and identified for a few disturbances in the equivalent external transmission grid. Results derived from the DE model suggest that their response is sufficient. Moreover, the signals of the DE model were closely identical to those of the main system for other disturbances not used during the optimization process. However, other grids should be studied as well to further validate the efficiency of the developed DE model.

3. **Is it feasible and computationally efficient to apply metaheuristic optimization to perform the parameter identification in an automated manner in RTDS?**
   Indeed the application of MVMO for parameter identification resulted in a reduction of the number of racks utilized for simulating the system. Therefore, computational resources are minimized due to the use of a metaheuristic optimization technique. Apart from the time delays that were deliberately included in the optimization script, the technique worked continuously without user interaction. The convergence plot shows that good results are achievable after about 100 evaluations. Furthermore, the simulation time for the system is significantly reduced. It takes less than half the time used for running the detailed model to run the DE.

7.3. CONTRIBUTIONS TO IEPG

1. Developed a practical understanding of the communication mechanism between MATLAB and RTDS, thereby implementing an optimization-enabled simulation involving MVMO, coded in MATLAB, and RTDS/Runtime.

2. A conference paper based on the results of this research was accepted by the Federated Conference on Computer Science and Information Systems (FedCSIS).

3. Developed a PV model which shall be used for subsequent studies on RTDS involving integration of solar PV generation.

4. Created a manual with step by step details of how to set up the communication between MATLAB and RSCAD for solving optimization problems. The manual would be used as a reference material for the laboratory session of Power System Dynamics (ET-4113) course.

7.4. FUTURE WORK

Research on developing dynamic equivalent models for active distribution network on RTDS is still in its early stages. Moreover, setting up an optimization-enabled simulation on RTDS can always be enhanced for better speed. Furthermore, an actual transmission system model can be used such that more scenarios can be implemented to validate the dynamic equivalent model. As such, the following are a few suggestions of what can still be done:

1. A detailed transmission system grid along with its distribution feeders can be simulated in RTDS. The implementation of disturbances in specific locations in the TS rather than randomly within an external grid would further validate the adequacy of the DE. Although many racks might be required to do this, however, successful results would help subsequent researches to simply use DE to reduce their network's complexity.

2. RTDS has parallel processing capabilities which means that multiple simulations can be run on different racks at the same time. The MVMO algorithm can be adapted to perform optimization on different systems and racks through MATLAB's parallel computing toolbox. This would further improve the overall time required to run several test cases sequentially. Implementation of this process would require computers with multicore processors and graphics processing unit (GPUs).

3. MVMO could be programmed into Field Programmable Gate Array (FPGA) to enhance how it is interfaced with RTDS. This would also reduce the time delay caused by the script written in MATLAB for connecting MVMO to RTDS.

4. Multiple distributed energy sources can be adapted to the detailed reference system to represent future grid scenarios more adequately. The control system of the solar PV generator model should include active and reactive power gradient control.

A

IEEE 34-Bus System Dataset

The parameters for the IEEE 34-Bus test feeder as published by the IEEE PES Committee in [2] are given in this appendix. The main distribution network is shown in Figure A.1. The line parameters, transformer data, load data etc. of the network are listed in the following tables. The load flow results can be obtained from [2].

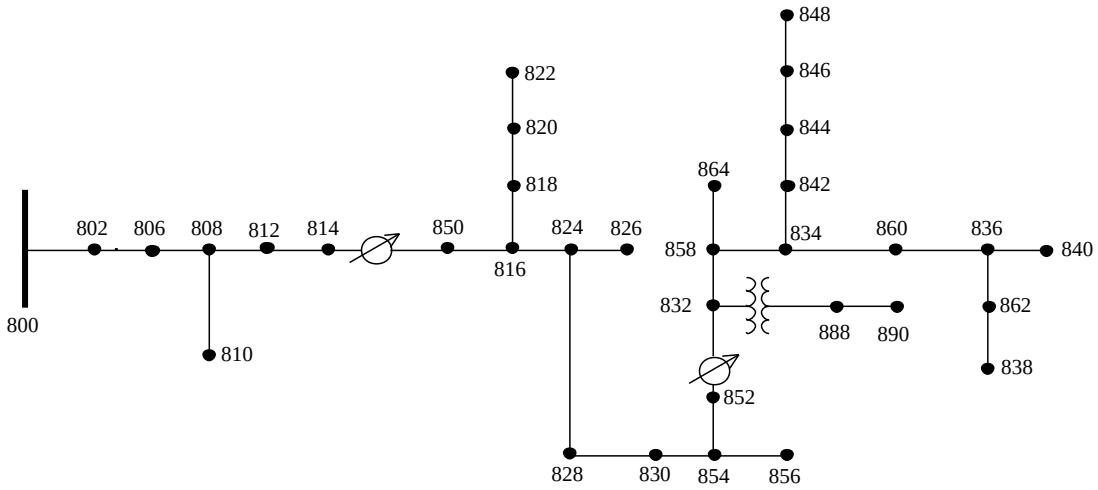

Figure A.1: IEEE 34-Bus Standard Test Feeder

Table A.1: Configurations for the Overhead lines

Overhead Line Configurations (Config.)				
Config.	Phasing	Phase ACSR	Neutral ACSR	Spacing ID
300	B A C N	1/0	1/0	500
301	B A C N	#2 6/1	#2 6/1	500
302	A N	#4 6/1	#4 6/1	510
303	B N	#4 6/1	#4 6/1	510
304	B N	#2 6/1	#2 6/1	510

Table A.2: Line Segment Data

Line Segment Data			
Node A	Node B	Length(ft.)	Config.
800	802	2580	300
802	806	1730	300
806	808	32230	300
808	810	5804	303
808	812	37500	300
812	814	29730	300
814	850	10	301
816	818	1710	302
816	824	10210	301
818	820	48150	302
820	822	13740	302
824	826	3030	303
824	828	840	301
828	830	20440	301
830	854	520	301
832	858	4900	301
832	888	0	XFM-1
834	860	2020	301
834	842	280	301
836	840	860	301
836	862	280	301
842	844	1350	301
844	846	3640	301
846	848	530	301
850	816	310	301
852	832	10	301
854	856	23330	303
854	852	36830	301
858	864	1620	302
858	834	5830	301
860	836	2680	301
862	838	4860	304
888	890	10560	300

Table A.3: Transformer Data

Transformer Data					
	kVA	**kV-high**	**kV-low**	**R - %**	**X - %**
Substation:	2500	69 - D	24.9 -Gr. W	1	8
XFM -1	500	24.9 - Gr.W	4.16 - Gr. W	1.9	4.08

Table A.4: Distributed Loads Data

Distributed Loads								
Node	Node	Load	Ph-1	Ph-1	Ph-2	Ph-2	Ph-3	Ph-3
A	B	Model	kW	kVAr	kW	kVAr	kW	kVAr
802	806	Y-PQ	0	0	30	15	25	14
808	810	Y-I	0	0	16	8	0	0
818	820	Y-Z	34	17	0	0	0	0
820	822	Y-PQ	135	70	0	0	0	0
816	824	D-I	0	0	5	2	0	0
824	826	Y-I	0	0	40	20	0	0
824	828	Y-PQ	0	0	0	0	4	2
828	830	Y-PQ	7	3	0	0	0	0
854	856	Y-PQ	0	0	4	2	0	0
832	858	D-Z	7	3	2	1	6	3
858	864	Y-PQ	2	1	0	0	0	0
858	834	D-PQ	4	2	15	8	13	7
834	860	D-Z	16	8	20	10	110	55
860	836	D-PQ	30	15	10	6	42	22
836	840	D-I	18	9	22	11	0	0
862	838	Y-PQ	0	0	28	14	0	0
842	844	Y-PQ	9	5	0	0	0	0
844	846	Y-PQ	0	0	25	12	20	11
846	848	Y-PQ	0	0	23	11	0	0
Total			262	133	240	120	220	114

Table A.5: Spot Loads Data

Spot Loads							
Node	Load	Ph-1	Ph-1	Ph-2	Ph-2	Ph-3	Ph-4
	Model	kW	kVAr	kW	kVAr	kW	kVAr
860	Y-PQ	20	16	20	16	20	16
840	Y-I	9	7	9	7	9	7
844	Y-Z	135	105	135	105	135	105
848	D-PQ	20	16	20	16	20	16
890	D-I	150	75	150	75	150	75
830	D-Z	10	5	10	5	25	10
Total		344	224	344	224	359	229

Table A.6: Total Distribution Load Data

Bus	Phase-A (KVA)	Phase-B (KVA)	Phase-C (KVA)
802	0	15+j7.5	12.5+j7
806	0	15+j7.5	12.5+j7
808	0	8+j4	0
810	0	8+j4	0
816	0+j0	2.5+j1	0
818	17+j8.5	0	0
820	84.5+j43.5	0	0
822	67.5+j35	0	0
824	0	22.5+j11	2+j1
826	0	20+j10	0
828	3.5+j1.5	0	2+j1
830	13.5+j6.5	10+j5	10+j5
832	3.5+j1.5	1+j0.5	3+j1.5
834	10+j5	12.5+j7	61.5+j31
836	24+j12	16+j8.5	21+j11
838	0	14+j7	0
840	18+j11.5	20+j12.5	9+j7
842	4.5+j2.5	0	0
844	139.5+j109.5	147.5+j111	145+j110.5
846	0	24+j11.5	10+j5
848	20+j16	44+j27.5	30+j21.5
854	0	2+j1	0
856	0	2+j1	0
858	6.5+j3	8.5+j4.5	9.5+j5
860	43+j27.5	35+j24	96+j54.5
862	0	14+j7	0+j0
864	1+j0.5	0	0
890	150+j75	150+j75	150+j75
Total	**606+j359**	**591.5+j348**	**574+j343**

Table A.7: Voltage Regulator Data

Regulator Data			
Regulator ID:	**1**		
Line Segment:	814 - 850		
Location:	814		
Phases:	A - B -C		
Connection:	3-Ph,LG		
Monitoring Phase:	A-B-C		
Bandwidth:	2.0 volts		
PT Ratio:	120		
Primary CT Rating:	100		
Compensator Settings:	Ph-A	Ph-B	Ph-C
R - Setting:	2.7	2.7	2.7
X - Setting:	1.6	1.6	1.6
Voltage Level:	122	122	122
Regulator ID:	**2**		
Line Segment:	852 - 832		
Location:	852		
Phases:	A - B -C		
Connection:	3-Ph,LG		
Monitoring Phase:	A-B-C		
Bandwidth:	2.0 volts		
PT Ratio:	120		
Primary CT Rating:	100		
Compensator Settings:	Ph-A	Ph-B	Ph-C
R - Setting:	2.5	2.5	2.5
X - Setting:	1.5	1.5	1.5
Voltage Level:	124	124	124

Table A.8: Capacitor Data

Shunt Capacitors			
Node	Ph-A kVAr	Ph-B kVAr	Ph-C kVAr
844	100	100	100
848	150	150	150
Total	**250**	**250**	**250**

BIBLIOGRAPHY

[1] A. D. Paz, *Modelling and aggregation of loads in flexible power networks - Scope and status of the work of CIGRE WG C4.605,* (2014).

[2] B.-H. Kim, H. Kim, and B. Lee, *Parameter Estimation for the Composite Load Model,* Journal of International Council on Electrical Engineering **2**, 215 (2012), http://dx.doi.org/10.5370/JICEE.2012.2.2.215 .

[3] K. Yamashita, S. Djokic, J. Matevosyan, F. Resende, L. Korunovic, Z. Dong, and J. Milanovic, *Modelling and aggregation of loads in flexible power networks - scope and status of the work of cigre wg c4.605,* in *IFAC Proceedings Volumes (IFAC-PapersOnline)|IFAC Proc. Vol. (IFAC-PapersOnline)*, Vol. 8 (2012) pp. 405–410.

[4] D. Gusain, J. L. Rueda, J. C. Boemer, and P. Palensky, *Identification of dynamic equivalents of active distribution networks through mvmo,* IFAC-PapersOnLine **49**, 262 (2016), iFAC Workshop on Control of Transmission and Distribution Smart Grids CTDSG 2016.

[5] L. Xiaofang, P. Minfang, H. Hao, and L. Tao, *Dynamic Load Modeling for Power System Based on GD-FNN,* in *2012 Third International Conference on Digital Manufacturing Automation* (2012) pp. 339–342.

[6] A. Oonsivilai and M. E. El-Hawary, *Power system dynamic load modeling using adaptive-network-based fuzzy inference system,* in *Engineering Solutions for the Next Millennium. 1999 IEEE Canadian Conference on Electrical and Computer Engineering (Cat. No.99TH8411)*, Vol. 3 (1999) pp. 1217–1222 vol.3.

[7] H. Andrei, P. C. Andrei, L. M. Constantinescu, R. Beloiu, E. Cazacu, and M. Stanculescu, *Electrical power systems,* in *Reactive Power Control in AC Power Systems: Fundamentals and Current Issues*, edited by N. Mahdavi Tabatabaei, A. Jafari Aghbolaghi, N. Bizon, and F. Blaabjerg (Springer International Publishing, Cham, 2017) pp. 3–47.

[8] R. Idema and D. Lahaye, *Computational Methods in Power System Analysis* (Atlantis Publishing Corporation, 2014).

[9] J. Ma, X. y. Zheng, Y. h. Tang, and Z. y. Dong, *Validating measurement-based composite load model,* in *8th International Conference on Advances in Power System Control, Operation and Management (APSCOM 2009)* (2009) pp. 1–6.

[10] W.-S. Kao, C.-T. Huang, and C.-Y. Chiou, *Dynamic load modeling in Taipower system stability studies,* IEEE Transactions on Power Systems **10**, 907 (1995).

[11] N. Martins, S. Gomes, R. M. Henriques, C. B. Gomes, A. de Andrade Barbosa, and A. C. B. Martins, *Impact of induction motor loads in system loadability margins and damping of inter-area modes,* in *2003 IEEE Power Engineering Society General Meeting (IEEE Cat. No.03CH37491)*, Vol. 3 (2003) p. 1384 Vol. 3.

[12] M. Rylander, W. M. Grady, A. Arapostathis, and E. J. Powers, *Power Electronic Transient Load Model for Use in Stability Studies of Electric Power Grids,* IEEE Transactions on Power Systems **25**, 914 (2010).

[13] A. J. Collin, I. Hernando-Gil, J. L. Acosta, and S. Z. Djokic, *An 11 kV steady state residential aggregate load model. Part 1: Aggregation methodology,* in *2011 IEEE Trondheim PowerTech* (2011) pp. 1–8.

[14] *Load representation for dynamic performance analysis of power systems,* IEEE Transactions on Power Systems **8**, 472 (1993).

[15] *Standard load models for power flow and dynamic performance simulation,* IEEE Transactions on Power Systems **10**, 1302 (1995).

[16] L. Wang, M. Klein, S. Yirga, and P. Kundur, *Dynamic reduction of large power systems for stability studies,* IEEE Transactions on Power Systems **12**, 889 (1997).

[17] R. Kearsley, *Restoration in Sweden and Experience Gained from the Blackout of 1983,* IEEE Power Engineering Review **PER-7**, 48 (1987).

[18] T. Ohno and S. Imai, *The 1987 Tokyo Blackout,* in *2006 IEEE PES Power Systems Conference and Exposition* (2006) pp. 314–318.

[19] D. Singh, R. K. Misra, and D. Singh, *Effect of Load Models in Distributed Generation Planning,* IEEE Transactions on Power Systems **22**, 2204 (2007).

[20] S. Li, X. Liang, and W. Xu, *Dynamic load modeling for industrial facilities using template and PSS/E composite load model structure CLOD,* in *2017 IEEE/IAS 53rd Industrial and Commercial Power Systems Technical Conference (I CPS)* (2017) pp. 1–9.

[21] P. K. Naik, W. A. Qureshi, and N. K. C. Nair, *Identification of coherent generator groups in power system networks with windfarms,* in *AUPEC 2011* (2011) pp. 1–5.

[22] D. J. Hill, *Nonlinear dynamic load models with recovery for voltage stability studies,* IEEE Transactions on Power Systems **8**, 166 (1993).

[23] *Bibliography on load models for power flow and dynamic performance simulation,* IEEE Transactions on Power Systems **10**, 523 (1995).

[24] J. V. Milanovic, K. Yamashita, S. M. Villanueva, S. . Djokic, and L. M. Korunović, *International Industry Practice on Power System Load Modeling,* IEEE Transactions on Power Systems **28**, 3038 (2013).

[25] J. Matevosyan, S. M. Villanueva, S. Z. Djokic, J. L. Acosta, S. M. Zali, F. O. Resende, and J. V. Milanovic, *Aggregated models of wind-based generation and active distribution network cells for power system studies - literature overview,* in *2011 IEEE Trondheim PowerTech* (2011) pp. 1–8.

[26] D. Salomonsson and A. Sannino, *Load modelling for steady-state and transient analysis of low-voltage dc systems,* IET Electric Power Applications **1**, 690 (2007), qC 20100908.

[27] K. Morison, H. Hamadani, and L. Wang, *Practical issues in load modeling for voltage stability studies,* in *2003 IEEE Power Engineering Society General Meeting (IEEE Cat. No.03CH37491)*, Vol. 3 (2003) pp. 1392–1397 Vol. 3.

[28] H. A. Toliyat and G. B. Kliman, *Handbook of Electric Motors* (CRC Press LLC, 2004) pp. 25–165.

[29] I. Boldea and S. A. Nasar, *The Induction Machine Handbook* (CRC Press LLC, 2002) Chap. 23.

[30] P. C. Krause, *Analysis of Electric Machinery* (New York: McGraw-Hill, Inc., 1986).

[31] P. Regulski, D. S. Vilchis-Rodriguez, S. Djurović, and V. Terzija, *Estimation of Composite Load Model Parameters Using an Improved Particle Swarm Optimization Method,* IEEE Transactions on Power Delivery **30**, 553 (2015).

[32] S. A. Y. Sabir and D. c. Lee, *Dynamic load models derived from date acquired during system transients,* IEEE Transactions on Power Apparatus and Systems **PAS-101**, 3365 (1982).

[33] T. Y. J. Lem and R. T. H. Alden, *Comparison of experimental and aggregate induction motor responses,* IEEE Transactions on Power Systems **9**, 1895 (1994).

[34] H.-D. Chiang, J.-C. Wang, C.-T. Huang, Y.-T. Chen, and C.-H. Huang, *Development of a dynamic zip-motor load model from on-line field measurements,* International Journal of Electrical Power Energy Systems **19**, 459 (1997).

[35] H. Renmu, M. Jin, and D. J. Hill, *Composite load modeling via measurement approach,* IEEE Transactions on Power Systems **21**, 663 (2006).

[36] D. Kosterev, A. Meklin, J. Undrill, B. Lesieutre, W. Price, D. Chassin, R. Bravo, and S. Yang, *Load modeling in power system studies: WECC progress update,* in *2008 IEEE Power and Energy Society General Meeting Conversion and Delivery of Electrical Energy in the 21st Century* (2008) pp. 1–8.

[37] A. Maitra, A. Gaikwad, P. Zhang, M. Ingram, D. L. Mercado, and W. D. Woitt, *Using System Disturbance Measurement Data to Develop Improved Load Models,* in *2006 IEEE PES Power Systems Conference and Exposition* (2006) pp. 1978–1985.

[38] K. Yamashita, M. Asada, and K. Yoshimura, *A development of dynamic load model parameter derivation method,* in *2009 IEEE Power Energy Society General Meeting* (2009) pp. 1–8.

[39] A. A. Rahim, M. F. Hashim, and M. F. M. Siam, *Dynamic load modelling based on power quality recorder data,* in *2013 IEEE 7th International Power Engineering and Optimization Conference (PEOCO)* (2013) pp. 119–123.

[40] J. Wen, S. Wang, S. Cheng, Q. H. Wu, and D. W. Shimmin, *Measurement based power system load modeling using a population diversity genetic algorithm,* in *Power System Technology, 1998. Proceedings. POWERCON '98. 1998 International Conference on*, Vol. 1 (1998) pp. 771–775 vol.1.

[41] F. Milano and K. Srivastava, *Dynamic rei equivalents for short circuit and transient stability analyses,* Electric Power Systems Research **79**, 878 (2009).

[42] J. M. Ramirez, B. V. Hernández, and R. E. Correa, *Dynamic equivalence by an optimal strategy,* Electric Power Systems Research **84**, 58 (2012).

[43] J. M. Undrill and A. E. Turner, *Construction of Power System lectromechanical Equivalents by Modal Analysis,* IEEE Transactions on Power Apparatus and Systems **PAS-90**, 2049 (1971).

[44] B. Marinescu, B. Mallem, and L. Rouco, *Large-Scale Power System Dynamic Equivalents Based on Standard and Border Synchrony,* IEEE Transactions on Power Systems **25**, 1873 (2010).

[45] A. M. Miah, *Study of a coherency-based simple dynamic equivalent for transient stability assessment,* IET Generation, Transmission Distribution **5**, 405 (2011).

[46] E. J. P. de Souza, *Identification of coherent generators considering the electrical proximity for drastic dynamic equivalents,* Electric Power Systems Research **78**, 1169 (2008).

[47] J. Machowski, A. Cichy, F. Gubina, and P. Omahen, *External subsystem equivalent model for steady-state and dynamic security assessment,* IEEE Transactions on Power Systems **3**, 1456 (1988).

[48] J. H. Chow, R. Galarza, P. Accari, and W. W. Price, *Inertial and slow coherency aggregation algorithms for power system dynamic model reduction,* IEEE Transactions on Power Systems **10**, 680 (1995).

[49] G. N. Ramaswamy, L. Rouco, O. Fillatre, G. C. Verghese, P. Panciatici, B. C. Lesieutre, and D. Peltier, *Synchronic modal equivalencing (sme) for structure-preserving dynamic equivalents,* IEEE Transactions on Power Systems **11**, 19 (1996).

[50] G. N. Ramaswamy, C. Evrard, G. C. Verghese, O. Fillatre, and B. C. Lesieutre, *Extensions, simplifications, and tests of synchronic modal equivalencing (SME),* IEEE Transactions on Power Systems **12**, 896 (1997).

[51] R. J. Galarza, J. H. Chow, W. W. Price, A. W. Hargrave, and P. M. Hirsch, *Aggregation of exciter models for constructing power system dynamic equivalents,* IEEE Transactions on Power Systems **13**, 782 (1998).

[52] J. Ma, D. Han, R. M. He, Z. Y. Dong, and D. J. Hill, *Reducing identified parameters of measurement-based composite load model,* IEEE Transactions on Power Systems **23**, 76 (2008).

[53] M. Rasouli, D. Westwick, and W. Rosehart, *Reducing induction motor identified parameters using a nonlinear lasso method,* Electric Power Systems Research **88**, 1 (2012).

[54] Q. Liu, Y. Chen, and D. Duan, *The load modeling and parameters identification for voltage stability analysis,* in *Proceedings. International Conference on Power System Technology*, Vol. 4 (2002) pp. 2030–2033 vol.4.

[55] I. A. Hiskens, *Nonlinear dynamic model evaluation from disturbance measurements,* in *2002 IEEE Power Engineering Society Winter Meeting. Conference Proceedings (Cat. No.02CH37309)*, Vol. 2 (2002) pp. 1010 vol.2–.

[56] K. S. Huang, Q. H. Wu, and D. R. Turner, *Effective identification of induction motor parameters based on fewer measurements,* IEEE Transactions on Energy Conversion **17**, 55 (2002).

[57] C. Kwon and S. D. Sudhoff, *Genetic algorithm-based induction machine characterization procedure with application to maximum torque per amp control,* IEEE Transactions on Energy Conversion **21**, 405 (2006).

[58] W. M. Lin, T. J. Su, and R. C. Wu, *Parameter Identification of Induction Machine With a Starting No-Load Low-Voltage Test,* IEEE Transactions on Industrial Electronics **59**, 352 (2012).

[59] A. Karimi, M. A. Choudhry, and A. Feliachi, *PSO-based Evolutionary Optimization for Parameter Identification of an Induction Motor,* in *2007 39th North American Power Symposium* (2007) pp. 659–664.

[60] E. Polykarpou and E. Kyriakides, *Parameter estimation for measurement-based load modeling using the Levenberg-Marquardt algorithm,* in *2016 18th Mediterranean Electrotechnical Conference (MELECON)* (2016) pp. 1–6.

[61] P. Ju, E. Handschin, and D. Karlsson, *Nonlinear dynamic load modelling: model and parameter estimation,* IEEE Transactions on Power Systems **11**, 1689 (1996).

[62] J. Y. Wen, L. Jiang, Q. H. Wu, and S. J. Cheng, *Power system load modeling by learning based on system measurements,* IEEE Transactions on Power Delivery **18**, 364 (2003).

[63] S. Z. Zhu, Z. Y. Dong, K. P. Wong, and Z. H. Wang, *Power system dynamic load identification and stability,* in *PowerCon 2000. 2000 International Conference on Power System Technology. Proceedings (Cat. No.00EX409)*, Vol. 1 (2000) pp. 13–18 vol.1.

[64] H. Bai, P. Zhang, and V. Ajjarapu, *A Novel Parameter Identification Approach via Hybrid Learning for Aggregate Load Modeling,* IEEE Transactions on Power Systems **24**, 1145 (2009).

[65] V. Vignesh, S. Chakrabarti, and S. C. Srivastava, *An experimental study on the load modelling using PMU measurements,* in *2014 IEEE PES T D Conference and Exposition* (2014) pp. 1–5.

[66] A. Rahim and A. Al-Ramadhan, *Dynamic equivalent of external power system and its parameter estimation through artificial neural networks,* International Journal of Electrical Power Energy Systems **24**, 113 (2002).

[67] A. M. Stankovic, A. T. Saric, and M. Milosevic, *Identification of nonparametric dynamic power system equivalents with artificial neural networks,* IEEE Transactions on Power Systems **18**, 1478 (2003).

[68] A. M. Stankovic and A. T. Saric, *Transient power system analysis with measurement-based gray box and hybrid dynamic equivalents,* IEEE Transactions on Power Systems **19**, 455 (2004).

[69] A. M. Azmy and I. Erlich, *Identification of dynamic equivalents for distribution power networks using recurrent ANNs,* in *IEEE PES Power Systems Conference and Exposition, 2004.* (2004) pp. 348–353 vol.1.

[70] J. L. Rueda, J. Cepeda, I. Erlich, D. Echeverría, and G. Argüello, *Heuristic optimization based approach for identification of power system dynamic equivalents,* International Journal of Electrical Power Energy Systems **64**, 185 (2015).

[71] J. C. Cepeda, J. L. Rueda, and I. Erlich, *MVMOS-based approach for identification of dynamic equivalents from PMU measurements,* in *2013 IEEE Grenoble Conference* (2013) pp. 1–6.

[72] J. C. Cepeda, J. L. Rueda, and I. Erlich, *Identification of dynamic equivalents based on heuristic optimization for smart grid applications,* in *2012 IEEE Congress on Evolutionary Computation* (2012) pp. 1–8.

[73] P. Forsyth and R. Kuffel, *Utility applications of a RTDS Simulator,* in *2007 International Power Engineering Conference (IPEC 2007)* (2007) pp. 112–117.

[74] *The massive integration of power electronic devices,* .

[75] R. Technologies, *RTDS Manuals and Documentation* (Winnipeg, 2009).

[76] H. W. Dommel, *Digital computer solution of electromagnetic transients in single-and multiphase networks,* IEEE Transactions on Power Apparatus and Systems **PAS-88**, 388 (1969).

[77] *Distribution System Analysis Subcommittee of the IEEE Power Engineering Society IEEE 34 Node Test Feeder,* `http://www.ewh.ieee.org/soc/pes/dsacom/testfeeders/`, accessed: 2016-12-30.

[78] M. G. Villalva, J. R. Gazoli, and E. R. Filho, *Comprehensive approach to modeling and simulation of photovoltaic arrays,* IEEE Transactions on Power Electronics **24**, 1198 (2009).

[79] Q. Xiong, X. Jin, D. Guo, and B. Zhang, *Modeling and simulation of large-scale grid-connected photovoltaic system on rtds,* in *Proceedings of the 6th International Asia Conference on Industrial Engineering and Management Innovation: Core Theory and Applications of Industrial Engineering (volume 1)*, edited by E. Qi (Atlantis Press, Paris, 2016) pp. 437–449.

[80] Y. Zhu, J. Yao, and D. Wu, *Comparative study of two stages and single stage topologies for grid-tie photovoltaic generation by pscad/emtdc,* in *2011 International Conference on Advanced Power System Automation and Protection*, Vol. 2 (2011) pp. 1304–1309.

[81] O. Nzimako and A. Rajapakse, *Real time simulation of a microgrid with multiple distributed energy resources,* in *2016 International Conference on Cogeneration, Small Power Plants and District Energy (ICUE)* (2016) pp. 1–6.

[82] A. Yazdani and R. Iravani, *Voltage-Sourced Converters in Power Systems: Modeling, Control, and Applications* (New Jersey: Wiley-IEEE Press, 2010).

[83] N. Z. B. Wu, Y. Lang and S. Kouro, *Power Conversion and Control of Wind Energy Systems* (Wiley-IEEE Press, 2011).

[84] A. Yazdani and P. P. Dash, *A Control Methodology and Characterization of Dynamics for a Photovoltaic (PV) System Interfaced With a Distribution Network,* IEEE Transactions on Power Delivery **24**, 1538 (2009).

[85] G. Farivar, B. Asaei, and S. Mehrnami, *An analytical solution for tracking photovoltaic module mpp,* IEEE Journal of Photovoltaics **3**, 1053 (2013).

[86] T. Thiringer and J. Luomi, *Comparison of reduced-order dynamic models of induction machines,* IEEE Transactions on Power Systems **16**, 119 (2001).

[87] W. Nakawiro, I. Erlich, and J. L. Rueda, *A novel optimization algorithm for optimal reactive power dispatch: A comparative study,* in *2011 4th International Conference on Electric Utility Deregulation and Restructuring and Power Technologies (DRPT)* (2011) pp. 1555–1561.

[88] J. E. Friedl, *Mastering Regular Expressions* (O'Reilly Media, 2002).